AGE AND UNFOLDED PROTEIN RESPONSE ENHANCEMENT IN STROKE-INDUCED INFLAMMATION.

EDAD Y RESPUESTA A LAS PROTEÍNAS MAL PLEGADAS EN EL ACCIDENTE CEREBRO VASCULAR. EL EFECTO DE LA EDAD

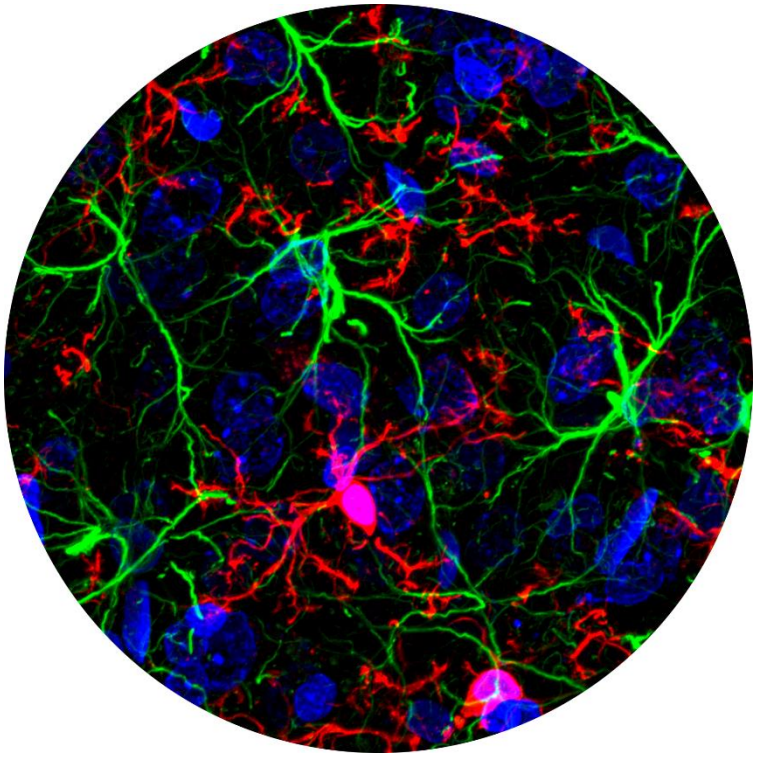

Memoria para optar al Grado de Doctor con Mención Internacional que presenta

Berta Anuncibay Soto

León, junio de 2017

A mi familia y a Diego, lo mejor que tengo.

A la memoria de Magdalena Benitez Saéz, lo mejor que tuve.

El cariño y el esfuerzo pueden cambiar las normas establecidas en el mundo.

Nunca he creído que por ser mujer deba tener tratos especiales,
de creerlo estaría reconociendo que soy inferior a los hombres,
y no lo soy a ninguno de ellos ***(Marie Curie)***

Al carro de la cultura española le falta la
rueda de la ciencia ***(Santiago Ramón y Cajal).***

El arte es yo, la ciencia
somos nosotros ***(Claude Bernard)***

PhD dissertation submitted to obtain a Doctorate degree in Molecular Biology and Biotechnology from the Universidad de León.

The studies summarized in this dissertation were made under the supervision of Professor Dr. Arsenio Fernández López, Área de Biología, Dpto. Biología Molecular, Universidad de León, Spain.

Experimental procedures were performed in the Animal House, and in the laboratories of Biología Molecular, Medicina, Anatomía y Cirugía Veterinaria and Instituto de Biomedicina in the University of León. Complementary assays were made in the School of Life, Sport & Social Sciences, Edinburgh Napier University, under the supervision of Drs. Mark G Darlinson and Jenny Fraser.

This work has been funded by Junta of Castilla y León (reference LE184A12-2); MINECO (reference BIO2013-49006-C2-2-R) and MINECO (reference RTC-2015-4094-1) all of them cofunded with FEDER FUNDS. The author has been supported by a MINECO (reference BIO2013-49006-C2-2-R) grant and by research contracts between University of León and Neural Therapies SL.

Agradecimientos

Durante tiempo he dicho que realmente la realización de mi tesis doctoral iba dirigida a la escritura de esta página, ahora que el sueño se hizo realidad la escritura de esta página es totalmente necesaria. Este maravilloso viaje ha requerido de muchos acompañantes totalmente necesarios, porque, aunque describiría este camino como un proceso de superación personal, soy totalmente consciente de que no hubiera sido posible si las personas que aparecen a continuación:

Me gustaría empezar agradeciendo al área de Biología Celular, la cual ha sido mi casa durante los últimos seis años (casi siete), desde que entre por la puerta buscando a Arsenio Fernández un octubre de 2010. Aún era estudiante de Licenciatura en ese momento, supongo que realmente ese fue el inicio de todo. Me gustaría darles las gracias a Carmen, Alberto, Paulino, Blanca y Paz. Aunque el área lo conforman más personas, son los que han cohabitado conmigo en esta experiencia. Gracias por la ayuda prestada y sobretodo perdón por aguantar de vez en cuando una voz más alta que la otra.

Este viaje no hubiera sido igual sin esa parte vivida en el Departamento de Cirugía Medicina y Anatomía Veterinaria. Muchas gracias a Carlos César por estar siempre pendiente de los problemas de los animales, y por todo lo aprendido de ellos durante estos años gracias a ti. Muchísimas gracias Manolo porque ese quirófano, siempre será mi segunda casa. Muchas gracias por estar siempre, por siempre decir que sí, por siempre encontrar un hueco para las ratas. Pero sobre todo por ese millón de conversaciones transcendentales en el quirófano sobre la vida y milagros, por las espichas con autobús incluido y por ese minivuelo (aún tenemos pendiente el real), que casi muero del miedo pero que, como todo, habrá una segunda oportunidad. A la reina de la anestesia, del orden, de la cirugía, de la paciencia, pero, sobre todo, a la persona que salvó a mi dragón, a mi pequeño corazón gatúnido, gracias Marta. Porque sé que de aquí me llevo a una amiga, no solo a una compañera. No me gustaría olvidarme de esas personas que también formaron parte de esto y que ahora siguieron su camino hacia delante: Fidel, Manu y sobre todo a Jenny!!!!!! O también conocida como Anabel, mil gracias chicos.

A mis compañeros becarios pertenecientes a las diversas Áreas que conforman la facultad: Alfonso, María, David, Cristina, Silvia, Marta Lombó, Yoli, Octavio, Sandra, Laura, Marta y Alberto. Muchas gracias a estos últimos por ser más que compañeros, por las noches de desconexión necesaria: Octavio rey de los chupitos, Laura y su gasolina necesaria para el parkineo, Marta y todo lo Indie a su alrededor, Sandra y su odio a lo Indie, también su amor al Indio y Alberto, que le monté un día en una bicicleta y así tanto le gusta venir a hacer parafina últimamente. Muchísimas gracias, chicos.

Cómo no al grupo de neurobiología mi "Dream Team"!!!. De vosotros no cambiaría NADA, repito NADA. Sería absurdo decir que sois mis compañeros, sois mucho más, muchísimo más. Una de las grandes cosas de este trabajo es hacerlo en equipo, las ilusiones son el doble y las penas son menos. A Jose, nuestra última incorporación, porque la vida siempre pega dos veces y hay que estar preparado para coger el tren, porque en este tiempo vas a bailar con flow. A María mi medio cerebro, como dice la canción "yo no necesito hablar para expresar una emoción, me basta solo con mirar", tú como poca gente entiendes esa mirada. A El Palomo, que es más lista que calista, porque te has superado no solo en lo profesional, también en lo personal, y porque nadie entiende el Traga como tú, guapi. Irene que está llamada a ser mi digna sustituta en lo económico, que apuesta por la apuesta completa, por la felicidad al 100%, porque es una valiente y más debiera haber en el mundo. A mi maicito, mi heredero de modelo (so, sorry), mi protegido, voy a usar contigo una gran frase que salvó a mi gata y que me parece un dogma de vida: porque hay que salir al sol, tomar unas cañas… la continuaría, pero no es el público adecuado. Vive, disfruta, convive con las dificultades, la vida es para salir al sol!!. A Diego, parte de este Dream Team pero parte de mucho, muchísimo más, porque sin ti muchas cosas no hubiesen sido posibles. Yo vine buscando un trabajo y encontré mucho más. Sabes que mil veces te mataría, pero diez mil solo te querría. Como una vez dijo Steve Jobs, las grandes relaciones son aquellas que mejoran con el tiempo. Ahora eso si, la custodia de Misi es mía. Gracias, gracias, gracias mil veces. No me gustaría olvidarme de los que ya no están como Irene que me enseñó que la vida es para pelearla, independientemente del tamaño que tengas, y a Severiano, que le hemos recuperado en los últimos tiempos, por esa forma que tienes de no dar puntada sin hilo, todo muy chic para tí y para mí.

No me gustaría olvidarme de esa gente que nos hace la vida más fácil a todos con su trabajo, pero, sobre todo, con su actitud ante ello: Benjamín, Domingo, Lorena, Iván y Maribel, gracias por todo vuestro trabajo y porque le dais sabor a esta Universidad. A Jorge y David por todo lo que me habéis enseñado. Me gustaría destacar aquí a esos técnicos que te lo enseñan todo y que cuando no encuentras algo te lo traen a las manos: a los dos Pedros (el nuestro y el de química), gracias chicos, pero sobre todo a esas dos grandes: Marta y Ana. Cuánto he aprendido del laboratorio, de la vida y de todo con vosotras, gracias por ser maravillosas, por seguir creyendo en el esfuerzo, pero especialmente gracias por ser como sois. No sé qué voy a hacer sin vuestra sabia palabra a partir de ahora.

A mis amigos fuera de aquí que me han ayudado a mantener la cordura necesaria para todo esto, que me han levantado cuando me caía y que me han sacado a bailar cuando creía que no podía más. A mis dos brothers, O y Carvi gracias por todo, incluso por reíros de mi, ay por favor!!!!, os quiero mucho. A Inés porque no siempre se tiene la suerte de tener un patito de siempre y para siempre. A Cris o debería decir SuperCris en los últimos tiempos, porque te mereces lo mejor del mundo, pero exactamente lo mejor te quiero con locura. A mi pollo que me enseñó mi segunda juventud, que la edad solo va en el carnet, porque conocerte ha sido de las mejores cosas de mi doctorado, ya sabes: Oye, abre tus ojos, mira hacia arriba, disfruta las cosas buenas que tiene la vida. Y a Fati, porque cuando nos juntamos las tres, está asegurado todo.

I also wish to thanks to the Edinburgh Napier University, the wonderful experience living in Edinburgh during mi PhD. I want to remember Mark G Dalinson, mi first director in Edinburgh, your efforts and implication in my job. But specially because you were present since my first moments in the PhD here in León, thank you Mark I will never forget you. I also want to thanks to Jenny Frasser and Amy Poole because you try to help me in everything, you advise me about what places I have to see in Edinburgh and because you treat me like family, thank you so much for everything. And, of course, I wish to thank the research students: Sophie, Kristie, Philipa, Hanna, Lee, Olga, Victor, Bea, Alva and of course Miguuuuuuelito, thank you because you are the reason because Edinburgh is one of the most especial place that I have visited in my life. I hope you know you have a friend in Spain.

Como no a Arsenio Fernández López, o Arse o Miniprep. Porque el respeto no se exige, se gana, y tú lo demuestras día a día. Gracias por no creer en lo que se veía de mí cuando entré a tu despacho (un número que encima era horrible), por creer más, por ver el potencial, gracias por esto porque es culpa tuya al 100%. Siempre serás quien lo hizo, quien tuvo fe en el corazón de las cartas. Te diría que me has enseñado muchas cosas científicas, pero creo que eso se sobreentiende. Me quedo con que me has enseñado lo maravilloso que es formar a alguien y verlo crecer, el esfuerzo personal y que el límite, ante todo, siempre es mental. Gracias por todo una y mil veces.

A mi familia, porque como una vez dijo alguien, yo si volviera a nacer solo pediría volver a nacer en la misma familia, que no son gente muy normal, pero les debo todo, lo sé, lo asumo y me encanta decirlo. A mi madre que es el altruismo personificado, gracias por ser lo mejor que podíamos esperar de ti cada día. A mi padre que nunca tuvo límites y eso te hace crecer en un mundo en el que sabes que con esfuerzo todo es posible. A mi hermano, mi medio corazón, braini perfecto, siempre los dos, siempre!. A mi abuela Pili, mi tía Pili, mi tío Álvaro, Albertito e Inés, mi familia gracias por esas maravillosas reuniones. Y por último a la memoria de mi abuela Magdalena, mi segunda madre, porque te encantaría estar aquí para verlo y a mí que estuvieras, aunque sé que alguien vive mientras se le recuerda, tú en mí vives todos los días.

"Tal vez lloré, tal vez reí, tal vez gané, tal vez perdí, ahora sé que fuí feliz, que si lloré también amé y todo fue, puedo decir, I did it my way"

¡Muchas gracias a todos!

Index

SUMMARY

Summary

The cerebrovascular accident (ACV) or stroke, is one of the main causes of mortality, the first cause of permanent disability and the second cause of dementia in the developed countries. Nowadays this pathology presents no effective treatments and it is under a very active research. This memory presents several studies performed in a global cerebral ischemia model where interactions between inflammation and stroke are analysed. The first chapter describes different responses in old and young animals at 48 h of I/R, including different patterns of apoptotic labelling, GFAP reactivity, and molecules involved in high and low affinity binding of neutrophils. These age-dependent differences seem represent changes in the time-course response to I/R and should be taken into account in the studies addressed for searching new therapeutic targets against stroke.

The second chapter shows that the treatment with the unfolded protein response (UPR) enhancer, salubrinal (Sal), presents a neuroprotective role in CA1, the hippocampal area with highest vulnerability to the ischemia. CA1 is suggested to present a limited UPR against the ischemia and Sal treatment is proposed to enhance this response thus reducing the cell delayed mortality. The neurovascular unit (NVU) presents structure-dependent inflammatory properties to ischemic injury mainly mirrored in the differences in the time course of the inflammatory response in the different brain areas. This is also supported by the Sal treatment. In addition, this chapter shows the responsiveness of endothelial cells and, to a much lesser degree, of astrocytes to the Sal treatment. Sal treatment affects in different way the different cell populations, resulting in local rather than systemic effects. This chapter evidences that UPR modulators are able to modify the inflammatory response. The effectiveness of Sal when administered after the ischemic insult suggest therapeutic possibilities for UPR modulators in stroke that, up to date, have not been taken into account.

The third chapter analysed the effect of the combined effect of Sal and a highly selective anti COX-2 agent, robenacoxib (Rob). Despite its anti-inflammatory effect, Rob moves the neuronal demise forward instead of increasing neuroprotection. However, the combined effect of Sal and Rob prevents the early neuronal loss induced by this anti-

inflammatory agent. Moreover, glial activation is strongly increased by Rob, poorly or non-activated by Sal, and reverted by the combined administration of Sal–Rob. Finally, the synergic action on the microglia by the combined effect of an anti-ER stress agent followed by an anti-inflammatory agent suggests that a proper combination of different neuroprotective agents could provide a stronger neuroprotective effect.

Resumen

El accidente cerebro vascular (ACV) es una de las principales causas de mortalidad, la primera causa de incapacidad permanente y la segunda causa de demencia en los países desarrollados. Actualmente no se dispone de una terapia efectiva frente a esta patología por lo que existe una investigación muy activa sobre la misma. Esta memoria presenta una serie de estudios hechos en un modelo experimental de isquemia cerebral global en el que se analiza la interacción entre el accidente cerebrovascular y la inflamación. En el primer capítulo se muestran las diferentes respuestas entre animales jóvenes y viejos a las 48 h de reperfusión, incluyendo los diferentes patrones de expresión de marcado de apoptosis, la reactividad de la proteína acídica fibrilar glial (GFAP) y las moléculas responsables de la adhesión de alta y baja afinidad entre el endotelio y los neutrófilos. Se considera que las diferencias dependientes de la edad representan cambios en la dinámica de respuesta a la isquemia/reperfusión (I/R), lo que debería tenerse en cuenta en los estudios encaminados a la búsqueda de nuevas dianas terapéuticas contra el ACV

El segundo capítulo muestra que el tratamiento con salubrinal (Sal), un potenciador de la respuesta a las proteínas mal plegadas (UPR), presenta un papel neuroprotector en una de las regiones del hipocampo más vulnerables a la isquemia, el área CA1. Se sugiere que CA1 presenta una capacidad limitada para desencadenar la UPR y el Sal potencia esta capacidad, lo que da lugar a una disminución de la mortalidad neuronal retrasada. También se sugiere que las propiedades inflamatorias en respuesta a la isquemia en la unidad neurovascular (NVU) dependen de la estructura, en particular en el tiempo de respuesta inflamatoria en las diferentes regiones cerebrales. Estas diferencias se ponen más claramente de manifiesto tras el tratamiento con Sal. Además, el estudio demuestra diferencias en los diferentes tipos celulares de la NVU. Las células endoteliales presentan una alta respuesta al tratamiento con Sal mientras que los astrocitos apenas responden. El tratamiento con Sal muestra la existencia de respuestas locales en la NVU. En este capítulo se pone de manifiesto la importancia de los moduladores de UPR en la respuesta inflamatoria. La efectividad del Sal administrado después de la isquemia

sugiere que los moduladores de la UPR pueden representar terapias efectivas contra el ACV que aún no han sido exploradas.

El tercer capítulo analiza el efecto combinado de Sal y un inhibidor muy selectivo de COX-2, robenacoxib (Rob), especialmente en CA1. A pesar de sus efectos anti-inflamatorios, Rob adelanta la pérdida neuronal en vez de aumentar la neuroprotección. Sin embargo, el efecto del tratamiento combinado con Sal y Rob impide la pérdida neuronal temprana inducida por el tratamiento con Rob. Además, la activación glial está enormemente aumentada por el tratamiento con Rob y contrarrestada por los tratamientos de Sal y de Sal y Rob. La acción sobre la microglia causada por el tratamiento combinado de un agente potenciador de la UPR, seguida por un agente anti-inflamatorio sugiere que una combinación apropiada de diferentes agentes neuroprotectores puede potenciar el efecto neuroprotector contra el ACV.

ABBREVIATIONS

Abbreviations

CVA: Cerebrovascular accident

CA: Cornu Ammonis

BBB: Blood brain barrier

NVU: Neurovascular unit

MPP: Matrix metalloproteinase

ICAM-1: Intercellular adhesion molecule 1

VCAM-1: Vascular adhesion molecule

TNF-α: Tumour necrosis factor

INOS: Inducible nitric oxidase synthase

ROS: Reactive oxygen species

NOS: Reactive nitrogen species

ER: Endoplasmic reticulum

UPR: Unfolded protein response

SOD: Superoxide dismutase

CNS: Central nervous system

OGD: Oxygen and glucose deprivation

qPCR: Quantitative qPCR

I/R: Ischemia/reperfusion

VO: Vessel occlusion

TJ: Tight junction

CAM: Cell adhesion molecule

IL: Interleukin

ISR: Integrated stress response

PG: Prostaglandin

COX: Cyclooxygenase

HIF-1: Inducible hypoxia factor 1

GFAP: Glial fibrillary acidic protein

IF: Intermediate filament

Cx: Cerebral Cortex

ANOVA: Analysis of variance

SEM: Standard error of the mean

PERK: Protein kinase RNA-like endoplasmic reticulum kinase

IRE-1: Inositol requiring enzyme 1

ATF-6: Activation transcription factor 6

CHOP: C/EBP homologous protein

ERAD: Endoplasmic reticulum associated degradation pathway

PDI: Protein disulfide isomerase

JAMs: junctional adhesion molecules

ZO: Zonula occludens

LFA-1: Lymphocyte function-associated antigen 1

VLA-4: Very late antigen factor 4

eIF2α: Eukaryotic initiation translation factor α subunit

TX: Tromboxane

NEMO: NF-κB essential modulator

PGH2: Unstable endoperoxide prostaglandin

IKK: IK kinase

IK: Inhibitor kβ

TGF-β: Tumour grow factor β

BCL-2: Endonuclease G and B-cell lymphoma 2

TNFR: Tumor necrosis factor receptor

AIF: Apoptosis inducible factor

BNIF3: Adenovirus E1B 19 kDa-interacting protein

ECM: Endothelial extracellular matrix

NF-kB: Nuclear factor kB

tPA: Tissue plasminogen activator

Sal: Salubrinal

Rob: Robenacoxib

Salrob: Salubrinal + robenacoxib

AD: Adherents junction

APO: Apochromatic

RT: Room temperature

INTRODUCTION

Stroke

Cerebrovascular accident (CVA), or stroke, has been defined by the World Health Organization (WHO) as "the rapid developing clinical signs of focal (at times, global) disturbances of cerebral function, lasting more than 24 hours or leading to death with no apparent cause other than that of vascular origin". Stroke is one of the leading causes of death in the developed world (WHO 2011), the main cause of permanent disability and the second leading cause of dementia (Olesen *et al.,* 2012). In Spain, CVA is the third leading cause of death (Table 1), only surpassed by cancer and pathologies of the vascular system, specifically heart diseases. Progressive ageing in the population plays a crucial role in the prevalence of CVA (INE 2017), which can result in hemiplegia, facial paralysis, aphasia, and other temporal or permanent disabilities that can affect functions such as walking, talking, speech, balance, co-ordination, vision, spatial awareness, swallowing, bladder control and bowel control. In Spain, social and sanitary costs of this pathology have been estimated to be 6% of the total sanitary costs (Spanish Neurology Society, 2015). In Spain, the average cost in 2000 for the treatment of a stroke patient was estimated to be about €5,000; 54% of the cost corresponded with the acute phase following the stroke, and the remaining 46% correspond to the first year after the stroke (Morales Ortiz *et al.,* 2010). More recent reports estimate costs at about €9,000 per patient and can reach up to €12,500 depending on the nature of the disability (Creutzfeldt and Holloway, 2012).

Table 1. Total mortality in Spain in 2014. Last data of Instituto Nacional de Estadística (INE) (2017)

Range*	Cause of death	Death number	Death percentag	Mortality rate
	All causes	395.830	100%	852.1
1	Cancer	106.269	26.9%	228.8
2	Hearth attack	79.707	20.2%	171.6
3	Cerebrovascular diseases	27.579	7%	59.4
4	Chronic diseases of the lower respiratory tract	15.546	3.9%	33.5
5	Alzheimer disease	14.022	3.5%	30.2
6	Unintentional accidents	10.313	2.6%	22.2
7	Diabetes mellitus	9.625	2.4%	20.7
8	Pneumonia and influenza	8825	2.2%	19
9	Nephritis, nephrosis and nephrotic syndrome	6556	1.7%	14.1
10	Hypertensive disease	4533	1.1%	9.8
	Rest of causes	98563	28.6%	242.8

*Range based on the number of death.

Risk factors

Risk factors for stroke are closely related to lifestyle. Being overweight and having a daily smoking habit increases the risk of stroke. Some pathologies, such as high blood pressure, diabetes mellitus, atrial fibrillation and high blood cholesterol, also contribute to an enhanced risk of stroke. Age is the most important risk factor of stroke (Ay *et al.,* 2005; Baltan *et al.,* 2008; Barnett, 2002; Broderick, 2004; Schaller, 2007; Seshadri *et al.,* 2006); the incidence of stroke starts to be relevant from the age of 60 and it increases almost exponentially from the age of 65 (Table 2) (INE 2017). This makes stroke one of the most important causes of death in the elderly population (Davis *et al.,* 1995; Suzuki *et al.,* 2003; Taoufik and Probert, 2008).

Table 2. Absolute deaths and death rate in Spain in 2014 caused by cerebrovascular diseases

	Range of age										
Sex	**< 1**	**1-4**	**5-14**	**15-24**	**25-34**	**35-44**	**45-54**	**55-64**	**65-74**	**75-84**	**> 85**
Men and women*	0	2	8	16	41	196	565	1101	2658	8725	14270
Men*	0	2	2	9	26	117	373	752	1589	4155	4548
Women*	0	0	6	7	15	76	192	349	1069	4570	9722
Rate of death											
Men and women	0	0.1	0.2	0.4	0.7	2.5	8	20.3	63	289.6	1118.3
Men	0	0.2	0.1	0.4	0.9	2.9	10.5	28.3	80.1	329.7	1089.9
Women	0	0.0	0.3	0.3	0.5	2	5.5	12.6	47.8	260.7	1132.1

* Number of deaths

Etiologic classification of human stroke

Approximately 85% of strokes are caused by a blockage of a blood vessel (ischaemic stroke). The remaining 15% of strokes are caused by a leaking blood vessel in the brain (haemorrhagic stroke) (Figure 1). Both cases result in the deprivation of blood flow in a brain area, and the size of the blood vessel that has been impaired is a crucial factor in how extensive the damage is to the brain (Isabel *et al.,* 2016).

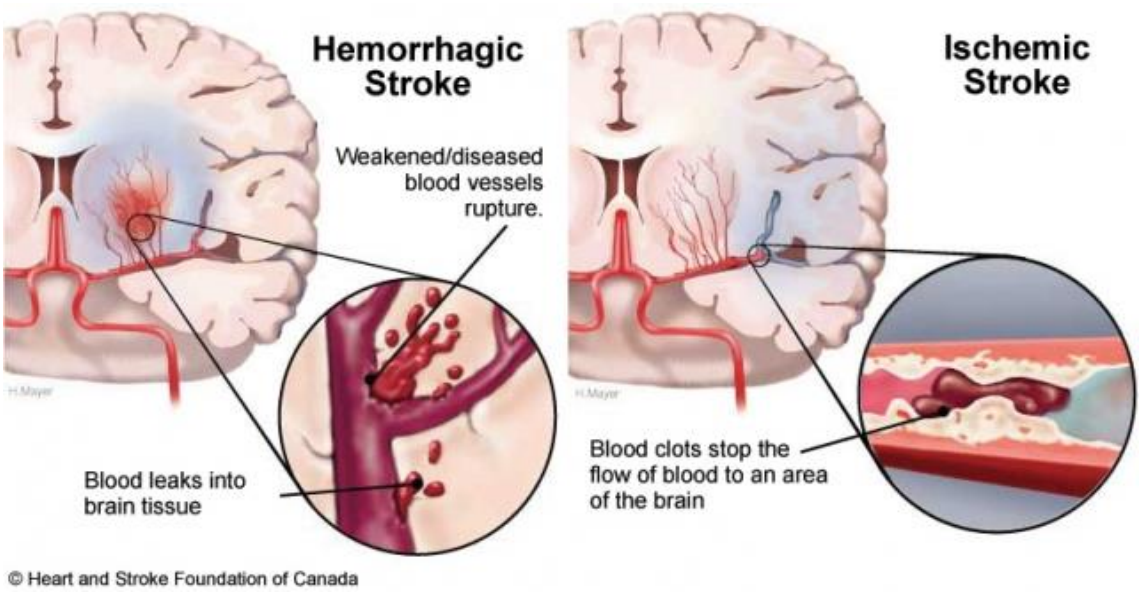

Figure 1. Types of stroke. Figure shows how the haemorrhagic and ischemic stroke are produced. *Taken from the Heart and Stroke Foundation of Canad*a

Ischemic insults

The Spanish Neurology Society clinic guide for the diagnosis and treatment of stroke (Arboix *et al.,* 2002) the divides ischaemic stroke into the following categories:

- *Atherothrombotic cerebral infarction* (15-20%): Characterised by a large infarction area in the cortical or subcortical regions. This type of infarction affects vessels in the carotid or vertebrobasilar systems Atherothrombotic cerebral is characterised in the following ways:
    - Aterosclerosis with stenosis: The reduction of the diameter of the vessels is equal to or greater than 50% by the stenosis.
    - Aterosclerosis without stenosis: Lesser stenosis and the presence of atherosclerotic clots. It has to present at least two of the following risk factors: high blood pressure, diabetes mellitus or high cholesterol levels.

- *Cardioembolitic infarction* (15-20%): Characterised by a large infarction area, usually in the cerebral cortex, and the presence of cardiopathologies such as the intracardiac presence of a tumour or a clot, atrial fibrillation, myocardial infarction or endocarditis.

- *Small vessel occlusive disease (lacunar stroke)* (25-30%): Characterised by a small infarction area (< 15 mm of diameter) in the cerebral perforating artery that usually causes a lacunar syndrome in patients with several stroke risks.

- *Cerebral infarction of unusual cause* (3-5%): Types of stroke of different sizes that affect the carotid or vertebrobasilar systems and for which an aterotrombotic, a carioembolic or a lacunar origin have been discarded.

- *Cerebral infarction of undetermined origin* (30%): Strokes included in this category present with a wide range of sizes and are of an origin that does not fit in any of the previous categories.

Haemorrhagic stroke:

Haemorrhagic stroke was defined in 1998 (Roda et al., 1998) and takes into account the localisation of the broken vessel. Haemorrhagic strokes localised in the brain parenchyma are named intracerebral haemorrhagic strokes, and haemorrhagic strokes localised in the large arteries that irrigate the brain are named subarachnoid haemorrhagic strokes (Roda et al., 1992).

Current therapies.

Currently, the sole effective drug therapy against stroke is the tissue plasminogen activator (tPA), which dissolves the clot. However, treatment can only be administrated following a few types of ischaemic stroke. This therapy, as well as the physical removal of the clot, are uniquely effective in the first hours after the onset of the stroke; treatment must usually be administered within the first four hours after the insult, and can sometimes can be expanded for up to six hours after the insult (Saver et al., 2009). After this time, a detrimental interaction has been reported between tPA and the N-methyl-D-aspartate receptors (Broderick, 1997).

Given the high incidence of stroke, its social and medical costs and the lack of effective therapies, the search for targets that will lead to the development of effective therapies against CVA is urgent.

Experimental models of stroke

Experimental models of stroke can be performed in large animals (for example, dog, cats and non-human primates) and small animals (for example, rodents). The structures and functions of the brain of large animals are closer to the human when compared to those of small animals, making easier to monitor and track the evolution of the damage using imaging techniques. However, the use of large animals presents several limitations, including economical costs, welfare concerns, and higher mortality and variability during the surgery procedures due to the procedures being more invasive compared to those in small animals. Altogether, these limitations make the use large animals in research more difficult.

In comparison, the development of genetically homogeneous strains of animals and the lower costs for production, genetic modifications and delivery of treatment, makes easier to use small animals. This use of small animals for research has allowed for the development of standardised models for ischaemic injury with high reproducibility and low economic costs. Behavioural tests in models of ischaemic stroke also have a better level of standardisation for small animals. Main limitations in small animal models are the number of samples required (especially in the case of blood volume or repetitive sampling) and the fact that their lissencephalic brain makes anatomical and functional aspects more distant from those of the human brain (Traystman, 2003)

Models of global cerebral ischemia

Global cerebral ischaemia models are usually classified as complete and incomplete cerebral ischaemia (Table 3). Complete ischaemia implies that brain blood flow has ceased completely. Incomplete ischaemia occurs when brain blood flow is severely reduced and insufficient to maintain cerebral metabolism and function. Table 5 1 illustrates different types of complete and incomplete cerebral ischaemia (Lo, 2008).

Table 3. Different models of global cerebral ischemia

Complete cerebral ischemia	Incomplete cerebral ischemia
Cardiac arrest: Ventricular fibrillation is used to simulate cardiac arrest.	**Haemorrhage:** Intracranial infusion of external blood or surgical brain vessel disruption.
Aortic occlusion: Clamping of aortic arteria.	**Intracranial hypertension:** Haemorrage as a consequence of increases in the intracranial pressure.
Neck Cuff: Carotid arteries are blocked by using a neck cuff that can swell. This model is only used in large animals. Moreover, the paravertebral arteries must be occluded separately due to vertebrae encapsulation. It presents many limiting factors such as vagal compression and venous congestions.	**2 Vessel occlusion (2VO):** Bilateral common carotid artery occlusion by clamping. It requires hypotension (under 50 mmHg) either by pharmacologic agents or by bleeding or partial exsanguination, to prevent that blood flow from the paravertebral arteries reach the brain.
Cephalic Artery Occlusion: Surgical blocking of a cephalic artery.	**4 Vessel occlusion (4VO):** It combines the blocking of carotid arteries and the electro-cauterization of paravertebral arteries. The surgical procedure has a low successful percentage (around 50-25%).
Decapitation: The head can be connect to an extracorporeal circulation system to simulate short reperfusions.	

Ageing and Stroke

Ageing is related to a progressive loss in the functionality of the locomotor, sensory and cognitive systems(Clayton *et al.,* 2002; Grady and Craik, 2000; Mesches *et al.,* 2004; Navarro *et al.,* 2005), which result in morphological, behavioural and neurochemical changes (He *et al.,* 2006; Sutherland *et al.,* 1996b). Unfortunately, studies that resulted in neuroprotection in animal models of stroke have not been successful in clinical assays (Fisher and Bastan, 2008; Gorelick, 2002; Petcu *et al.,* 2008). A possible explanation of the discrepancies between research results in animals and clinical assays could be the different response to an ischaemic insult that occurs as a consequence of age. Most studies in animal models are performed in young animals, which are not accurate models since. This is because the transformation of ischaemic tissue to infarcted tissue increases with age (Ay *et al.,* 2005) and, therefore, do not correctly represent the ischaemic effects on the neural tissues in the elderly individuals (Brown *et al.,* 2003; Markus *et al.,* 2005; Popa-Wagner *et al.,* 1998; Wang *et al.,* 1995).

Thus, age should be taken into account in experimental models of research on this pathology (Baltan *et al.,* 2008).

Ischaemic cascade and oedema

After an ischaemic insult in the brain, two different areas of damage can be recognised on the basis of blood flow deprivation (Figure 2). The area where the blood flow is less than 12 ml/100g/min represents the ischaemic core where the complete or partially lack of energy results in the rapid cell death by necrosis. The surrounding area is characterised by partial blood flow that is estimated to be less than 30 ml/100g/min from close arteries and is called penumbra. The energetic metabolism in the penumbra presents some activity that can be restored when the normal perfusion of blood (reperfusion) is recovered (Dirnagl *et al.,* 1999; Hossmann, 2008). The lack of recovery of blood flow over time causes the penumbra area to become part of the ischaemic core, preventing the tissue from having the possibility of being rescued. The impairment of this region is characterised by hypoxia and reoxygenation stress, brain blood barrier (BBB) disruption, oedema and inflammation. The crosstalk between neurons, endothelial cells and glial cells (in particular astroglia and microglia) is crucial in the recovery of penumbra (Østergaard *et al.,* 2013). This area is considered to be the most important therapeutic target in post-ischaemic treatments that are aimed at preventing neuronal death after an ischaemic stroke. Penumbra is estimated to remain viable for 16 to 48 hours after stroke, allowing possible clinical actions (Candelario-Jalil, 2009; Dirnagl *et al.,* 1999; Durukan and Tatlisumak, 2007; Kadhim *et al.,* 2008; Kriz, 2006; Lakhan *et al.,* 2009; Meisel *et al.,* 2005).

Neuronal tissue requires a high level of oxygen and glucose, and the blood flow deprivation causes a rapid loss of energy, represented by ATP depletion. This leads to the depolarisation of plasmatic membranes, the accumulation of intracellular Ca^{2+} and the lipolysis caused by lipid peroxidation. The Ca^{2+} influx induced by ischaemia elicits the release of large amounts of the excitotoxic neurotransmitter, glutamate, another characteristic of ischaemia/reperfusion (Figure 3) (Kuroda and Siesjo, 1997).

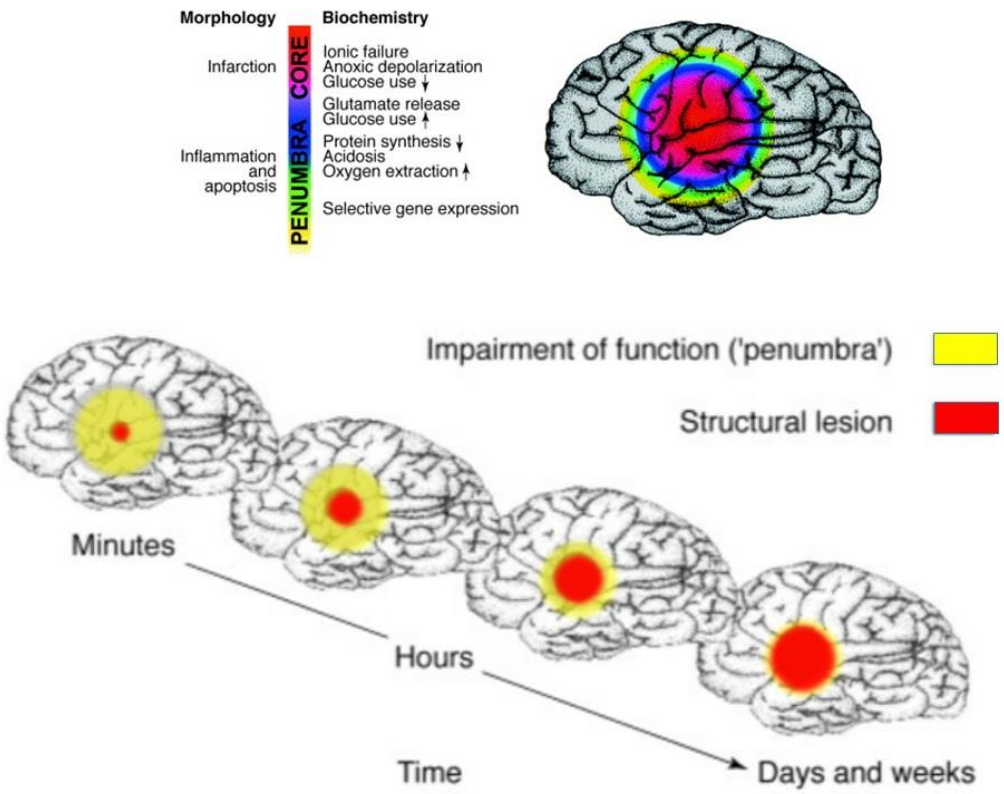

Figure 2. Ischemic core and penumbra regions. ***Modified from Dirnagl et al., 1999***

Furthermore, Ca^{2+} increases in the cytosol promotes the influx of water into the neurons. The sum of these events leads to the excitotoxic oedema, which causes rapid cell death by necrosis (Liang *et al.,* 2007). A large amount of compounds that are derived from the lipid breakdown remain during reperfusion. Those compounds react with oxygen, yielding an overproduction of reactive oxygen species (ROS) (J.Marc Simard *et al.,* 2007). In addition, arachidonic acid and products of lipid peroxidation inhibit the reuptake of glutamate, which causes an increase in excitotoxicity (Braughler *et al.,* 1985; Chan *et al.,* 1983).

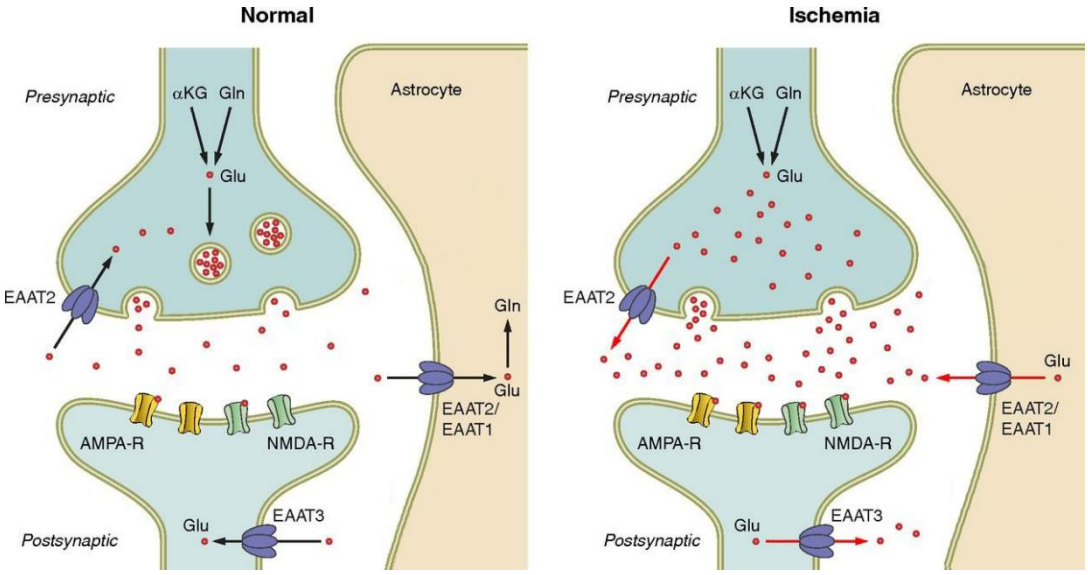

Figure 3. Excitotoxicity process in brain ischemia. ***Modified from Vandenberg and Ryan, 2013***

The release of ROS and reactive nitrogen species (NOS) promotes the production of cytokines and quimioquines, the activation of extracellular enzymes such as matrix metalloproteinases (MMPs) and the activation of microglia. MMPs degrade the extracellular matrix of the endothelium and contribute to the inflammatory response (Jin et al., 2010a). After hours to days of ischaemic stroke, the BBB disruption, oedema cytotoxicity and neuroinflammation may lead to the haemorrhagic transformation of the ischaemic tissue (Wang et al., 2003).

Cytosolic microvacuolation of neurons appears from the first stages of ischaemia and the subsequent reperfusion (Krause et al., 1988). Some brain areas, such as cortical pyramidal layers 3 and 5, hippocampal Cornu Ammonis 1 (CA1) and Purkinje neurons, present high vulnerability to ischaemia (Sato et al., 1990). Protein synthesis is strongly suppressed in these vulnerable neurons during reperfusion (Cooper et al., 1977). CA1 is reported to have the highest vulnerability to global ischaemia (Kirino, 1982; Petito et al., 1987; Zhu et al., 2012). A summary of this processes can be observed in the Figure 4.

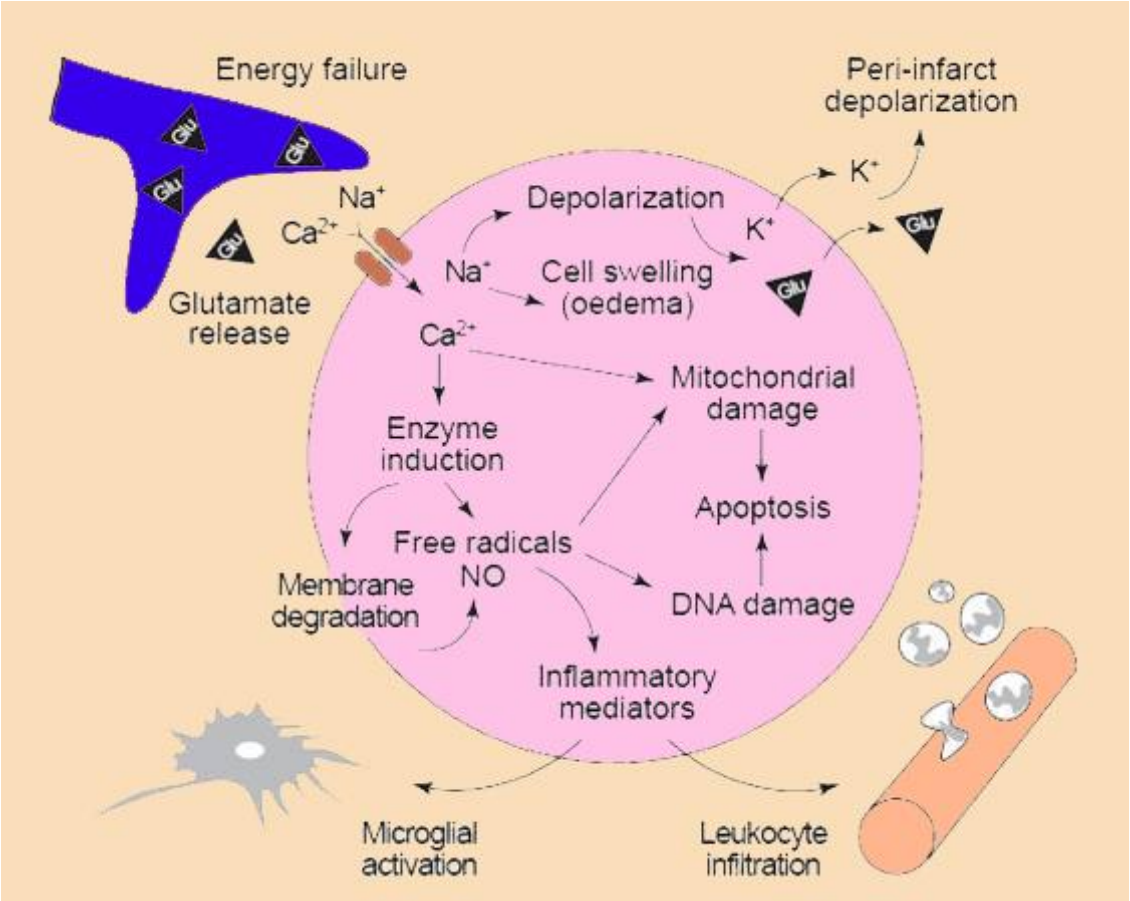

Figure 4 Ischemic cascade. ***Modified from Dirnagl et al., 1999***

Oedema

Brain excitotoxic and vasogenic oedema are the main alterations observed following a CVA. Excitotoxic oedema occurs when there is an intracellular accumulation of water from the extracellular space. It starts in the first minutes after the loss of blood flow but before BBB impairment. This oedema produces astrocyte and neuronal dendrite swelling. Vasogenic oedema occurs after BBB impairment. It drives the diffusion of blood protein into the nearest neuronal parenchyma, followed by the accumulation of water in the extracellular space (Unterberg *et al.,* 2004).

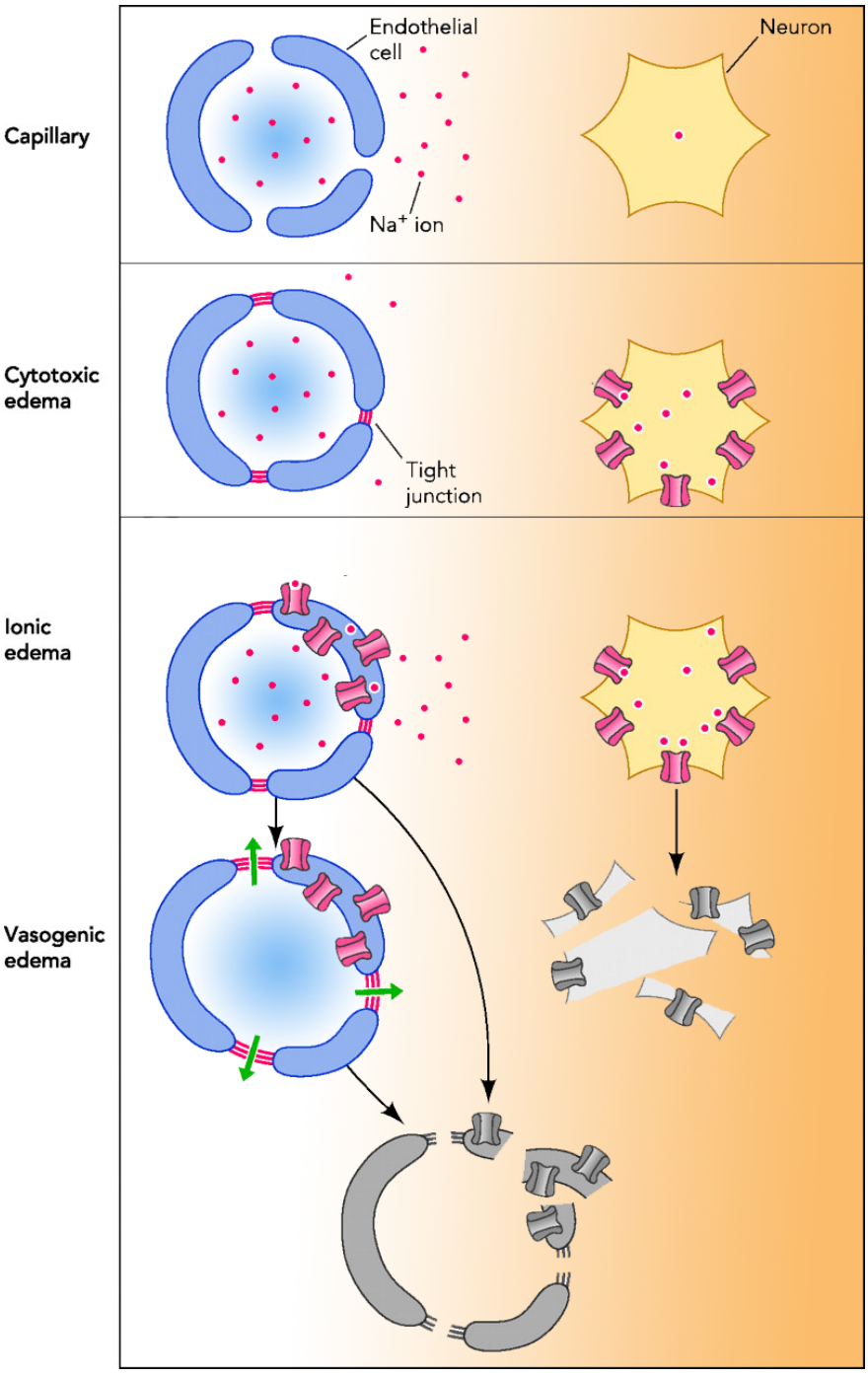

Figure 5: Different oedemas after brain ischemia. ***Modified from Kahle et al., 2009***

Shortly after excitotoxic oedema occurs, oxygen and glucose deprivation modifies the ionic equilibrium in the endothelial membranes, allowing an influx of Na^{2+} and a depletion of ATP depletion in the endothelial cells. This ionic oedema is a new type of oedema that is not currently included in the traditional classification (Figure 5) (Simard *et al.,* 2007). Endothelial cells also require high levels of energy, and ATP depletion impairs the cell function. Furthermore, the part of the vascular tree that is not subjected

to reperfusion suffers an overpressure; the overpressure causes laminar shear stress, which produces an early transitory permeability of the BBB; the impairment in the BBB results in an influx of water (through endothelial cells) into the neural parenchyma; and the influx of water leads to the ionic oedema that is observed 30 minutes after reperfusion. Early reperfusion would probably mitigate the BBB alterations; however, the delayed reperfusion enhances the damage in endothelial cells (Hirt *et al.,* 2009). The later vasogenic oedema occurs when tight junctions (TJs) in endothelial cell are damaged. This increases the BBB permeability to blood proteins, such as albumin, and activates MMPs feeding positiverly the vasogenic oedema and the degradation of the basal lamina (Berezowski *et al.,* 2012).

Reperfusion

The delayed re-establishment of the blood flow in the penumbra area, associated with neuronal apoptosis, increases ROS production and decreases the concentration of antioxidants that appear to be responsible for most of the cellular damage that is observed in ischaemic stroke (Figure 6). In several animal models of stroke, putative irreversible changes have been described that occur during reperfusion and that lead to neural death (Kidwell *et al.,* 2001; Kuroda and Siesjo, 1997). These changes involve increases in the expression of hypoxia inducible factor-1 (HIF-1) and nuclear factor-κb (NF-κB) in endothelial and glial cells, especially in microglia cells. The upregulation of the signalling pathways activated by these transcription factors plays a key role in the disruption of the BBB and in the neuroinflammation (Lochhead *et al.,* 2012) that is responsible for most of the brain damage that occurs during reperfusion (Pan *et al.,* 2007), as detailed below in the BBB disruption and neuroinflammation sections. Activated platelets are also involved in the damage caused by reperfusion because they increase ROS and NOS levels, thus contributing to oxidative stress of the surrounding tissue and an enhanced inflammatory response (Chong *et al.,* 2001; Wong and Crack, 2008; Zeller *et al.,* 2005). In addition, areas with post-ischaemic hyperperfusion contribute to brain oedema and occasionally to brain haemorrhage.

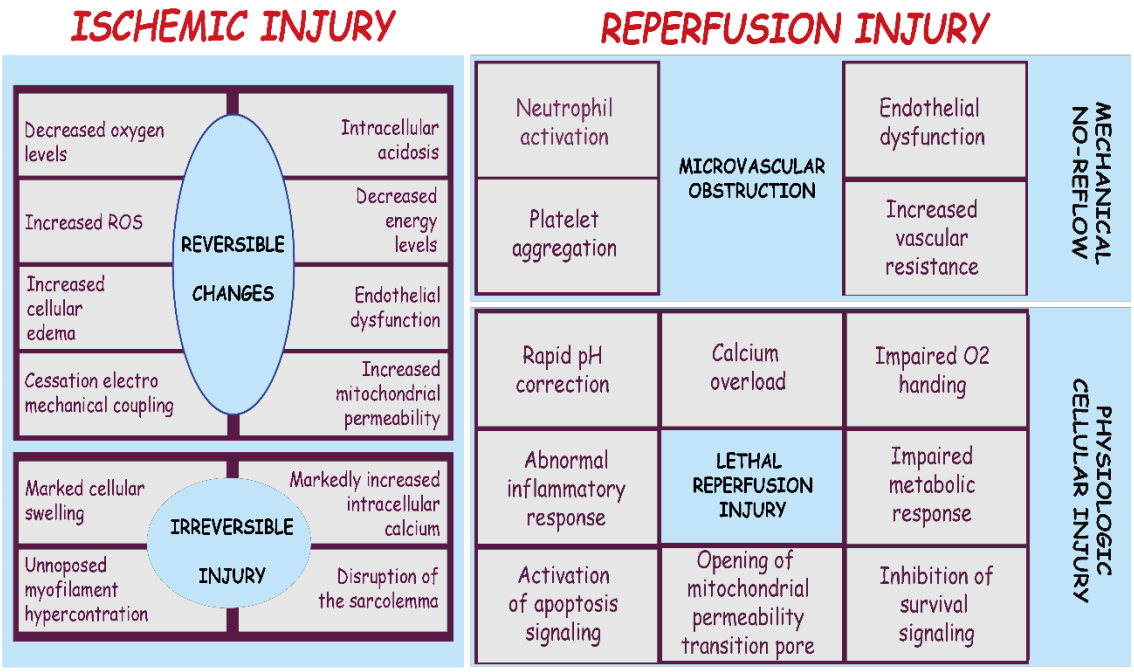

Figure 6: Events after ischemia reperfusion.

Recanalization and reperfusion

Recanalisation is defined as the ''reopening of an occluded artery'', whereas reperfusion means the ''restoration of microcirculatory blood flow downstream of the recanalised artery''. Complete recanalisation does not necessarily result in reperfusion, a state named as ''no-reflow phenomenon'' (Bai and Lyden, 2015a). Human and animal studies show that most cases of recanalisation do not lead to proper reperfusion of brain tissue (Anwar *et al.,* 1988; Christou *et al.,* 2000; Marler *et al.,* 2000; del Zoppo *et al.,* 1991). Mechanisms involved in impaired reperfusion include capillary constriction and vessel luminal narrowing, which results when swollen astrocyte endfeet cause extra-luminal compression and when the intraluminal space becomes filled with entrapped erythrocytes, leukocytes and platelets. These events increase the BBB permeability and activate tissue factors that elicit fibrin deposition, microvascular occlusion, and uninterrupted shrinkage of pericytes despite the recanalisation of an occluded artery (Belayev *et al.,* 2002; Choudhri *et al.,* 1998; Garcia *et al.,* 1994; Liu *et al.,* 2002; Yemisci *et al.,* 2009; del Zoppo *et al.,* 1991). During reperfusion, the damage to the vascular endothelium exposes the subendothelial extracellular matrix to blood components. This triggers the adhesion and aggregation of blood platelets to the brain microvasculature (del Zoppo, 1998), which is assumed to play a major role in the pathogenesis of

reperfusion failure after recanalization (Adams *et al.,* 2008; Elvers *et al.,* 2010; Kleinschnitz *et al.,* 2007).

Mitochondria and reperfusion

Under physiological conditions, mitochondria constantly produce ROS, which are inactivated by superoxide dismutase, glutathione peroxidase and other antioxidants (including glutathione and ascorbic acid). Overproduction of ROS in the mitochondria during reperfusion rapidly exhausts endogenous antioxidant scavenging capacity (Li *et al.,* 2012; Saito *et al.,* 2005). High ROS levels directly oxidise cellular macromolecules (such as proteins, lipids and nucleic acids) and cause mitochondrial swelling, cell injury and death (Figure 7). Indirectly, ROS lead to the exhaustion of superoxide dismutases, which inhibit molecular switches for apoptosis signalling pathways during cerebral ischaemia and reperfusion (Chan, 2001; Schild and Reiser, 2005).

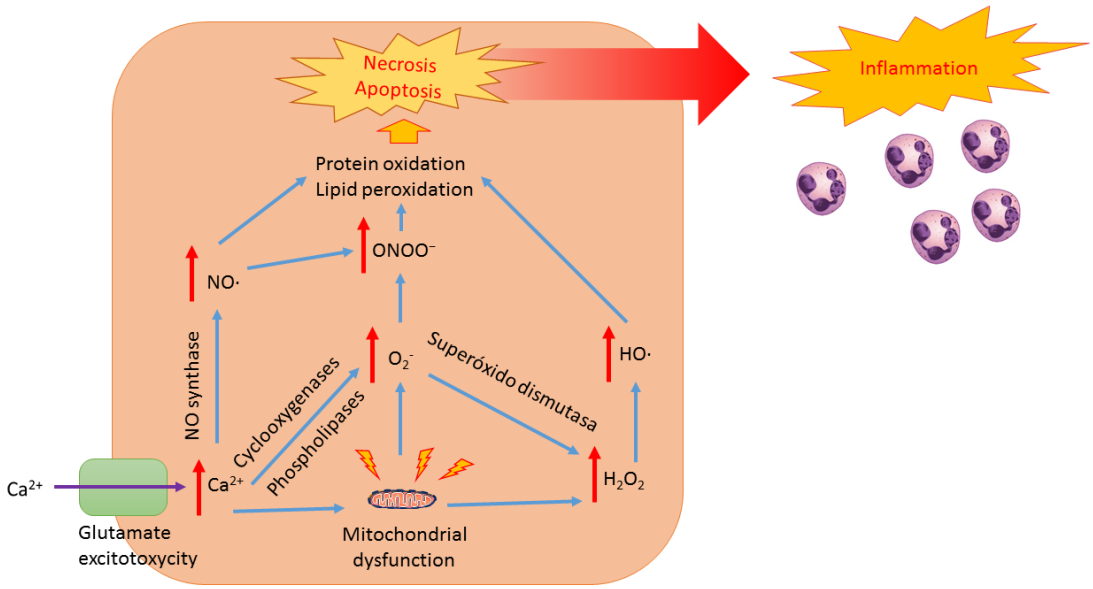

Figure 7: Reperfusion events that leads to mitochondrial dysfunction.

Furthermore, an excess of ROS inactivates NO produced by the endothelial NO synthase, causing the dysfunction of cerebral arteries and arterioles (Didion *et al.,* 2002; Iadecola *et al.,* 1999). Excess ROS production is only one of the initial causes that results in cell injury because mitochondrial dysfunction drives a variety of other subcellular processes. The impaired capacity of mitochondria to regulate calcium homeostasis leads to the mitochondrial membrane permeability transition, which is a Ca^{2+}-dependent increase in

the permeability of the mitochondrial membrane. This results in the loss of the mitochondria transmembrane potential, mitochondrial swelling and rupture of the outer mitochondrial membrane (Jornayvaz and Shulman, 2010; Solenski *et al.,* 2002; Tsujimoto *et al.,* 2006).

Protein synthesis inhibition during reperfusion

Decreases in the incorporation of [^{14}C]-labelled amino acids in the brain after ischaemia and during reperfusion are thought to be the result of the suppression of protein synthesis (Kleihues and Hossmann, 1971). The suppression of protein synthesis also occurs in the unfolded protein response (UPR) that is elicited by the overload of unfolded proteins, a state called endoplasmic reticulum (ER) stress (Walter and Ron, 2011). Post-ischaemic reperfusion promotes several factors that contribute to ER stress, such as ATP depletion, decreased ER-associated degradation, inhibition of protein glycosylation, ER-reducing conditions and Ca^{2+} depletion in the ER (Bai and Lyden, 2015b). UPR and ER stress will be explained in more detail in the section ER stress and UPR.

Apoptosis

The characterisation of the pathways that lead to cell death following CVA is crucial in the search for new therapies against stroke. Traditionally, necrosis has been believed to be the main type of cell death type following CVA; however, in recent years, other cell death processes, mainly apoptosis and necroptosis, have been discovered (MacManus and Buchan, 2000; Mehta *et al.,* 2007; Vieira *et al.,* 2014). Many vulnerable neurons, particularly in the penumbra area, undergo ischaemic-induced damage that can trigger a delayed cell death, mainly by different types of apoptosis. The hallmark of apoptosis is the activation of specific proteases called caspases, although the concept of programmed cell death is under active redefinition and caspase-independent apoptosis has been described (Galluzzi *et al.,* 2015). Intrinsic apoptosis can be elicited by ischaemic-induced mitochondrial damage that releases cytochrome c into the cytosol and activates procaspase-9 which, in turn, activates caspase-3 (Figure 8).

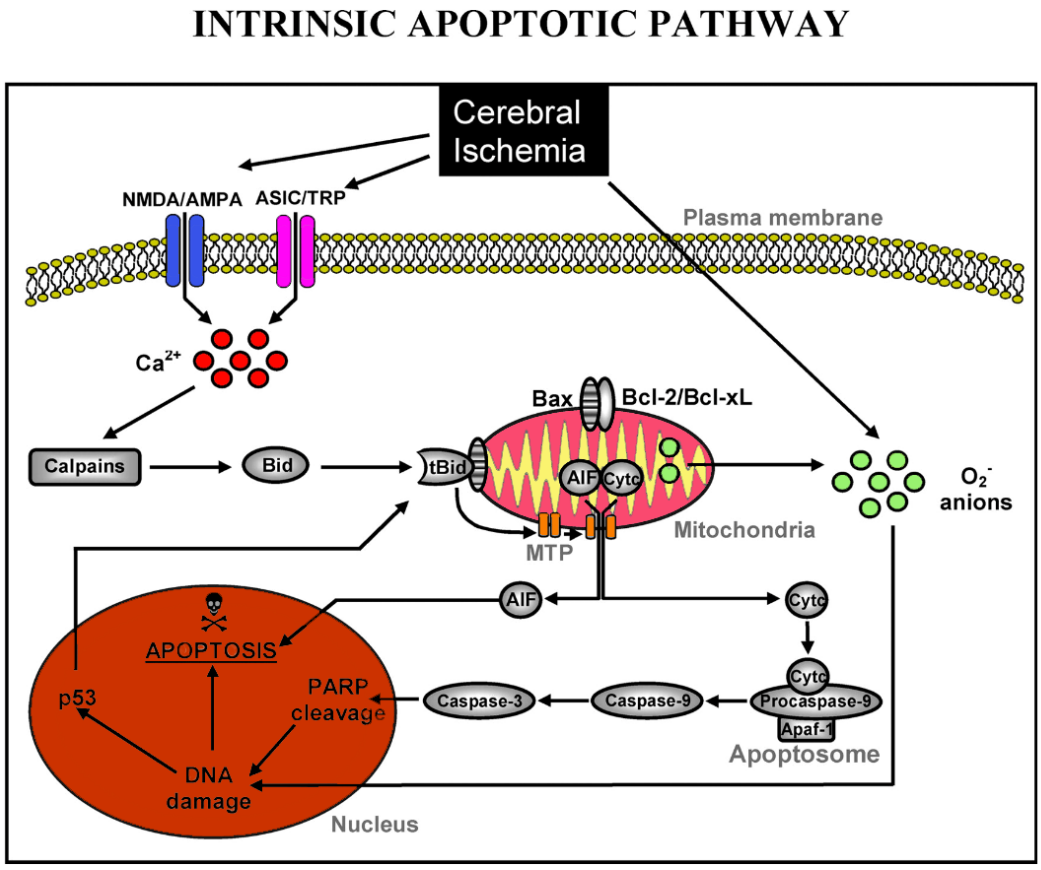

Figure 8: Intrinsic apoptotic pathway after ischemia. ***Modified from Broughton et al., 2009***

Ischaemia also elicits extrinsic apoptosis that is triggered through cell-surface receptors belonging to the tumour necrosis factor receptor (TNFR) family. Once triggered, TNFR activates procaspase-8, which results in activation of caspase-3 (Figure 9). The effector caspase-3 is a key mediator of apoptosis, and its cleavage leads to the proteolysis of multiple proteins and causes the cell to be dismantled. Ischaemia has also been reported to induce caspase-independent apoptosis, during which proapoptotic proteins other than caspases (for example, apoptosis-inducing factor, endonuclease G and B-cell lymphoma-2 and adenovirus E1B 19 kDa-interacting protein (BNIP3) are released via mitochondrial transition pores (Broughton *et al.,* 2009).

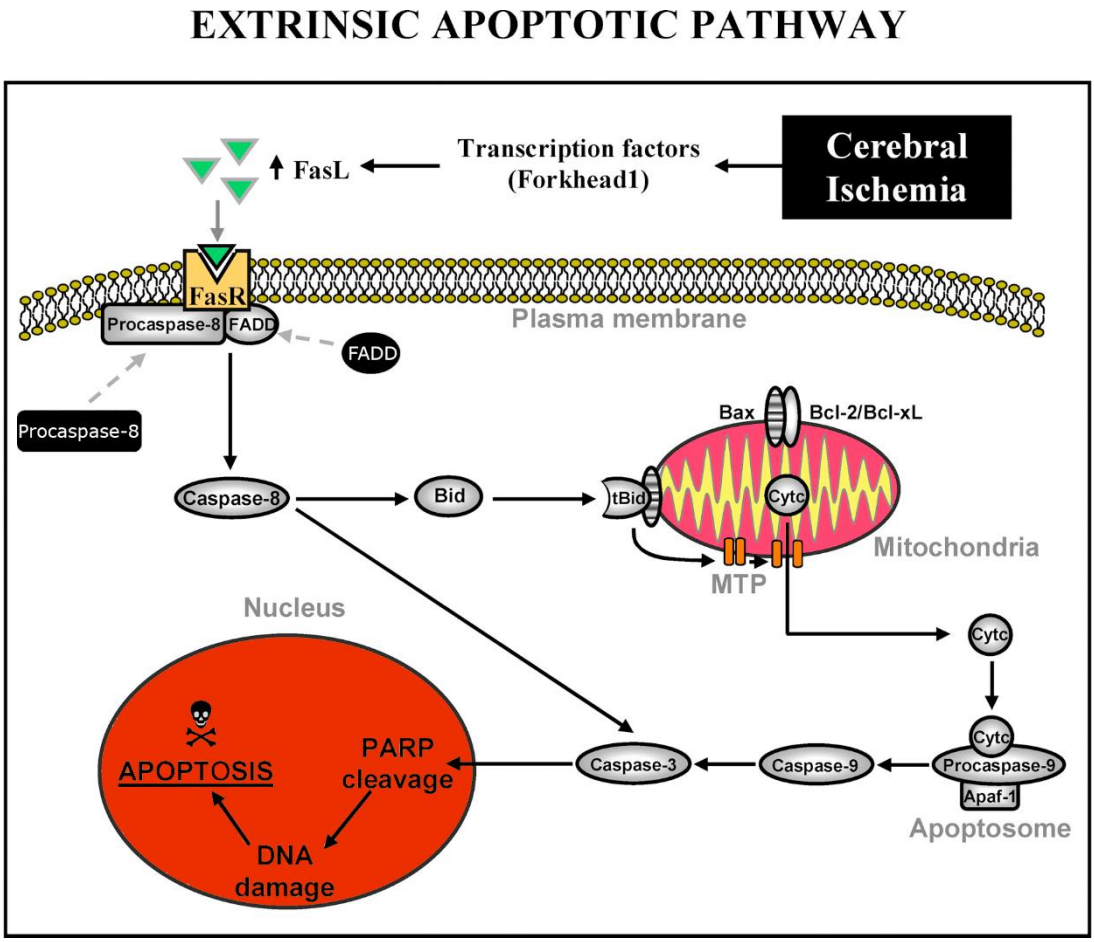

Figure 9: Extrinsic apoptotic pathway after ischemia. ***Modified from Broughton et al., 2009***

Inflammatory response after cerebral ischemia

After stroke, neuronal death in the damaged areas, especially the resultant necrotic-cell debris, elicits an inflammatory process that modifies BBB permeability. This increases the expression of endothelial cell adhesion molecules (CAMs) that are responsible for the recruitment and infiltration of leukocytes into the neural parenchyma (Wang *et al.,* 2007). Inflammation triggers the activation of cells in the immune system, mainly phagocytic cells (Lelekov-Boissard *et al.,* 2009; Lucas *et al.,* 2006; Luheshi *et al.,* 2011; Simi *et al.,* 2007). A part of these cells are derived from microglia that, upon activation, are transformed into phagocytes, which are recruited to areas of cell damage as part of the ischaemic process (Abraham and Lazar, 2000; Bendel *et al.,* 2005). An inflammatory response has been classically been considered to be beneficial in the restoration of damage following the ischaemic accident. In recent years, the post-ischaemic

inflammatory response has been linked to the progression of brain ischaemia-induced damage (Amantea *et al.,* 2009; Chamorro and Hallenbeck, 2006; Rodriguez-Yanez and Castillo, 2008; Barone and Feuerstein, 1999), revealing that the inflammatory response could also be detrimental (Ceulemans *et al.,* 2010).

Inflammation without benefits for the body is often referred to as sterile inflammation (Figure 10). Thus, part of the cell damage that occurs happens rapidly after the ischaemic insult, but the remaining inflammation during the next several days contributes to the damage and delayed cell death (Wang *et al.,* 2007). Thus, the prolonged inflammatory response makes it possible to use new long-term therapeutic strategies that treat the damaged area after the ischaemic accident (Barone and Feuerstein, 1999b).

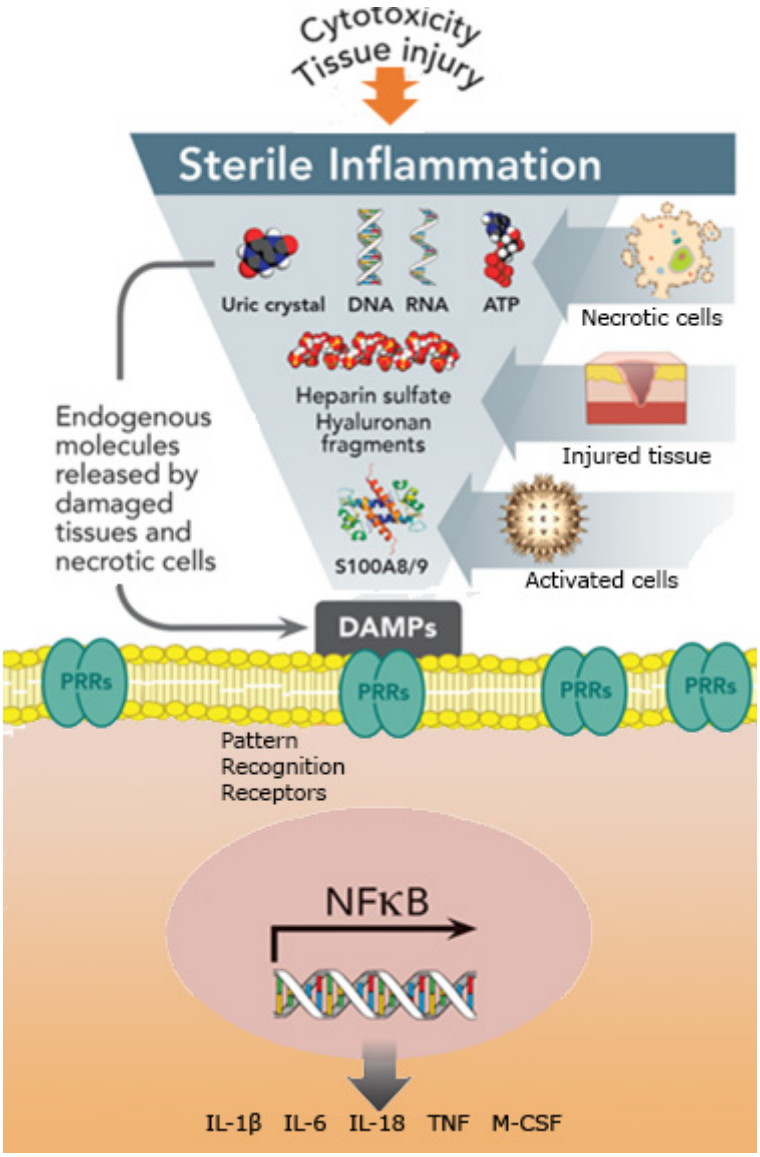

Figure 10 Sterile inflammation. ***Modified from Monsel et al., 2014***

A crucial role in the inflammatory process is the ischaemic-induced increase of ROS that modifies the homeostasis of several types of cells, including endothelial cells, astroglia, microglia and leukocytes (that is, granulocytes, macrophages and lymphocytes). ROS has an important role in the activation of microglia cells and astrocytes, which exacerbates the inflammatory reaction. The inflammatory response involves many mediators, including chemokines and cytokines such as interleukins [IL]-1, IL-6 and IL-10; tumour necrosis factor α (TNF-α); tumour grow factor-β; cell adhesion molecules (for example, selectins, integrins and immunoglobulins); eicosanoids and other proinflammatory mediators that contribute to neural damage (Brouns and De Deyn, 2009; Iadecola and Alexander, 2001).

NFkB activation after cerebral ischemia

Nuclear factor kappa-light-chain-enhancer of activated B cells (NF-κB) is a transcription factor that belongs to the Rel-homology domain (RHD). Its interaction with the inhibitor κB (IκB), which is regulated by IκB kinase (IKK), acts a regulated molecular switch known as the NF-κB pathway. NF-κB subunits (RelA [p65], cRel, RelB, p50 [NF-κB1] and p52 [NF-κB2]) present a nuclear localisation sequence. These subunits also bear homodimerisation and heterodimerisation motifs that bind to κB sites in DNA promoter regions in the genes controlled by NF-κB (Hoffmann and Baltimore, 2006).

A large number of genes are NF-κB dependent. The most prominent gene transcription programs associated with NF-κB are: (1) inflammation (for example, IL-6, inducible oxide nitric synthase, intercellular adhesion factor [ICAM-1], MMP-9 and cyclooxygenase [COX]-2; (2) regulation of apoptosis, typified by the B-cell lymphoma-2 family; and (3) regulation of IκBs (α, β, ε, γ, ζ, p105 and p100). Different isoforms of NF-κB bind to specific IκB types, which are involved in a classic negative feedback loop for which the transcription factor is sequestered in the cytosol by binding their ankyrin repeats to the nuclear localisation sequence. Inhibition of NF-κB by IκB is eliminated by a series of events, beginning with the phosphorylation of specific serines (32 and 36 in IκBα) by the IKK complex. The IKK complex is composed of two serine kinases (IKK1/α and IKK2/β) and a regulatory subunit (IKKγ/NF-κB essential modulator[NEMO]) (Chariot, 2009; Israël, 2010). The phosphorylation of IκB triggers its polyubiquitination by ubiquitin ligases. It

is then led to 26S proteasome for degradation and NF-κB is released so that it can translocate to the nucleus.

Interesting IκB exceptions are p105 and p100, which contain both Rel homology and ankyrin repeat domains. Upon phosphorylation they are cleaved into p50 (NF-κB1) and p52 (NF-κB2), respectively, and join to other subunits (RelA for example) to become transcription factors.

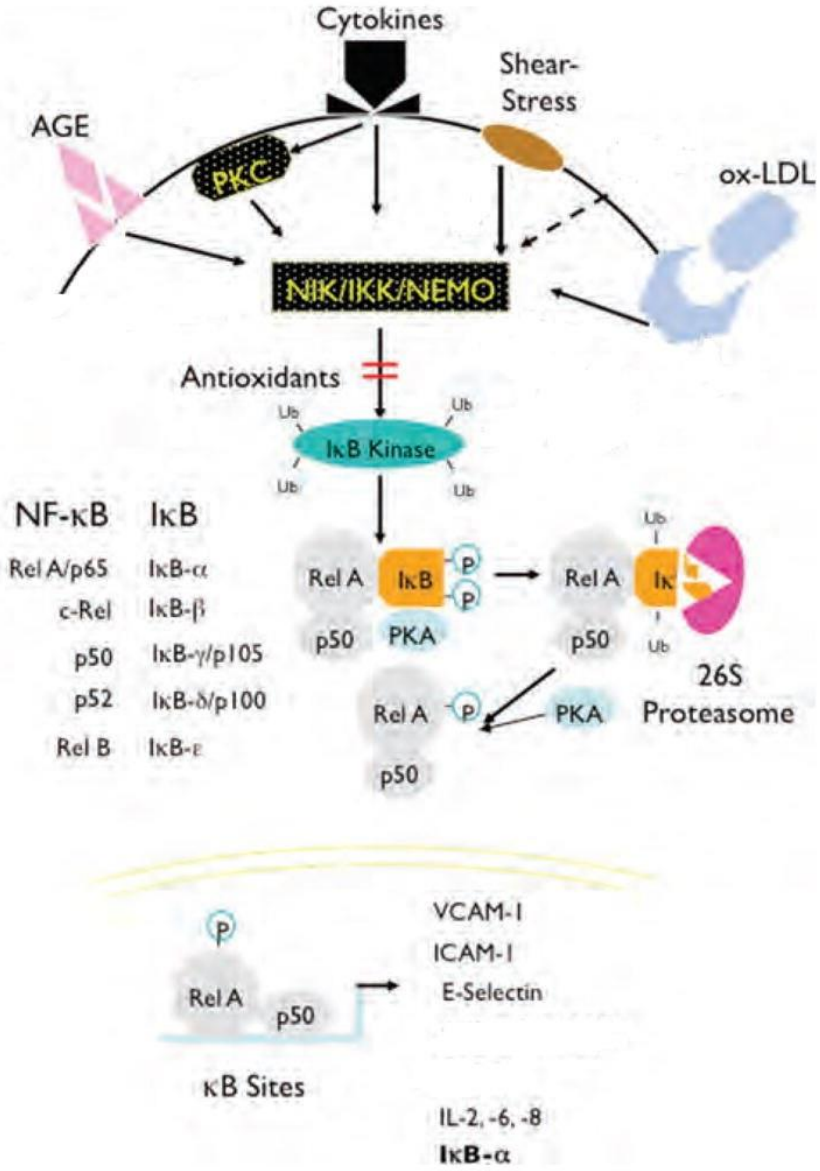

Figure 11 NF-κB regulation. ***Modified from Harari and Liao, 2010***

For example, the canonical NF-κB switch that is associated with inflammation is dependent on NEMO,the NF-κB essential modulator which integrates upstream stimuli, activates IKK2 and drives to the RelA/p50 heterodimer (Hayden and Ghosh, 2004; Viatour *et al.,* 2005). In the resting state, this switch is "off", and upon activation, the

"*de novo*" synthesis of IκBs produce a negative feedback loop. This feedback presents different "on" peaks (two to four) during the next three days after stroke and each successive peak presents progressively less amplitude. IκBs tightly control the strength and duration of the signal, which provides specificity to the different pathways that are modulated by NF-κB. This control has proven to be dependent on the duration of the inducing stimulus rather than its strength. Short-length stimulus results in typical patterns of activation and downregulation over one hour, while prolonged stimulation results in more variable activation (Hoffmann and Baltimore, 2006; Oeckinghaus and Ghosh, 2009). This provides a differential response to different inflammatory triggers in order to prevent an excessive inflammation response and subsequent damage (Shih *et al.,* 2015; Simmons *et al.,* 2016).

The contribution of COX-1 and COX-2 to global ischemia

COXs are highly conserved enzymes (Grosser *et al.,* 2002) with two distinct isoforms — COX-1 and COX-2 — that are encoded by two separate genes. Both COX-1 and COX-2 catalyse the transformation of arachidonic acid, released from cell membranes by phospholipases, into the unstable endoperoxide prostaglandin (PGH2). PGH2, in turn, is metabolised by PG-synthases and isomerases into thromboxane and D, E, F and I series of prostaglandins (PGs) (Smith and Langenbach, 2001). PGs are local mediators and, therefore, only activate neighbouring membrane receptors that trigger different signalling events. COX-2 was characterised by several research groups in the early 1990s as the isoform that is inducible by cytokines, growth factors and tumour promoters and that is responsive to glucocorticoids (Marnett and DuBois, 2002). COX-2 is considered as the main enzyme responsible for the formation of PGs in inflammation, pain and possibly tumour growth (Seibert *et al.,* 1995). COX-1 isoform is constitutively expressed in most tissues (Figure 12) and has been suggested to be the main enzyme responsible for homeostatic functions, and it is considered the sole isoform involved in the protection of the gastroduodenal mucosa (Grosser *et al.,* 2010).

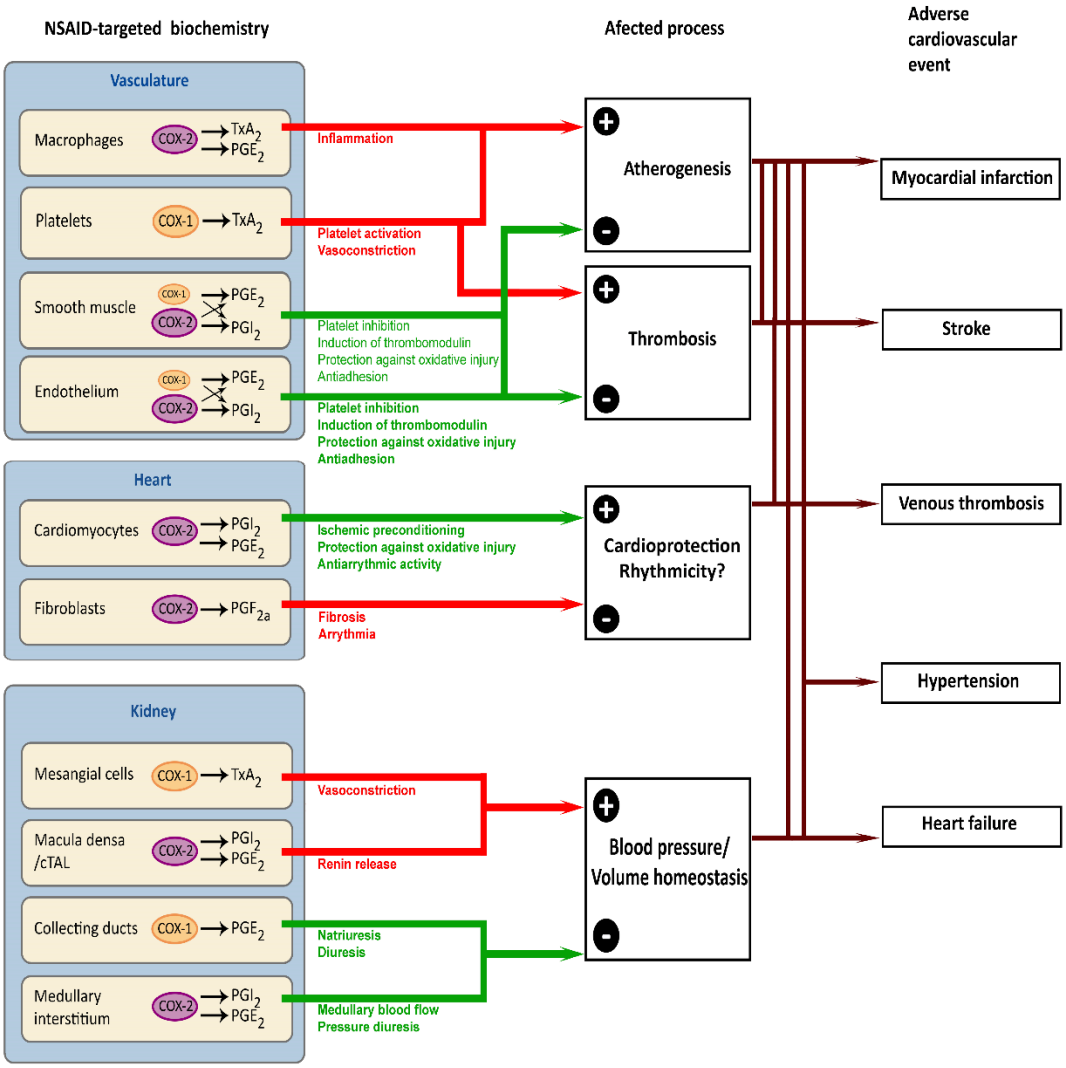

Figure 12: Effects of COX-1 and COX-2 in different organs *Modified from Grosser et al., 2010*

The development of preferential inhibitors for COX-2 in recent years has led to new conclusions about the contribution of both COX-1 and COX-2 isoforms to the inflammatory process. COX-2 is more inducible by inflammatory stimuli (O'Banion *et al.,* 1992), but both isoforms are expressed in circulating inflammatory cells.COX-1 was found to be upregulated in some inflammatory conditions, for example in arthritic synovia (Crofford *et al.,* 1994) and in atherosclerotic plaque (Schönbeck *et al.,* 1999). COX-1 also contributes to the synthesis of PGs in experimental inflammation in humans (McAdam *et al.,* 2000). Additional support to the notion that both COX-1 and COX-2 play important roles in inflammation and pain is derived from mouse genetics (Vardeh *et al.,* 2009; Yu *et al.,* 2005). The relative contributions of each isoform to these processes are still not well understood. Recent studies reveal that COX-2 is expressed not only during

inflammation, pain, and fever but also under physiological conditions (Grosser *et al.,* 2010).

Both isoforms are expressed during development, are co-regulated in some embryonic tissues (Grosser *et al.,* 2002) and are postnatally expressed in uninflamed tissues, including the vasculature, kidney, spinal cord, brain and gastric epithelium. Interestingly, COX-2 has been observed to be induced at the margins of gastric erosions and ulcerations (Hatazawa *et al.,* 2007; Schmassmann *et al.,* 2006), suggesting a role for COX-2 in ulcer healing. PGI2 is a potent inhibitor of platelet function and a vasorelaxant in vitro, and it is thought to confine local prothrombotic and proatherogenic stimuli *in vivo*. Endothelium is a major source of PGI2, and laminar shear stress induces COX-2 expression in endothelial cells, suggesting that COX-2-dependent PGI2 formation in the vasculature can be regulated by hemodynamic control (Cairns, 2007). These observations have led to the conclusion that the suppression of COX-2-induced PGI2 might increase thrombotic events. In addition, mature platelets do not express COX-2 and therefore their activation is COX-1 dependent. Thus, the platelet activation results in thrombotic activity that cannot be inhibited by selective COX-2 inhibitors (Grosser *et al.,* 2010). COX-1 is also crucial in microglia activation that occurs in the neuroinflammatory response (Aïd and Bosetti, 2011; Fiebich *et al.,* 2014). More information is still required to understand the contribution of COX isoforms to the neuroinflammatory response.

Anti-inflammatory agents

The critical role of the inflammatory response in the progression of tissue damage, particularly damage caused by sterile inflammation, has been studied for many years in the search for stroke therapies (Perez-Polo *et al.,* 2013; Szekely and Zandi, 2010; Yilmaz and Granger, 2010). The administration of anti-inflammatories after stroke has been widely tested in both *in vivo* and *in vitro* models of ischaemia (Llorente *et al.,* 2015; De los Reyes and Céspedes 2014; Ugidos *et al.,* 2017). The search for targets and new agents to treat the damage caused by stroke is a very active field, and particularly with regard to the role of COX-1 and COX-2 in the neuroinflammatory process (Grosser *et al.,* 2010).

The first studies of anti-inflammatory agents as putative neuroprotectors used acetylsalicylic acid and traditional non-steroidal anti-inflammatory drugs (NSAIDs) that inhibited both isoforms of COX. NSAIDs present a wide range of percentages for the inhibition of COX-1 and COX-2 (Figure 13) (Patrono, 2016b). Nimesulide and meloxicam are the preferred COX-2 inhibitors, and they also present some ability to inhibit COX-1. COX-1 plays an important role in the maintenance of the gastrointestinal barrier; therefore, the inhibition of COX-1 has a detrimental effect in peripheral area (Patrono, 2016a). For that reason, the prolonged used of NSAIDs can lead to gastrointestinal haemorrhages and even death (Cairns, 2007).

The studies that investigated acetylsalicylic acid revealed that COX-1 inhibition plays an important role in the subacute phases of stroke because the inhibition of COX-1 in platelets prevents their activation. In this regard, the antithrombotic effect of acetylsalicylic acid has led to its common use in clinic as a preventative treatment for ischaemic stroke in patients with previous episodes of stroke (Antithrombotic Trialists' (ATT) Collaboration *et al.,* 2009; Antithrombotic Trialists' Collaboration, 2002). Moreover, the inhibition of this isoform has a critical role in microglia activation, as mentioned above (Aïd and Bosetti, 2011; Fiebich *et al.,* 2014). The results obtained in traditional NSAID studies reveal a neuroprotective effect in most models of stroke.

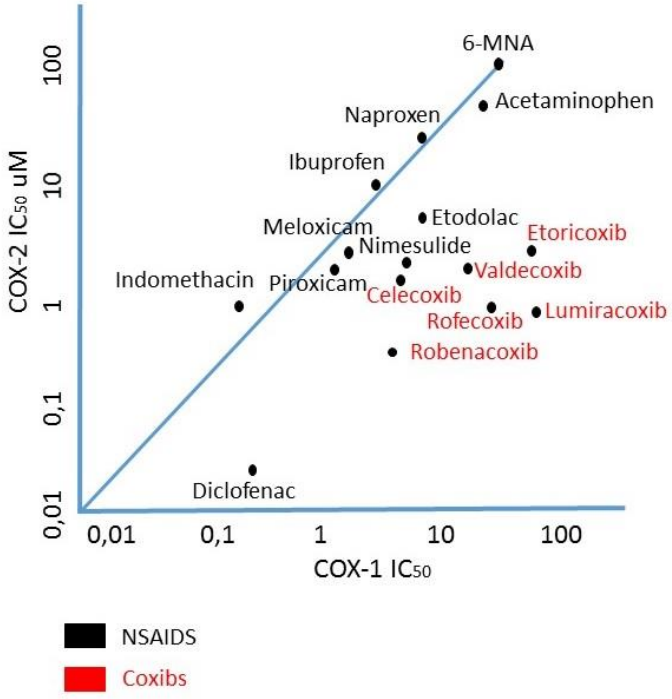

Figure 13: Percentage of inhibition of COXs by NSAIDs and "coxibs". *Modified from Cairns, 2007*

Because of the detrimental peripheral effect of inhibiting COX-1, the pharmaceutical industry put much effort into creating COX-2 inhibitors that were more and more selective, and they have developed a new generation of very selective COX-2 agents called the ''coxib'' family (Figure 13). These agents have provided very good results in the prevention of the general inflammatory response in non-central nervous system (CNS) pathologies (King *et al.,* 2009). However, the use of "coxibs" in clinic has revealed that some of them, such as rofenacoxib and valdecoxib, enhance the risk of the cardiac arrest and stroke, especially as age increases; in fact, rofenacoxib and valdecoxib were withdrawn from the market (Cairns, 2007; Jüni *et al.,* 2004; Patrono, 2016a, 2016b). The increased risk of stroke and cardiac arrest are associated with the COX-1 induced platelet activation and the protective effects of COX-2 on the BBB as a consequence of the constitutive expression of this isoform in the vascular endothelial cells. Therefore, blocking the expression of both isoforms seems to be necessary to prevent the thrombotic effect (FitzGerald *et al.,* 2001; Roumie *et al.,* 2008). Additional effects have also been described for different coxibs. For example, celecoxib presents pro-apoptotic effects in cell culture but (Schonthal, 2007), interestingly, is used as a neuroprotector in haemorrhagic stroke (Chu *et al.,* 2004). Etoricoxib has been described as having a neuroprotective effect in focal ischaemia; it triggers the translocation of the cAMP responsive element binding protein into the nucleus and cjun transcription factors control the expression of pro-survival genes (Maheshwari *et al.,* 2011). The different responses of members of the ''coxib'' family make it necessary to test each one to find out whether it has a neuroprotective effect in stroke.

The debacle in the inhibition of these two isoforms provides a final lesson because each COX isoform has different indispensable functions that do not overlap and cannot functionally replace each other (Fiebich *et al.,* 2014).

Astrocytes as inflammatory markers after cerebral ischemia

Following cerebral ischaemia, activation of astrocytes increases the glial fibrillary acidic protein (GFAP) expression, a typical marker of "reactive gliosis" that is characterised by both functional and morphological changes. GFAP is an intermediate filament protein that is expressed in astrocytes and ependymal cells of the CNS, but not expressed in

oligodendrocytes or neurons (Sofroniew and Vinters, 2010). Reactive astrocytes increase in size and acquire a characteristic star-shaped morphology (Badawi *et al.,* 2012; Che *et al.,* 2001; Pekny and Nilsson, 2005). The phosphorylation of GFAP is increased after the ischaemic process (Gudino-Cabrera and Nieto-Sampedro, 2000; Sullivan *et al.,* 2012). Astrocytes are also capable of secreting inflammatory factors, such as cytokines, chemokines and inducible oxide nitric synthase (Dong and Benveniste, 2001; Lively and Schlichter, 2012). These cells normally perform functions related to the maintenance of neurons, but activated astrocytes can also contribute to ischaemic brain damage. (Lively and Schlichter, 2012; Sullivan *et al.,* 2012; Wang *et al.,* 2007). GFAP could be a possible blood biomarker of cerebral haemorrhage in patients with symptoms of acute stroke because it is rapidly released into the blood after haemorrhagic stroke and in a more gradual way after ischaemic stroke (Wasserman *et al.,* 2008).

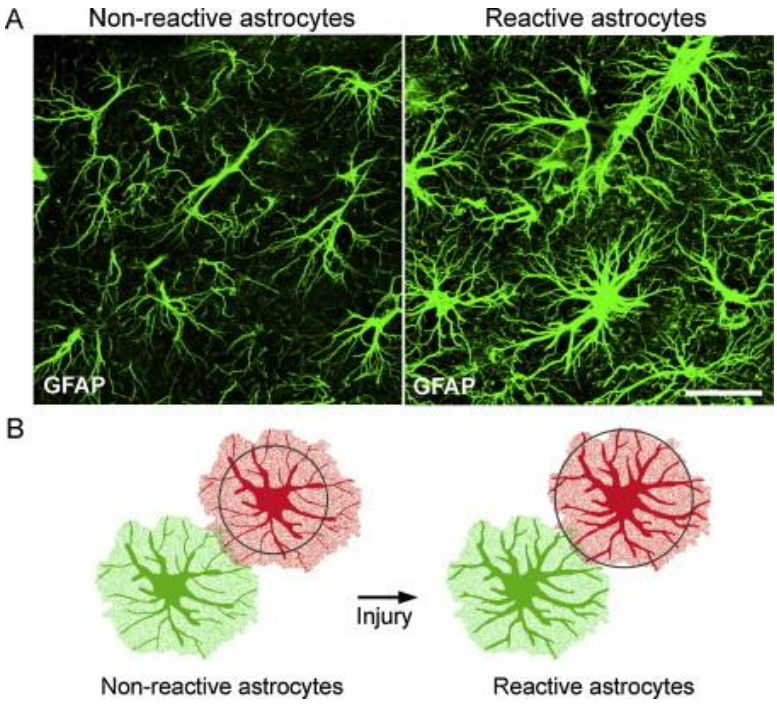

Figure 14 Reactivity of astrocytes following brain injury. ***Modified from Pekny and Pekna 2014***

Neurovascular unit (NVU)

Blood brain barrier (BBB)

In mammals, including humans, endothelial cells that line capillary walls form the most external layer of the BBB that separates the blood and the neural parenchyma (Figure 15). Epithelial cells of the choroid plexus form a blood–cerebrospinal fluid barrier. Vascular arachnoid epithelium, which underlies the dura mater, completes the seal between the extracellular fluids of the CNS and the rest of the body (Abbott *et al.,* 2006).

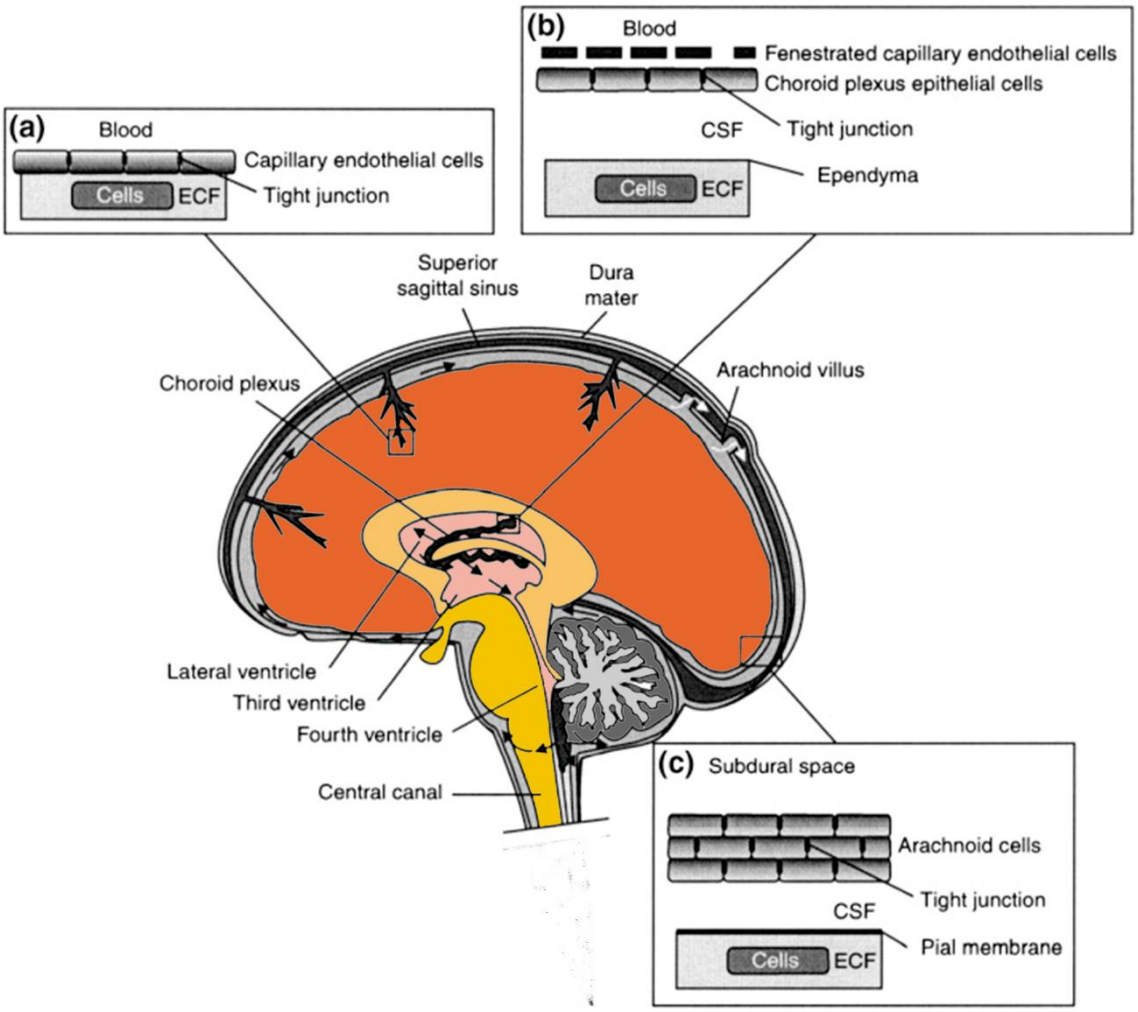

Figure 15 Barriers in brain. ***Modified from Abbott et al., 2006***

The BBB represent the largest interface between blood and brain. It has many different functions (Abbott *et al.,* 2010), for example:

- *Ion regulation*: The BBB contributes to ion homeostasis in combination with specific ion channels and transporters, keeping the ionic composition optimal for neural signalling.
- *Neurotransmitters:* The BBB maintains separate pools of some molecules that act as either neurotransmitters or as metabolites in different molecular pathways. For example, blood plasma contains high concentrations of the amino acid glutamate, which is a metabolite in the Krebs cycle, but glutamate is also an excitatory neurotransmitter in some neurons. The BBB prevents the movement of some of these blood molecules because they can result in synaptic signalling in the CNS.
- *Macromolecules:* The protein content in cerebrospinal fluid is much lower than blood plasma, and the BBB preserves the difference in protein concentrations. In addition, the leakage of some serum protein macromolecules (for example, plasminogen and thrombin) into the neural parenchyma as a consequence of BBB impairment can result in severe pathological consequences.
- *Neurotoxins*: Endogenous metabolites or proteins, as well as xenobiotics ingested in the diet or otherwise acquired from the environment, can act as toxins in the neural parenchyma. The BBB prevents these molecules from reaching the neural tissue.
- *Brain nutrition:* The BBB provides a low, passive permeability to many essential water-soluble nutrients and metabolites that are required by nervous tissue. The presence of specific transport systems that are expressed in the BBB ensures that there is an adequate supply of these substances.
- *Immunoprivileged state*: The BBB allows an immune surveillance that is specific to the neural parenchyma (microglia) with minimal inflammation and cell damage, and it prevents the action of the blood cell immune response.

Tight junctions

TJs are dynamic structures that consist of transmembrane and membrane-associated cytoplasmic proteins assembled in a multimolecular complex. TJs are composed of integral membrane proteins (occludin, claudins and junctional adhesion molecules) that

are involved in intercellular interactions with cytoplasmic scaffolding proteins such as zonula occludens (ZO). TJs are also composed of actin cytoskeleton and associated proteins such as protein kinases, small GTPases and heterotrimeric G-proteins (Figure 16). Extremely tight TJs (for example, ZO) are a key feature in the BBB function. They reduce the permeation of polar solutes through paracellular diffusional pathways between vascular endothelial cells into the brain extracellular fluid (Wolburg *et al.,* 2009). Adherens junctions maintain endothelial cells, which gives the tissue structural support, and they are critical for the formation of TJs. The disruption of TJs leads to impairment of the BBB (Wolburg and Lippold, 2002).

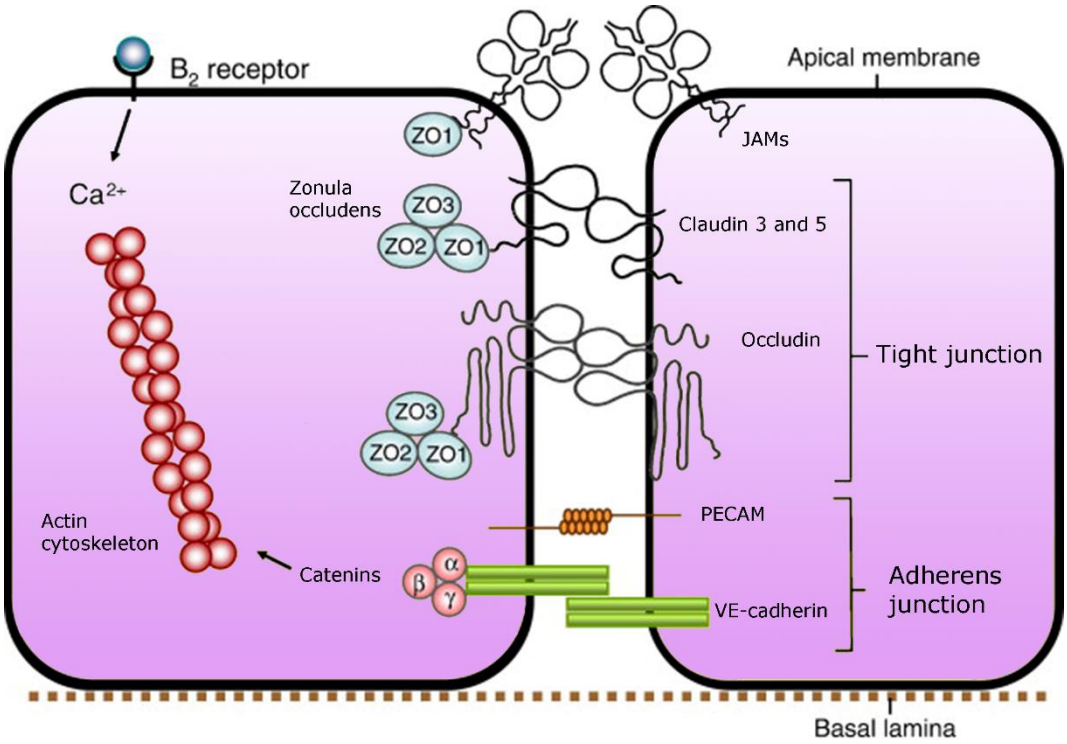

Figure 16 The composition of the tight junctions. ***Modified from Abbott et al., 2010***

The blocking of paracellular diffusional pathways by TJs results in a high *in vivo* electrical resistance of the BBB (about 1800 Ω/cm^2). TJs seem to be regulated via intercellular scaffold proteins (ZO-1, ZO-2 and ZO-3) which link claudins and occludin to intercellular actin and the cytoskeleton (Lauer *et al.,* 2004; Wolburg *et al.,* 2009). Modifications of Ca^{2+} concentrations or changes to electrical resistance limit the effectiveness of the TJs as a barrier. Many cell types associated with brain microvessels — for example, astrocytes, neurons, pericytes, monocytes and microglia — release reactive vasoactive agents and cytokines that can modify the assembly and permeability of TJs (Abbott *et al.,* 2006; Nakagawa *et al.,* 2009).

Transport across the BBB

Excellent reviews such as Abbot *et al.,* 2010 of potential routes for different molecules (figure17) to cross BBB can be summarized as follows:

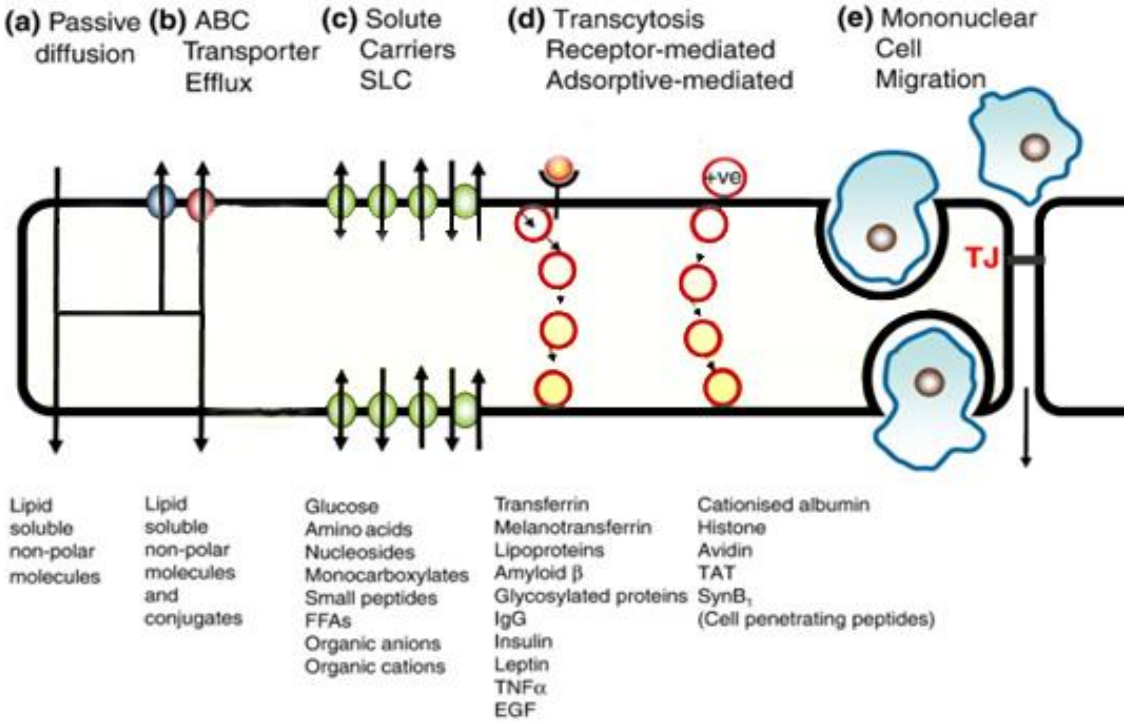

Figure 17: Different routes from blood to the neural parenchyma. ***Modified from Abbott et al., 2010***

- *Passive transport:* Bases with a positive charge have an advantage over acids when crossing the BBB. The cationic nature of these molecules likely interact with the negatively charged glycocalyx and phospholipid head groups, facilitating their entry. The exchange of blood gases oxygen and carbon dioxide across the BBB is diffusive, and dissolved gases move according to a concentration gradient. The bicarbonate anion has a very restricted passive permeability across the BBB.
- *Solute transporters across the BBB*: The blocking of paracellular diffusion potentially isolates the brain from many essential polar nutrients that are necessary for brain metabolism, such us glucose and amino acids. This requires the brain endothelium to contain specific solute transporters that allow the entry of these substances into the neural parenchyma. The structure of TJs makes the BBB behave as a continuous cell membrane whose permeability

depends essentially of the membrane lipid bilayer and its specific transporters. Endothelial cell transporters are specific for a wide variety of solutes and nutrients, and they mediate the traffic into and out of the neural parenchyma.

- *ATP-binding cassette transporters (ABC transporters) across the BBB:* ABC transporters in the BBB play a major role as ATP pumps that transport diverse lipid-soluble compounds out of the brain capillary endothelium and the CNS. They consume ATP and are responsible for decreasing the concentration of some lipid-soluble drugs in the brain.
- *BBB transport of macromolecules:* Transcytosis of macromolecules across the BBB provides the main route via which macromolecules, such as proteins and peptides, reach the intact neural parenchyma. Two vesicle transcytotic mechanisms — receptor-mediated transcytosis (specific) and adsorptive-mediated transcytosis (non-specific) — allow the transport of a variety of macromolecules into the brain.
- *Cell movement across the BBB:* Cells derived from monocyte lineage are recruited in the brain during embryonic development and become resident microglia (Glezer *et al.,* 2007). In addition, mononuclear leukocytes, monocytes and macrophages can reach the neural parenchyma in pathological conditions, displaying a microglial phenotype and playing complementary roles to those of the resident microglia (Bechmann *et al.,* 2005; Davoust *et al.,* 2008). Sites of BBB inflammation attract circulating neutrophils and mononuclear cells that cross the BBB. They accumulate between endothelia cells and the parenchyma basal membrane, forming special zones named perivascular cuffs (especially in venules) (Konsman *et al.,* 2007). This strictly regulated immune cell traffic makes the CNS an immunoprivileged site, where the neutrophil infiltration is much lower than in peripheral tissues. This immunoprivileged condition is lost after trauma or ischaemia events when activated neutrophils damage the BBB (Scholz *et al.,* 2007).

The NVU components

The BBB is formed by specialised vascular endothelial cells, but it is tightly controlled by pericytes embedded in the vascular basement membrane, perivascular microglial cells, astrocytes and neurons. Taken together, the components constitute the neurovascular unit (NVU), a concept that highlights the functional cell–cell interactions that support BBB function (Figure 18).

The NVU concept integrates many aspects of cellular function, including the BBB integrity and physiology (Sengillo *et al.,* 2013; Winkler *et al.,* 2013). The different cell types of NVU are closely associated. In this regard, TJs of cerebral endothelial cells restrict paracellular pathway diffusion; pericytes partially envelop the endothelial cells and share a common basal lamina with them; and astroglial endfeets ensheath the blood microvessel wall and neurons. Pericytes and astrocytes are important in the BBB maintenance and its embryonic development. Thus, the initial concept of a static barrier has been replaced in recent years by a dynamic concept that implies different cell types working together in the homeostasis maintenance of the CNS (Wong *et al.,* 2013; Yepes, 2013). The NVU underlies neurovascular coupling, which allows cerebral blood flow to be locally regulated according to the neuronal activity in specific areas of the brain, which in turn contributes to the normal functioning of the CNS (da Fonseca *et al.,* 2014). Recent *in vivo* studies provide evidence that perivascular microglia in the neural parenchyma interact with CNS blood microvessels, and studies suggest that the microglia cells play a role in regulating BBB properties in both development and disease (Tammela *et al.,* 2011).

Microglia cells represent the population of innate immune cell in e CNS, which migrate from the yolk sac into the neural parenchyma during embryogenesis (Alliot *et al.,* 1999). Microglia perform an essential role in the immune response, but they are also included by some authors as a component of the NVU (Spindler and Hsu, 2012).

Microglia are dynamic cells that are able to change their morphology. Thus, in physiological conditions (resting state), microglia cells present a ramified morphology with small somata and dynamic processes showing an extensive arborisation. These cells are rapidly activated in response to an ischaemic insult, which is evidenced by striking morphological changes that are characterised by deramification —that is, the branch

number and the length of processes are progressively attenuated, leading to an amoeboid morphology (activated state). Changes in the microglial morphology mirror the extent of severity of ischaemic damage (Walker *et al.,* 2014; Yenari *et al.,* 2010). Microglia become activated under brain injury and undergo several alterations from the resting state to the active state. This last state mirrors the presence of neuroinflammation, which is involved in the progression of neurodegenerative diseases (Kettenmann *et al.,* 2011).

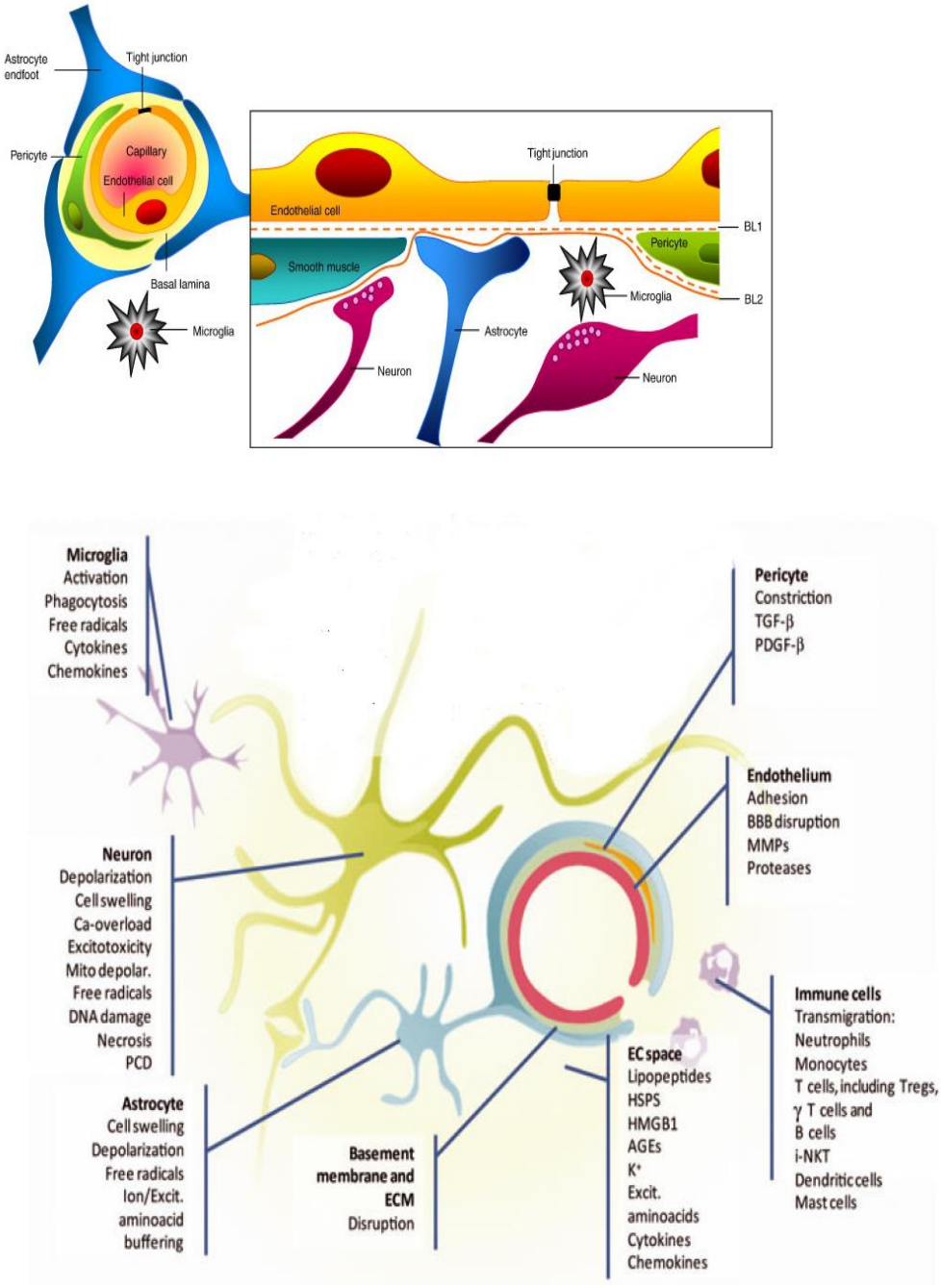

Figure 18 The neurovascular unit. ***Modified from Abbott et al., 2006***

The contribution of the microglia to the BBB maintenance has been highlighted in recent years, suggesting that microglial activation may be related to BBB disruption (Fonseca *et al.,* 2014). Activated microglia have been suggested to increase ROS concentration through the nicotinamide adenine dinucleotide phosphate (NADPH) oxidase system (a typical immune mechanism of microglia), which seems to be the main producer of superoxide anion and an important contributor to increase the BBB impairment (Rojo *et al.,* 2014; Sumi *et al.,* 2010). The reduction in ROS concentrations by inhibiting both microglial activation and infiltration of blood macrophages would limit disruption to the BBB and would reduce vasogenic oedema in ischaemic stroke (Jiao *et al.,* 2011; Sandoval and Witt, 2008).

The importance of microglia in recovery following ischaemic damage has also been highlighted by the results of research studies. In this regard, the absence of proliferating microglia cells contributes to the extension of the damage, while the intracerebroventricular injection of microglia protects the BBB integrity (Kitamura *et al.,* 2004; Lalancette-Hebert *et al.,* 2007). All these data support a role for microglia in endothelial damage and BBB disruption in stroke, making microglia a putative target for the minimisation of ischaemic damage in stroke patients (da Fonseca *et al.,* 2014).

Cell adhesion molecules (CAMs) in vascular endothelium

Leukocyte traffic across the brain endothelium is strictly regulated by the low expression of luminal CAMs under normal healthy conditions, minimising the first stages of leukocyte adhesion. Leucocyte transmigration during inflammation occurs predominantly in vessels on the meningeal pial surface of the brain and postcapillary venules (Engelhardt and Ransohoff, 2012).

Selectins mediate cell–cell adhesion, particularly between leukocytes and vascular endothelium of the post-capillar venules. Three main types of selectins have been identified: P-selectin, E-selectin and L-selectin (Carlos and Harlan, 1994; Hallenbeck, 1996; Kim, 1996). These molecules are expressed in the luminal endothelial membrane immediately after their activation by stimulants such as thrombin and histamine. P- and E-selectin are involved in the recruitment of leukocytes during first stages of leukocyte

activation while L-selectin helps to discard non-activated leukocytes (Bargatze *et al.,* 1994).

The low affinity binding: rolling

The recruitment of the leukocytes and platelet in the brain venules after the BBB impairment is a striking coordinated process, regulated by the expression of different CAMs in the vascular endothelium membranes and their ligands in leukocyte membranes (Figure 19).

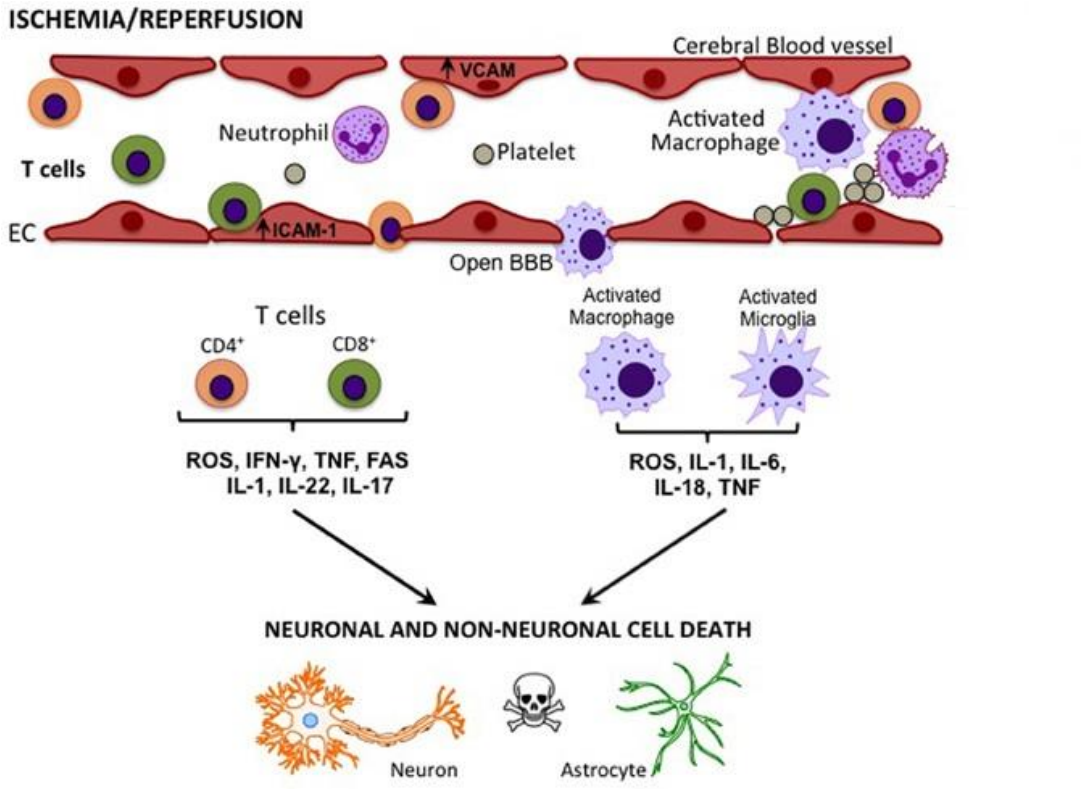

Figure 19: Adhesion process. Modified from Broughton *et al.,* 2013

The recruitment involves two different stages. The first stage is called “labile adhesion” and is characterised by a low-affinity binding adhesion between leukocytes and endothelial cells. This process requires the rolling of the leukocytes and is followed shortly thereafter by high-affinity binding (“firm adhesion”) between leukocytes and endothelial cells. The “labile adhesion” process requires an initial capture process mediated by P-selectin (Yilmaz and Granger, 2008). In the leukocytes, the main ligand for P-selectin is PSGL-1 (P-selectin glycoprotein ligand) (Frenette *et al.,* 2000). This is followed by a characteristic leukocyte rolling process mediated by E-selectin, which is

not pre-synthetised in the vascular endothelial cells (except in the skin where is constitutively expressed together with P-selectin) (Hwang *et al.,* 2004). The expression of E-selectin can be observed after two hours of stimulation by TNF-alpha. During inflammation, cytokine-induced E-selectin expression presents maximal transcript levels between two and four hours, and after 24 hours it returns to the baseline (Kansas, 1996). E-selectin overlaps with that of P-selectin and contributes to the enhanced recruitment of the leukocytes during the inflammatory process. E-selectin reduces the speed of leukocyte rolling, increasing the probability of adhesion (Kunkel and Ley, 1996).

The high affinity binding

Rolling leukocytes bound through E-selectin are induced to express β2 integrin (CD11) as a consequence of laminar shear stress, which leads to the high-affinity binding stage (Green *et al.,* 2004; Kunkel *et al.,* 2000). In particular, neutrophil adhesion is mediated by the β2 integrin lymphocyte function-associated antigen 1 (LFA-1) to the endothelium intercellular ICAM-1. This binding is extremely important to prevent the loss of adhesion that results from the lamina shear stress from the blood flow. Interaction between β2 integrin and its ligands, ICAM-1 and ICAM-2, is also crucial for the proper diapedesis of leukocytes in the transmigration sites (Schenkel *et al.,* 2004).

Transmigration of leukocytes through the vascular endothelial cells is a dynamic process for both cell types. Endothelial cells play a crucial role in this process and proactively form microvilli-like projections that are enriched in ICAM-1 and vascular adhesion molecule 1 (VCAM-1), and that form cup-like structures around populations of adherent leukocytes dependent on LFA-1 and very late antigen-4 (VLA-4) (Barreiro *et al.,* 2002; Carman and Springer, 2004; Shaw *et al.,* 2004). ICAM-1 and VCAM-1 are connected to the endothelial cell cytoskeletal actin by scaffold proteins. This protein complex leads to the cytoskeleton reorganisation that allows the leukocyte to cross the vascular endothelial cells (Barreiro *et al.,* 2004).

The presence of pro-inflammatory mediators (such as TNF-α) increases ICAM-1 expression, which is related to increases in BBB permeability as observed in acute inflammation. A region-specific correlation has been reported between the ICAM-1 induction and microglial activation (Huber *et al.,* 2006). During cerebral ischaemia, the platelet accumulation in microvessels triggers the activation of brain endothelial cells.

ICAM-1 expression is then increased, which enhances neutrophil infiltration into the brain parenchyma and contributes to cerebrovascular inflammation (Thornton *et al.,* 2010).

Leukocyte transmigration

Perivascular macrophages and microglia are activated in several pathological states. Normal blood mononuclear cells are able to cross the BBB by a process of diapedesis through the cytoplasm of the endothelial cells without TJs disruption. Instead, the mononuclear cells use the paracelullar route that involves the opening and re-arrangement of TJs (Abbott, 2013). The BBB plays an essential role in the control of the leukocyte traffic, the immune response during brain infection and the cleaning of the debris by microglia and macrophages after brain trauma (Shechter and Schwartz, 2013). The brain inflammatory response is characterised by the rapid activation of brain resident cells, especially microglia, followed by the infiltration into the neural parenchyma of blood immunoreactive components, including neutrophils, T cells and monocytes and macrophages (Yilmaz and Granger, 2010). The recruitment of blood immune cells occurs under conditions that represent biphasic dynamics. In the acute phase (minutes to hours), the damaged tissue releases ROS, cytokines and chemokines that promote the rapidly recruitment of microglia to the injury site. Activated microglia enhance ROS release (mediated by nicotinamide adenine dinucleotide phosphate oxidase), cytokines (IL-6, TNF-α) and chemokines. In this phase, mediators are also released to stimulate endothelial cells, which results in the expression of the adhesion molecules P-selectin, E-selectin, ICAM-1 and VCAM-1. Adhesion ligands (lectins) are also upregulated in circulating leukocytes, allowing the cell diapedesis in the subacute phase(Enzmann *et al.,* 2013; Obermeier *et al.,* 2013). All of these processes enhance the adhesion of leukocytes to the endothelium and their subsequent transmigration (Figure 20) (Jin *et al.,* 2010b). The degradation of the basal lamina of the vascular endothelial cells by MMPs facilitates contact between the leukocytes and the endothelial CAMs, allowing transmigration. In the subacute phase (hours to days), the infiltrated leukocytes release chemokines and cytokines that increase ROS production and activates MMPs (especially MMP-9). In turn, ROS and MMPs enhance the inflammatory response, increase the activation of the resident brain macrophages and facilitate the

transmigration of neutrophils and peripheral macrophages. Finally, these events result in BBB disruption, which can lead to the neuronal death (Berezowski *et al.,* 2012; Rosell *et al.,* 2006; Stanimirovic and Satoh, 2000).

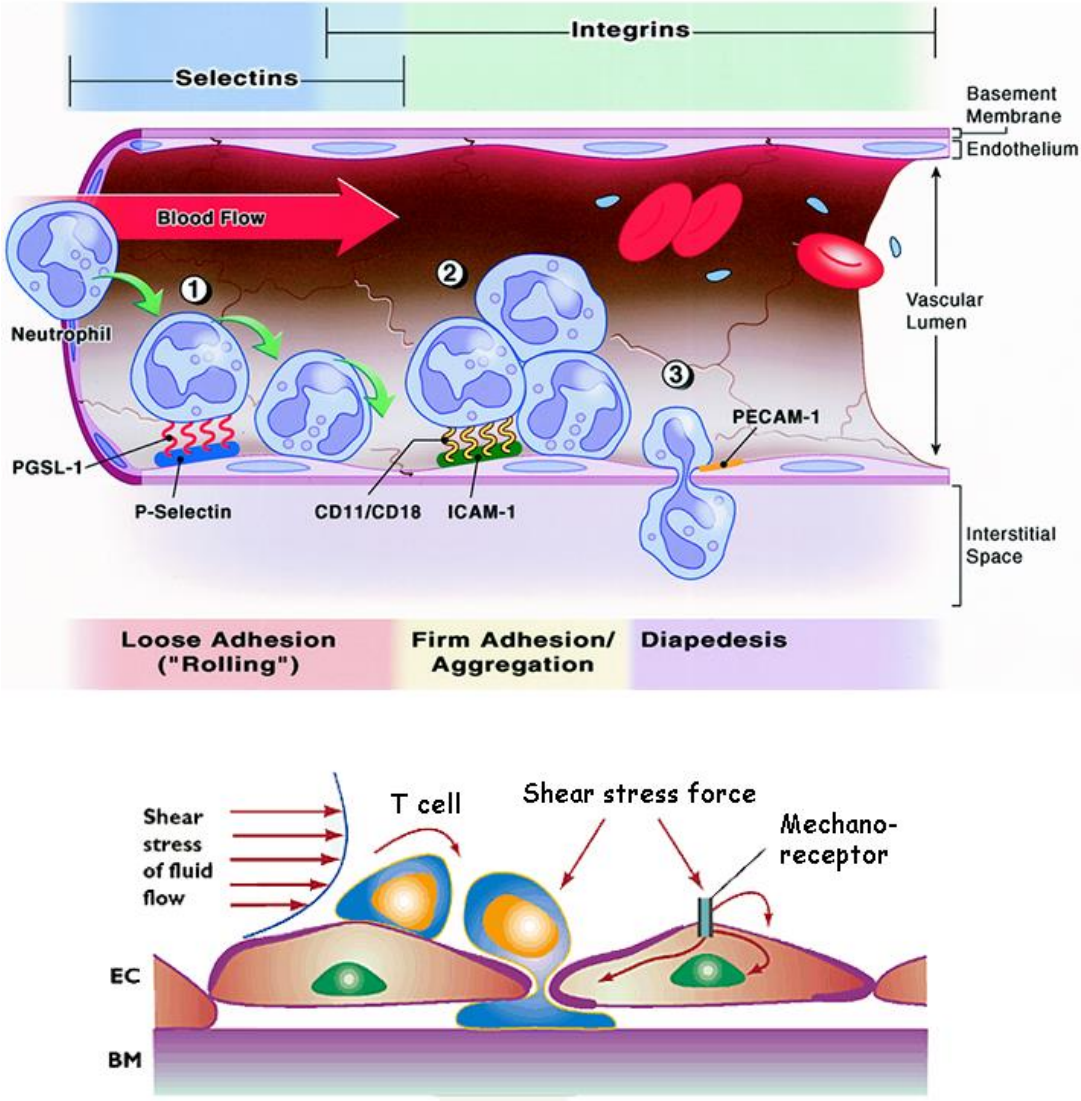

Figure 20: Leukocyte transmigration. ***Modified from Collard and Gelman, 2001.***

Blood brain barrier impairment

In inflammatory pathological states, the BBB TJs may be opened by the action of cytokines and other agents, allowing mononuclear cells to reach the neural parenchyma by both paracellular and transcellular routes (Abbott, 2013; Konsman *et al.,* 2007). In most CNS disorders, a BBB impairment appears that is associated with inflammation

prior to the neuronal loss. This impairment may play a causative or exacerbating role in neuronal dysfunction or loss. Neuroinflammation with microglial activation is detectable before the neuronal loss and involves the BBB impairment with extravasation of large molecular weight tracers (Farfel-Becker *et al.,* 2011; Vitner *et al.,* 2012).

BBB disruption after stroke also presents with biphasic dynamics. The reversible early opening (around 12 hours after insult) of the BBB is mainly caused by oxidative stress; the most important mediators are ROS produced predominantly by astrocytes and microglia. In addition, ROS and NO can induce a reorganisation of endothelial cytoskeleton, modulate TJs and activate latent MPP-2. The activated MPP-2 is the most important factor in the early disruption of the BBB. Despite its reversibility, the first opening of the BBB activates microglia and upregulates inflammatory mediators during the first 48 hours (Bauer *et al.,* 2010; Lee *et al.,* 2004; Obermeier *et al.,* 2013).

A delayed secondary opening of the BBB occurs in the following 48 to 72 hours, and the sustained inflammatory response in the brain parenchyma causes a continuous BBB impairment. In this second opening, MPPs (MPP-2 and MPP-9) are the most important mediators released by astrocytes and pericytes, which are stimulated by the increase of the microglial ROS and NO and cytokines production (Rosenberg *et al.,* 2001; Takahashi *et al.,* 1999). This permeability contributes to haemorrhagic transformation and vasogenic oedema. MPPs are stimulated by NF-kB and HIF-α and disrupt TJs, contributing to the BBB impairment (Gu *et al.,* 2012; Obermeier *et al.,* 2013). The most active metalloprotease is MPP-9. It is considered to be the main molecule responsible for the disruption of the TJs and the irreversible phase of the BBB impairment (Bauer *et al.,* 2010; Lee *et al.,* 2004).

The continuous production of proinflammatory mediators in the damaged area, such the mediators TNF-α, IL-6 and NO, also interferes with the late phase of the BBB disruption. TNF-α and IL-1beta downregulate the TJ protein expression in vascular endothelial cells (Jiao *et al.,* 2011) and, together with IL-6, modulate the expression of ICAM-1 and VCAM-1 (Hallenbeck, 2002). These actions enhance the diapedesis of peripheral leukocytes and contribute to the vasogenic oedema, allowing the diffusion of sodium and water into the neural parenchyma (Sandoval and Witt, 2008).

ER-stress, UPR and stroke.

The ER is a highly specialised organelle where the proper folding of proteins occurs. Those proteins are destined to be secreted or delivered to different cellular organelles. These events require ATP and Ca^{2+}-dependent post-translational modifications to the nascent peptides, including disulfide bond formation, glycosylation, controlled proteolysis and chaperone-mediated folding (Schroder and Kaufman, 2005). To carry out these functions and for a protein to achieve is final functional conformation, the ER must maintain an oxidising environment, elevated Ca^{2+} concentrations and an environment rich in molecular chaperones, isomerases and glycosylation enzymes (Kaufman, 1999).

The ER is highly sensitive to changes in cytoplasm and the extracellular environment. Thus, when neuronal homeostasis is impaired, ATP levels drastically decrease and Ca^{2+} is released from the ER. The accumulation of damaged and misfolded proteins in the cytoplasm and ER lumen is known as ER stress, a situation that happens during an ischaemic insult and is accompanied with increases in ROS and NOS (Wu and Kaufman, 2006). ER-stress has been reported in models of global and focal ischaemia and in cultured neurons subjected to oxygen and glucose deprivation (OGD) (Llorente *et al.,* 2013; Petito and Pulsinelli, 1984; Wu and Kaufman, 2006). Moreover, ER stress can result in inflammatory signalling (Hasnain *et al.,* 2012).

Unfolded protein response (UPR)

In response to ER-stress, cells ignite an adaptive response known as UPR. UPR includes a number cellular responses, such as 1) a reduction in the rate of protein synthesis; 2) an upregulation in genes that encode for ER chaperones, enzymes and structural components of the ER, thus increasing its capacity for processing proteins; 3) the activation of degradation pathways to overcome the excess of misfolded and damaged proteins and 4) the initiation of a program of delayed cell death (apoptosis) if the stress is too severe or impossible to overcome (Meusser *et al.,* 2005; Muchowski, 2002; Schröder and Kaufman, 2005).

There are three transmembrane proteins, known as “UPR sensors, that are located in the membrane of the ER and that are involved in UPR ignition: inositol-requiring enzyme 1 (IRE1), double-stranded RNA-activated protein kinase-like ER kinase (PERK) and activating transcription factor 6 (ATF6). Each of the three transmembrane proteins activates a different UPR pathway (Figure 21). The ER molecular chaperone glucose-related protein-78/binding immunoglobulin protein (GRP-78/BiP) is considered to be the main protein that is responsible for the activation of th UPR “sensors”. GRP-78 is expressed constitutively in ER lumen and, under physiological conditions, binds the luminal domains of PERK, IRE1 and ATF6. Upon accumulation of misfolded proteins in the ER lumen, GRP-78 binds the exposed hydrophobic residues of misfolded proteins which leads to its dissociation from the UPR sensors (Chapman *et al.,* 1998. However, the activation of UPR sensors independently of GRP-78 has been described in recent years, indicating that the mechanism of UPR-sensor activation may be more complex than just GRP-78 dissociation (Gardner and Walter, 2011).

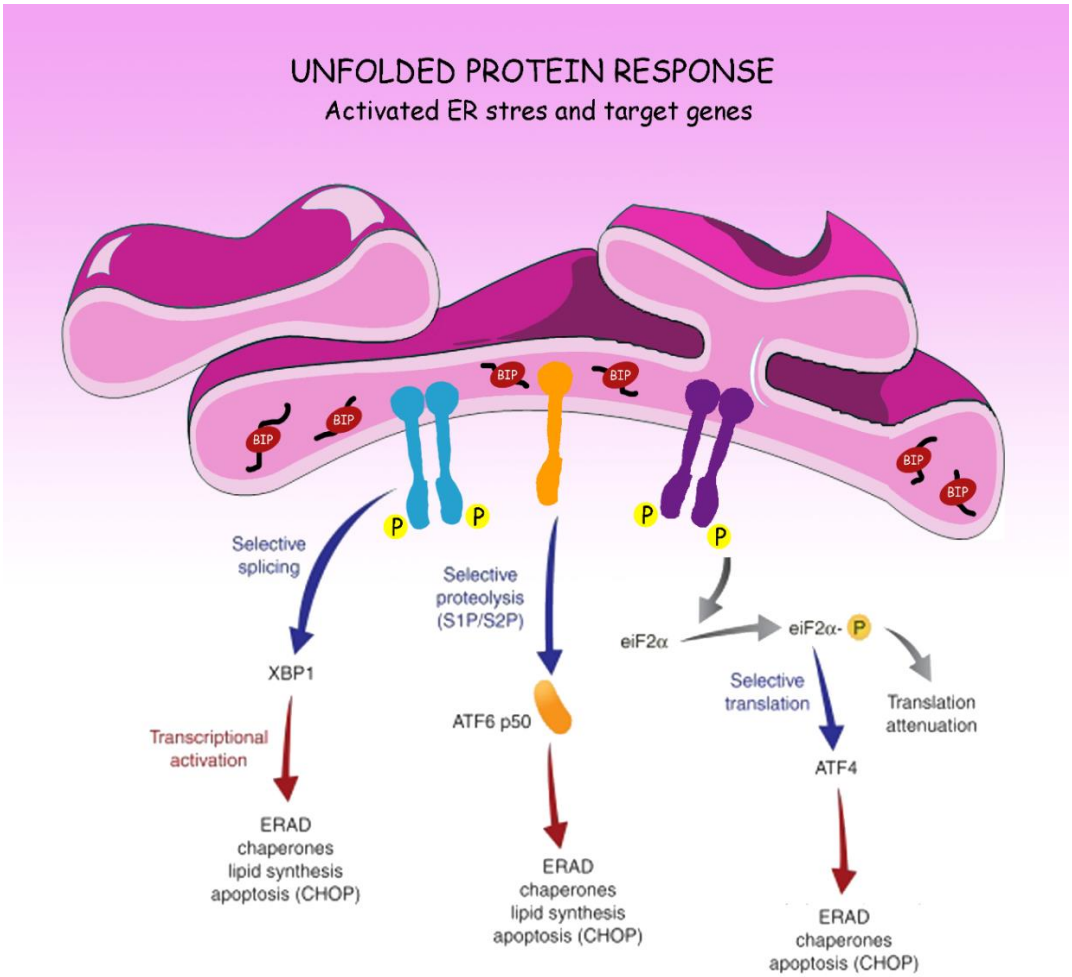

Figure 21: The UPR pathways. ***Modified from Malhotra and Kaufman, 2011***

The immediate response to cellular stress is a decrease in protein synthesis, which reduces the cargo load in the ER. This early pathway of the UPR is elicited by PERK. The increase in the folding capacity of the ER takes one to two hours and involves later transcriptional regulation that is elicited by IRE1 and ATF6 (DeGracia *et al.,* 2002).

1.- *PERK-pathway*

When the folding capacity of the ER is compromised, GRP-78 dissociates and promotes the PERK homodimerisation. The subunits of the homodimer activate each other by autophosphorylation, which activates PERK. Next, PERK phosphorylates the eukaryotic initiation factor 2 subunit α (eIF2α) at serine 51, a crucial component of the ribosome-initiation complex. This event attenuates the translation of most proteins in the cell,

thus contributing to the prevention of ER overload. Nevertheless, several mRNAs are preferentially translated when eIF2α is phosphorylated. Moreover, some other cytosolic kinases that are able to phosphorylate eIF2α in response to cellular stress contribute to the integrated stress response, linking the cytosol and ER lumen events (Wiseman and Balch, 2005).

The PERK pathway is attenuated by the dephosphorylation of eIF2α by a protein complex containing the enzyme phosphatase protein phosphatase 1(PP1) and its essential non-enzymatic cofactor growth arrest and DNA damage (GADD34). The expression of GADD34 is upregulated by eIF2α phosphorylation, resulting in a tight auto-feedback loop (Anderson and Kedersha, 2002; Novoa *et al.,* 2003). After global ischaemia, protein synthesis inhibition initially affects the whole brain, but normal translation levels are not recovered in the most vulnerable CA1 hippocampal region (Hossmann, 1993).

2.- ATF6 pathway

ATF6 is an ER-membrane-bound transcription factor. After dissociating from GRP78, the inactive 90 kDa ATF6 translocates from the ER membrane to the Golgi apparatus. In the Golgi apparatus, ATF6 is cleaved by site 1 proteases (S1P) and site 2 proteases (S2P). Cleaved ATF6 (50 kDa) is the active transcription factor that is able to translocate to the nucleus, bind to ER stress response elements and form complexes with several co-activators. This pathway increases the expression of molecular chaperones (GRP78, GRP94 and protein disulfide isomerase) and CCAAT-enhancer-binding proteins (C/EBP) homologous protein (CHOP). CHOP is a transcription factor that promotes the activation of the apoptotic pathway (Korennykh *et al.,* 2009)..

3-*IRE1-XBP1 pathway*

IRE1 follows the same activation mechanism as PERK. After the release of GRP-78, IRE1 oligomerises, which leads to its autocatalytic phosphorylation and endoribonuclease activation. Activated IRE1 splices a 26-nucleotide sequence in the coding region of X-box binding protein 1 (XBP1) mRNA, which promotes a change in the reading frame. In the absence of stress, XBP1 mRNA is translated into a 33 kDA XBP1 protein; after IRE1 activation, the spliced XBP1 mRNA form is translated into a 54 kDa protein, the

processed XBP1 (XBP1^{proc}). XBP1^{proc} is a transcription factor that activates the expression of molecular chaperones and the components of the ER-associated degradation (ERAD) system, thus counteracting the accumulation of misfolded proteins in the cell (Korennykh and Walter, 2012).

ER stress modulators

Therapeutic agents that target the components involved in ER stress have a putative high value for the treatment of pathologies for which ER stress and UPR play prominent roles. This is mainly accomplished by controlling the pro-apoptotic signalling that is associated with ER stress. This signalling pathway following ischaemia is primarily mediated by three signalling pathways: CHOP, c-Jun N-terminal kinase and caspase-12 (Ivanova and Orekhov, 2016).

One of the possible mechanisms to alleviate ER stress is the use of chemical chaperones, for example, phenylbutyrate and tauroursodeoxycholic acid (Engin and Hotamisligil, 2010). These agents facilitate protein folding and trafficking in a non-selective way, thereby decreasing the protein load when the ER is under conditions of stress. Protein kinase A activators, such as isoproterenol and forskolin, use this mechanism to attenuate ER stress and associated apoptosis (Asai *et al.,* 2009).

Other agents act by inhibiting p-eIF2α dephosphorylation, which results in protective effects against ER stress. In this regard, by inhibiting the eIF2α phosphatases and CHOP-mediated pro-apoptotic signalling, salubrinal prevents ER stress-induced apoptosis in cardiomyocytes (Fu *et al.,* 2010).

Agents such as SB203580, which inhibits p38 mitogen-activated protein kinase (MAPK), or SP600125, which inhibits c-Jun N-terminal kinase (JNK), could suppress mechanical stress induced by the activation of CHOP phosphorylated (Cheng *et al.,* 2009; Wang and Ron, 1996). A different pathway can be elicited by valproate, which induces the expression of the ER chaperone BiP, thus blocking the induction of CHOP and caspase-12 activation (Zhang *et al.,* 2011). Other compounds, for example EN460 and QM295, have been shown to alleviate the ER stress by inducing an adaptive UPR response (Blais *et al.,* 2010; Kim *et al.,* 2009). On the other hand, activators of AMP-activated protein kinase, which acts as an energy sensor in the cell, have protective effects on cardiac cells

by reducing the ER stress; examples include 5-aminoimidazole-4-carboxyamide-1-β-D-ribofuranoside (AICAR), atorvastatin, A-769662 and PT1 (Jia *et al.,* 2012; Kimata and Kohno, 2011).

The recovery of calcium homeostasis in the ER is another promising avenue for the alleviation of ER stress-induced apoptosis. Several drugs, including verapamil and diltiazem, can inhibit ER calcium efflux and enhance its protein folding capacity (Mu *et al.,* 2008; Ong and Kelly, 2011). Literature related to a wide spectrum of natural components that have the potential to alleviate ER stress and prevent apoptosis has recently been reviewed. Those include proteasome inhibitors (such as brefeldin A, tunicamycin and lactacyclin); regulators of calcium homeostasis (such as thapsigargin, basiliolide A1 and agelasine B); and IRE1/PERK signalling inhibitors (such as resveratrol and withaferin A) (Pereira *et al.,* 2015).

Salubrinal

The relevance of ER stress to the damage of a cell has led researchers to look for small molecules that modulate UPR and that could potentially be useful for the treatment of several human diseases. One of these molecules, salubrinal, has been reported to confer resistance to apoptosis induced by ER stress. This small molecule inhibits PP1-GADD34 phosphatase activity, which results in sustained eIF2α phosphorylation (Boyce *et al.,* 2005). Salubrinal does not interfere with the induction of XBP1 or ATF6; therefore, it is a very selective tool for the analysis of the UPR–PERK pathway. Salubrinal is cytoprotective against ER stress at micromolar concentrations, and it has the advantage of having low toxicity (Li and Herlyn, 2005).

Crosslinking between UPR and inflammation.

The effect of ER stress on inflammation

ER stress initiates a molecular cascade that involves the coordinated activation of specific enzymes and transcription factors that recover ER homeostasis. However, this cascade can result in inflammatory signalling or apoptosis in chronic or severe ER stress (Kimata and Kohno, 2011). ER stress-induced inflammation can be dependent or independent of UPR. In the UPR-dependent mechanism, the IRE1 alpha subunit forms a complex with the IkB kinase leading to the degradation of IkBα. When TNF-receptor

activation 2 is induced, NF-κB transcription factor becomes activated and is translocated to the nucleus(Kaneko and Nomura, 2003) , providing one of the direct links between ER stress and NF-κB activation. In addition, PERK-induced inhibition of protein synthesis in ER-stressed cells results in a decreased translation of IkBα. As mentioned above, this increases the translocation of NF-kB transcription factors into the nucleus (Deng *et al.,* 2004; Jiang *et al.,* 2003).

ER stress overload (even in the absence of significant misfolding) can also result in NF-kB activation in a UPR-independent, but Ca^{2+}- and ROS-dependent manner. This activation is the consequence of the leaking of GRP-78 into the cytosol during ER stress and of the direct interaction with the NF-kB protein–IkB kinase complex (Shkoda *et al.,* 2007).

Evidence mentioned above suggests that ER stress activates NF-kB, but there is an emerging body of evidence that ER stress can, conversely, make some cell types refractory to NF-kB activation and inflammatory stimulation. In this regard, a previous exposure to ER stressors, such as tunicamycin or thapsigargin, decreases the severity of the disease in models of renal inflammation (Cybulsky *et al.,* 2005; Inagi *et al.,* 2008). In a similar way, mesangial cells preconditioned to ER stress show a decrease in NF-kB activation in response to lipopolysaccharides. This response is mediated by a PERK- and IRE1-dependent increase of CHOP, which is known to act as an NF-kB inhibitor in the presence of inflammatory cytokines (Hayakawa *et al.,* 2010; Nakajima *et al.,* 2011). The zinc finger protein A20 is thought to be the main protein responsible for NF-kB inhibition in preconditioning studies (Nakajima *et al.,* 2010).

ER stress can also contribute to inflammation by an NF-kB-independent mechanism. The apoptosis triggered by UPR can interfere with the normal functioning of antigen-presenting cells, leading to an increased production of inflammatory cytokines (Peters and Raghavan, 2011). Also, ER stress or an impaired UPR can increase the cytokine production of T and B immune cells (Goodall *et al.,* 2010; Iwakoshi *et al.,* 2003).

The effect of inflammation on the ER stress

Inflammatory cytokines can induce oxidative stress and activate granulocytes and the release of oxidative stressors by macrophages, which is known to increase protein misfolding. ROS and NOS can activate UPR by inhibiting the production of protein

disulphide isomerases, resulting in the accumulation of proteins within the ER (Uehara *et al.,* 2006; Xue *et al.,* 2005). Inflammatory cytokines can also induce ER stress by increasing the synthesis of secretory proteins, which arese produced in mucosal defence and which are complex proteins that are susceptible to misfolding. In a very limited study, TNF-α has also been reported to induce ER stress in colon cells(Hao *et al.,* 2011). The interconnection between ER stress and inflammatory signalling pathways in general is supported by substantial evidence. However, there is still limited evidence for this link in cerebral ischaemia (Anuncibay-Soto *et al.,* 2016). Neuroprotective agents that target both ER stress and neuroinflammation will possibly result in strong beneficial effects against cerebral ischaemia injury (Xin *et al.,* 2014)..

AIMS

WORK HYPOTHESIS AND AIMS

Stroke is one of the main health problems in developed countries, both in terms of its clinical and its social effects. The search for therapeutic targets and putative therapies, either palliative or regenerative, is the basic aim of many research teams working on stroke. As previously described, inflammation and the subsequent events related to its response, leukocyte adhesion and BBB impairment appear to play crucial roles in the damage that follows a stroke. In addition, the close relationship between ER stress, UPR and inflammation that has been discovered in recent years provides researches with new and relevant therapeutic targets to alleviate the damage caused by stroke. In this research, the differences in vulnerability to ischaemia in different parts of the brain make it necessary to choose models that allow for a comparison between structures of similar conditions, such as the global cerebral ischaemia model.

Our research aims to analyse the inflammatory response following a stroke. Our proposed working hypothesis is that local properties of the BBB, including age-dependent changes, explain the differences in vulnerability and that the BBB could be used as the main target for the reduction of sterile inflammation. This inflammation could be alleviated not only by a direct effect on inflammation, but also by controlling ER stress or by combining agents that affect both ER stress and inflammation.

To test this hypothesis, we proposed the following objectives and questions:

1) Are there local differences or age-dependent differences in the BBB? To answer these questions, we analysed the steps involved in the adhesion process in structures with different vulnerabilities and in young and old animals.
2) Does ER stress modify the inflammatory response acting on the BBB? We used a blocker of ER stress, salubrinal, to analyse the role of UPR in the adhesion process and the inflammatory response triggered by ischaemia.
3) Can we observe a synergic neuroprotective effect combining an ER stress blocker and an anti-inflammatory agent? We checked the effect of salubrinal and the preferred COX-2 inhibitor independently and combination, and we analyised the effects on different NVU components.

CHAPTER 1

Age-dependent modifications in vascular adhesion molecules and apoptosis after 48-h reperfusion in a rat global cerebral ischemia model

Background

Stroke is one of the most important cause of death worldwide according to the WHO (Llorente et al. 2013a) and the main cause of permanent disability (Donnan et al. 2008). Ischemia causes necrosis in neurons in the first hours after insult in the area where blood flow has been reduced to less than 15% (ischemic core) (Tamura et al. 1981; Nedergaard et al. 1986; Duverger and MacKenzie, 1988). After longer periods, areas with blood flow up to 40% (penumbra areas) (Ginsberg and Pulsinelli, 1994; Hossmann, 1994; Back, 1998) present delayed cell death, mainly by apoptosis (Mehta et al. 2007). Thus, the goal of neuropharmacological targeting is mainly addressed to preserve or rescue the neurons in the penumbra area of apoptotic delayed cell death (Rami et al. 2008; Fricker et al. 2013). Apoptosis is also tightly related with the strong neuroinflammation elicited by stroke and the impairment of the BBB (Amor et al. 2010). In the inflammatory response, adhesion molecules play crucial roles since they mediated recruitment and infiltration of neutrophils across the vascular endothelium (Sughrue et al. 2004; Petri et al. 2008). This process requires the sequential action of different selectins and CAMs (Stanimirovic and Satoh, 2000; Yilmaz and Granger, 2008) and we hypothesised that the balance of these molecules could mirror the time-course of this recruitment. In addition, the impairment of the BBB is neutrophil-dependent (Anthony et al. 1997; Perry et al. 1997; Blamire et al. 2000) and, therefore, should be mirrored by the expression of these molecules. This expression could help to identify the BBB permeability at different ages. The impairment of the BBB is also related to astrocyte activation (Ivens et al. 2007; Cacheaux et al. 2009), where quiescent astrocytes become reactive astrocytes. This process modified these cells substantially, inducing crucial changes in the expression of cytoskeletal molecules, such as GFAP (Sofroniew and Vinters, 2010; Colangelo et al. 2014). Reactive astrocytes release soluble factors that are related to the recruitment of

leukocytes for crossing the BBB and initiate neuroinflammation in the central nervous system (CNS) (Li et al. 2011).

Ischemia focal models reveal an intrinsic gradient of damage from the ischemic core that has to be considered when a structure is studied (Ayuso et al. 2010). Most of the results from focal models are morphological data based on immunofluorescence and magnetic resonance imaging (MRI) (Dziennis et al. 2011; Liu and McCullough, 2012), and many of them are based on the leukocyte response (Stevens et al. 2002a; Gelderblom et al. 2009). In addition, despite the fact that strokes mainly occur in the elderly, current studies are mainly performed on young animals and data from old animals are very scarce (Collins et al. 2003; Wasserman et al. 2008). Particularly, studies on transcriptional expression of specific molecules that bind neutrophils (e.g. selectins and CAMs) are very limited and are practically non-existent in old animals (Liu and McCullough, 2012), despite their importance for gaining insight into the leukocyte infiltration process.

Age is considered the most relevant factor for stroke risk (Rojas et al. 2007; Rosamond et al. 2008). Since many biochemical parameters are decrease with aging (Sinha et al. 2005; Bala et al. 2006; Arumugam et al. 2010; Liu and McCullough, 2011; Liu et al. 2012), it would be expected a lessened ability of response to the stroke. However, age-dependent differences in the time-course of the stroke-induced response of different molecules could play crucial roles in the discovery of new therapeutic targets or therapies (Anyanwu, 2007). In this regard, we present here a study comparing for the first time the ischemic-induced apoptotic damage (delayed cell death), GFAP, and selectin and CAM adhesion molecules involved in leukocyte infiltration and GFAP, and show their age dependence.

Material and Methods

Animals

Young (3 months old) and old (18 months old) male Sprague–Dawley rats, 400 ± 50 g and 750 ± 80 g, respectively, were housed at 22 ± 1 °C in a 12 h light/dark controlled environment with free access to food and water. Twenty rats of each age group were

divided randomly into ischemic and sham-operated groups. Experiments were performed in accordance to the Guidelines of the Council of the European Union (63/2010/EU), following Spanish regulations (RD 53/2013, BOE 8/2/2013) for the use of laboratory animals. Experimental procedures were also approved by the Scientific Committee of the University of Leon. All efforts were made to minimise animal suffering and to reduce the number of animals used.

Transient global ischemia

Animals were anesthetised in an anaesthesia induction box supplied with 4% halothane (Sigma-Aldrich) at 3 L/min in 100% oxygen. After induction, anaesthesia was maintained with 1.5 to 2.5% halothane at 800 mL/min in 100% oxygen using a rat face mask. Trimetaphan (kindly provided by Roche Applied Science) was used as the main hypotensor agent (15 mg/mL, 0.3 mg/min), administered through the femoral artery, to obtain moderate hypotension (40–50mm Hg). This prevents blood flow through the circle of Willis in the two vessel occlusion models of global ischemia. Arterial tension was also modulated by changing the halothane concentration, which has intrinsic hypotensive effects (Bendel et al. 2005). Body temperature was controlled with a rectal probe and maintained at 36 ± 1 °C during surgery using a feedback-regulated heating pad. Both common carotid arteries were exposed and occluded with atraumatic aneurysm clips for 15 min of transient global ischemia. Then, animal arterial blood pressure was left to recover, the femoral artery catheter was removed, and the animal was sutured.

After recovering consciousness, rats were maintained in standard conditions for 48 h (reperfusion time). Procedures in sham-operated rats were performed exactly as for ischemic animals except that carotid arteries were not clamped.

RNA and protein studies

Forty-eight hours after the ischemic insult, animals were decapitated, their brains quickly removed and transferred into a brain rodent matrix (ASI instruments) at 4 °C in order to obtain2 mm thick sagittal slices at a distance of 1 mm to the medial line. The Cornu Ammonis 1 hippocampal region (CA1), Cornu Ammonis 3 hippocampal region (CA3) and cerebral cortex (CX) were dissected from those slices under a microscope, frozen in dry ice, and stored at -80°C. Total RNA and protein of each of these regions

were extracted using the TripureTM isolation reagent (Roche Applied Science) following the manufacturer's instructions, and then stored at -80 °C.

Reverse transcription (RT) and quantitative real-time PCR (qPCR)

RNA integrity was assessed using the Experion RNA HighSens Analysis Kit (Biorad Laboratories) following the manufacturer's instructions. Possible contamination with DNA was prevented by incubation with DNase (Sigma-Aldrich) and checked by PCR.

The concentration of the total RNA in each sample was determined by measuring its absorbance (260/280 nm) using a NanoDrop ND-3300 spectrophotometer (NanoDrop Technologies). Six hundred nanograms of total RNA of each sample was used as a template for reverse transcription using the High Capacity cDNA Reverse Transcription Kit (Applied Biosystems) according to the manufacturer's instructions. The cDNA obtained was used as a template for the qPCR assays. Primers were designed using Primer Express software (Applied Biosystems) and those with efficiencies lower than 90% were discarded. Forward and reverse primers used in this study (efficiency values between 90 and 110%) are shown in Table 1.

Table 1. Sequences of the primers used for RT-qPCR and GenBank Accession Numbers.

Gene	Forward primer	Reverse primer	Accession number
p-selectin	5'acaggcagccctccaatgtgtg	5'atttgacggctctgcacacggg	[NM_013114.1]
e-selectin	5'tgcttcccgtctttgccacacc	5'tccgtccttgctcttctgtgcg	[NM_ 017211.2]
vcam-1	5'tgctcctgacttgcagcaccac	5'tgtcatcgtcacagcagcaccc	[NM_ 012889.1]
icam-1	5'tgcagccggaaagcagatggtg	5'atggacgccacgatcacgaagc	[NM_012967.1]
gapdh	5'gggcagcccagaacatca	5'tgaccttgcccacagcct	[NM_017008]

Real-time PCR was performed using a StepOnePlus ™ Real-Time PCR System, and SYBR Green PCR Master Mix (Applied Biosystems) was used as the fluorescent DNA binding dye. Optimal qPCR conditions in our assays were obtained with 2 µl of 1/10 cDNA and 300 nM of primers. Glyceraldehyde-3-phosphate dehydrogenase (GAPDH) was used as a reference gene for normalisation of different transcript values The normalised messenger RNA (mRNA) levels were expressed as $2^{-\Delta Ct}$ (ΔCt=Ct target−Ct GAPDH), and fold changes were compared using the $2^{-\Delta\Delta Ct}$ method (Livak and Schmittgen, 2001). All of the qPCR assays in this study were performed according to MIQE Guidelines (Taylor et al. 2010).

Western blot

Proteins were resuspended in 8 M urea and 4% SDS in the presence of a protease inhibitor (complete protease inhibitor cocktail, EDTA free; Roche Applied Science) and their concentrations were determined using the DC Protein Assay (BioRad) based on the Lowry method. Protein samples (25 µg per lane) were resolved on a 10% polyacrylamide gel (SDS-PAGE; BioRad) at 110 V for 120 min. Then, proteins were transferred onto a nitrocellulose membrane using a dry transfer system (Invitrogen) at 20 V for 7 min. Nitrocellulose membranes were blocked in 5% bovine serum albumin and 0.2% Tween-20 (Sigma Aldrich) in Tris-buffered saline (TBS-T) for 60 min at 25 °C. Then, membranes were incubated overnight, at 4 °C, with the primary antibodies (Table 2).

Table 2. Primary antibodies and concentration used.

Primary antibodies	Manufacturer	Concentration
P-selectin raised in rabbit	Abcam	1 µg/ml
E-selectin raised in rabbit	Abcam	0.67 µg/ml
ICAM-1 rabbit in rabbit	Abcam	0.75 µg/ml
GFAP raised in mouse	Dako	1 µg/ml
β-Actin raised in mouse	Sigma Aldrich	0.2 µg/mL

Primary antibodies were labelled with their appropriate secondary anti-rabbit or anti-mouse antibodies complexed with horseradish peroxidase (Dako) at a dilution of 1:3000. After incubation in Chemiluminescence Luminol Reagent (Life Technologies), the nitrocellulose membranes were exposed onto the proper films (ECL films, Amersham) to obtain images of the protein bands labelled with the enzyme. Densitometry analysis of the bands was performed with ImageJ 1.46r (ImageJ software).

Immunofluorescence assays

Animals used for this technique were perfused via the aorta with a saline solution followed by a fixer solution (PFA) made of 4% paraformaldehyde (Merck) in 50 mM phosphate buffer saline (PBS; pH 7.4) at 4 °C. The brains were removed, maintained overnight in PFA at 4 °C, and then stored until sunk in a cryoprotectant solution made of 30% sucrose in PBS, pH 7.4. Brains were sectioned into 40 µm thick sagittal slices with a freezer microtome, and then were maintained in 0.025% sodium azide (Sigma-Aldrich) in PBS (pH 7.4) at 4 °C until analysis. Sections were labelled with a rabbit primary antibody against the activated caspase 3 (Cell Signalling) overnight at 4 °C. A biotinylated goat anti-rabbit antibody (Vector; 1:500) was used as the secondary antibody and was labelled with stravidin complexed with Dyelight Alexa 592 (Molecular probes; 1:100).

Nuclei were labelled with DAPI (Sigma Aldrich; 1:1000) and mounted in 3% DABCO (Sigma Aldrich) in glycerol-water (1:1) to preserve the fluorescence. Slices were kept at 4 °C in the dark. Images were obtained using a confocal Nikon TE 2000 EZ.C1 microscope (Nikon).

Quantification of cleaved caspase-3-positive cells was performed on six 40 µm thick equidistant sagittal sections that were between 1 and 4 mm lateral to the middle line per rat. An optical dissector method modified from (Zarow et al. 2005) was used. A 60X objective was used to perform the quantification. The counting frame for the dissector was a 35 x 35 µm square, and for the fractionator volume, we used a 30 µm height (discarding five microns of both lateral and medial sides that were damaged in the cutting process). In each of the sections, seven equidistant dissectors along the cerebral cortex internal pyramidal layer, seven along CA1, and four along the CA3 pyramidal layers were used per section. Cells were scored as apoptotic when the nucleus was stained by the cleaved caspase 3 antibody and was condensed, or if at least 30% of the cytosol surrounding the nucleus was labelled. Other staining patterns were considered as artefacts. The results were expressed as the percentage of cleaved caspase-3-positive cells with respect to the total number of cells.

Statistical analysis

Two-way ANOVA tests followed by Bonferroni t-test were conducted to detect interactions between age and ischemia. The significance was set at the 95% confidence level. The statistical analysis was carried out using Graph Pad Prism 5 (Graph Pad software).

Results

E-selectin mRNA levels on the hippocampus and cerebral cortex

The analysis of the effect of age revealed that the cerebral cortex and CA1 showed significantly lower mRNA levels in the aged sham-operated animals than in the young sham-operated animals. However, we failed to find differences in CA3. In contrast, we only detected an age-dependent effect, with increased E-selectin transcript levels, in the CA3 of injured animals (Figure 1A). In all of the structures studied, the ratios between

old/young sham-operated animals were significantly lower than the ratios for old/young ischemia/reperfusion (I/R) injured animals.

In young animals, we only detected the I/R effect in the CA1 and CA3 hippocampal structures where E-selectin mRNA levels of ischemic animals were significantly lower than those of their respective sham-operated animals. In old animals, E-selectin transcript levels were significantly higher than those of their respective sham-operated animals in all of the structures studies. Also, E-selectin mRNA levels were higher in old injured animals than in young injured animals (Figure 2A).

Two-way ANOVA analysis of E-selectin transcripts revealed significant interactions for both age and ischemia in all of the structures studied.

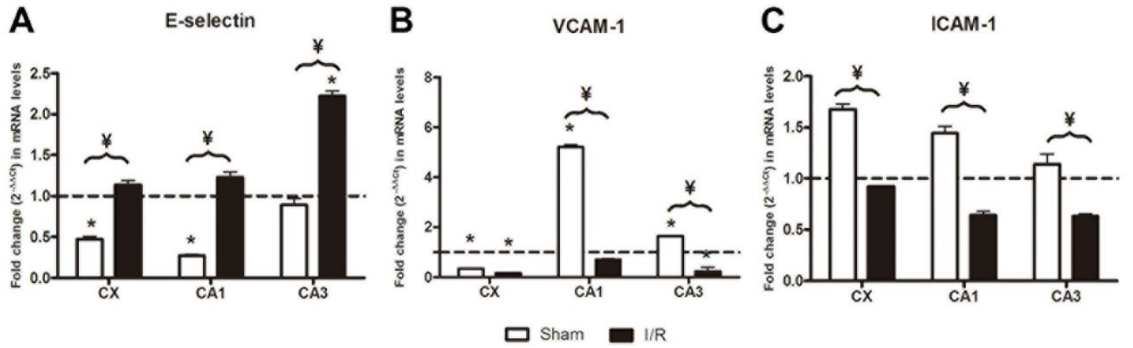

Figure 1. Effect of age on mRNA levels. Fold change ($2^{-\Delta\Delta Ct}$) in A) E-selectin, B) VCAM-1, and C) ICAM-1 mRNA levels in old sham-operated animals (open columns) as compared with young sham-operated animals (represented as a value of 1, dotted line) in the CA1 and CA3 hippocampal structures and the CX. Black columns represent old I/R injured animals as compared to their respective young I/R animals (represented as a value of 1, dotted line). Age-dependent significant differences are represented by * and significant differences between old animals are indicated by ¥ ($p < 0.05$, two way ANOVA, n = 5).

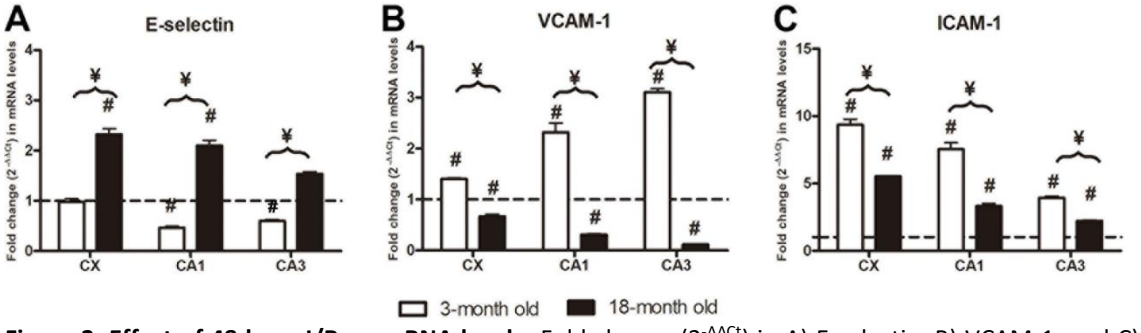

Figure 2. Effect of 48 hour I/R on mRNA levels. Fold change ($2^{-\Delta\Delta Ct}$) in A) E-selectin, B) VCAM-1, and C) ICAM-1 mRNA levels between I/R injured animals when compared with their respective sham-operated animals in the CA1 and CA3 hippocampal structures and the CX. Three month old I/R animals (open columns) and 18 month old animals (black columns) are compared with their respective sham-operated animals (represented as a value of 1, dotted line). I/R-dependent significant differences are represented by # and significant I/R difference as a consequence of age is represented by ¥ ($p < 0.05$, two way ANOVA, n = 5).

E-selectin protein levels on the hippocampus

In the cerebral cortex, E-selectin protein levels were significantly higher in both sham-operated and injured old animals when compared to the young animals. However, in the hippocampus, we failed to detect significant differences in old animals when compared to young animals.

I/R elicited increases in E-selectin in the cerebral cortex and CA3 in young animals, but we could not detect I/R-dependent differences in any of the structures in the old animals (Figure 3D-F).

P-selectin protein levels on the hippocampus and cerebral cortex

We only detected age-dependent significant P-selectin decreases in the cerebral cortex of sham-operated animals and in the CA3 of old I/R animals when compared with the respective young animals. I/R induced significant changes only in young animals, with significant decreases in P-selectin levels in the cerebral cortex and significant increases in P-selectin in the CA3. Age and I/R showed a significant interaction only in the CA3 of old animals (Figure 3A-C).

ICAM-1 mRNA levels on the hippocampus and cerebral cortex

In the hippocampus and cerebral cortex, I-CAM1 transcripts of old sham-operated animals were significantly higher when compared to young sham-operated animals. In contrast, I-CAM 1 transcripts in old injured animals were significantly lower than those of young animals in both the cortex and hippocampus (Figure 1C).

I/R elicited increases in I-CAM transcript levels in all the structures of both young and old animals. However, in young animals this effect was more noticeable. We found significant interactions between I/R and age in all structures studied (Figure 2C).

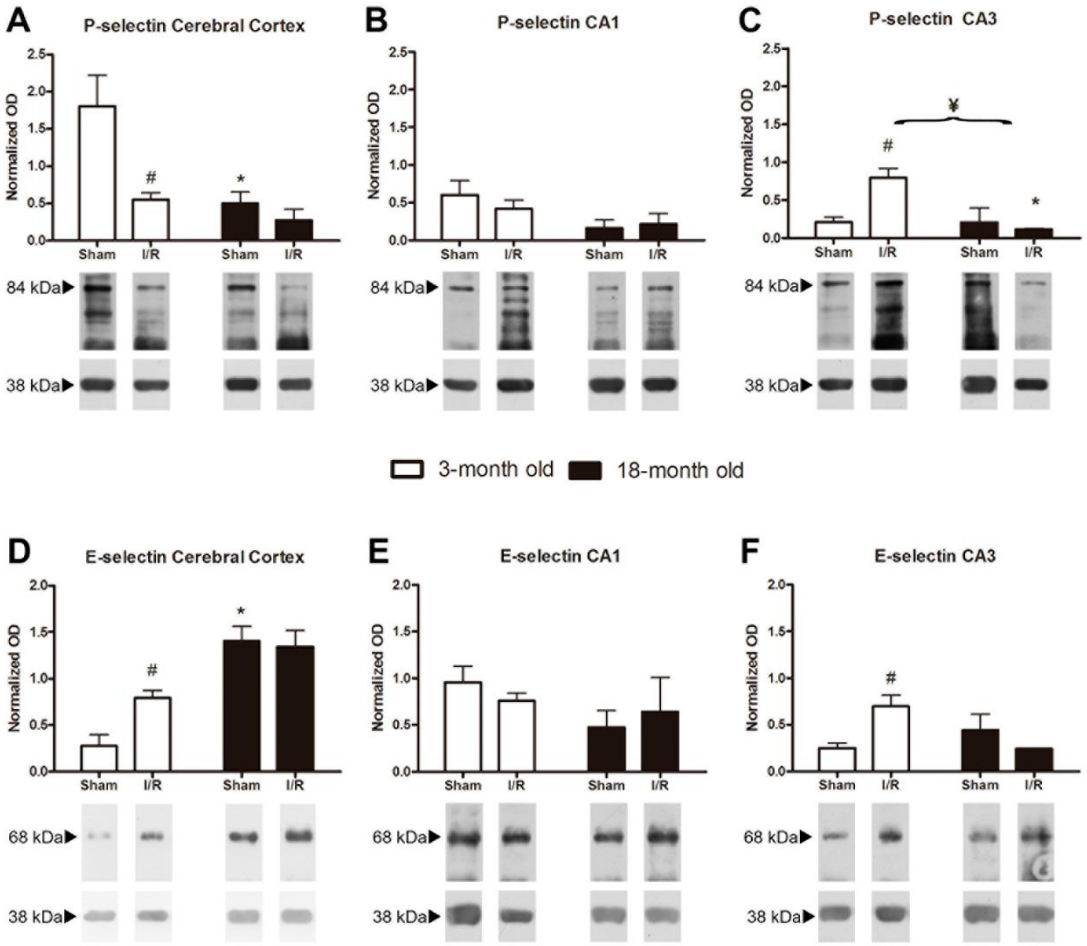

Figure 3. Effect of age and I/R on selectin protein levels. Representative protein bands of P-selectin (84 kDa) and E-selectin (67 kDa) in the CX (A and D), CA1 (B and E), and CA3 (C and F) in young (open columns) and old animals (black columns). The averages of the densitometric analysis corresponding to five rats (mean ± SEM) normalised to respect to β-actin (40 KDa) are indicated above the bands. Age-dependent significant differences are represented by *, I/R-dependent significant differences are represented by #, and significant interactions between and age and I/R are represented by ¥ ($p < 0.05$, two way ANOVA, n = 5).

ICAM-1 protein levels on the hippocampus and cerebral cortex

We only found age-dependent significant increases in ICAM-1 protein levels in the CA1 of sham-operated animals. However, old injured animals had higher levels of this protein in the cerebral cortex and CA1 than young injured animals. We only found I/R-dependent increases of ICAM-1 levels in the CA3 in both young and old injured animals (Figure 4A-C).

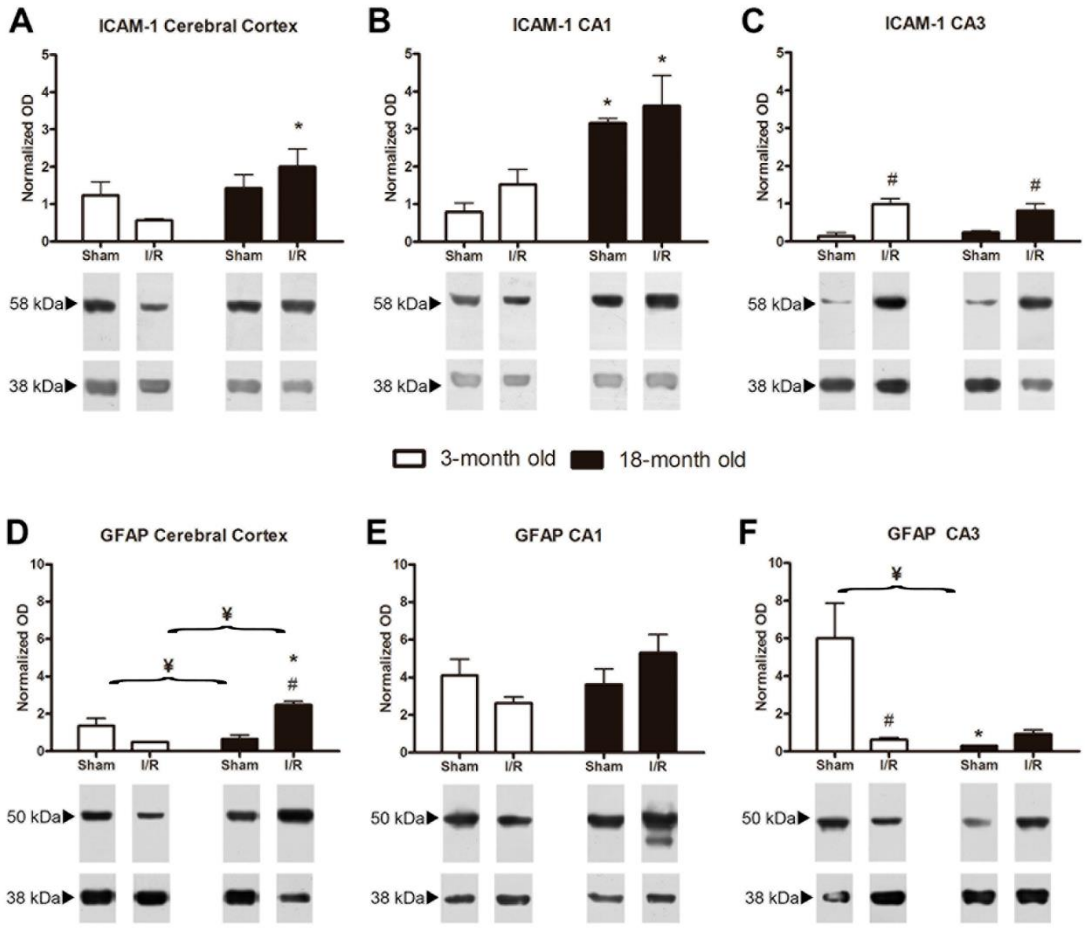

Figure 4. Effect of age and I/R on ICAM-1 and GFAP protein levels. Representative protein bands of ICAM1 and GFAP in the CX (A and D), CA1 (B and E), and CA3 (C and F) in young (open columns) and old animals (black columns). The averages of the densitometric analysis corresponding to five rats (mean ±SEM) normalised to respect to β-actin (40 KDa) are indicated above the bands. Age-dependent significant differences are represented by *, I/R-dependent significant differences are represented by #, significant interactions between and age and I/R are represented by ¥ ($p < 0.05$, two way ANOVA, n = 5).

VCAM-1 mRNA levels on the hippocampus and cerebral cortex

Considering the effect of age, VCAM-1 transcripts in the cerebral cortex were significantly lower in the old animals when compared to the young animals in both sham-operated and I/R-injured animals. However, VCAM-1 mRNA levels in the hippocampus of old sham-operated animals were significantly higher than in the young animals. The transcripts in old injured animals were significantly lower than in young injured animals in both the cerebral cortex and hippocampus (Figure 1B).

The result if the effect of I/R are shown in Figure 2B. Significant I/R-dependent increases in VCAM-1 transcript levels were observed in young animals for all of the structures studied when compared with their young sham-operated animals. This is in contrast to the significant decreases observed in old injured animals with respect to old sham-operated animals in all the structures studied.

GFAP protein levels on the hippocampus and cerebral cortex

GFAP mRNA levels at 48 hours after reperfusion in young and old animals has been previously described (Montori et al. 2010c) and, therefore, we only present the results corresponding to the GFAP protein levels. Regarding the effect of age, young sham-operated animals had significantly lower GFAP levels in the cerebral cortex when compared with the hippocampal structures. In contrast, GFAP levels of old sham-operated animals were lower in the hippocampus than in the cerebral cortex. With respect to the effect of I/R, we observed that GFAP levels decreased 48 h after I/R in young animals in all structures when compared with the sham-operated animals. This is in contrast with the increase in GFAP levels observed in the old injured animals when compared with their respective sham-operated animals (Figure 4D-F).

Cleaved caspase-3 immunolabelling on the hippocampus and cerebral cortex

In the cerebral cortex, the quantification of the apoptosis was performed in the cerebral cortical layer V pyramidal cells and in the CA1 and CA3 pyramidal cells by determining the percentage of cleaved caspase 3-positive with respect to the total number of cell pyramidal DAPI stained nuclei. Two different immunocytochemical patterns of cleaved caspase 3 labelling were observed (Figure 5). One of them was characterised by a cytoplasmic labelling, while the other showed labelling of mainly the nuclear area that correlated with abnormal nuclear morphology (Figure 6D). The first pattern was significantly higher in the pyramidal cells of old animals than in young animals, while the nuclear staining was significantly higher in young animals than in old animal (Figure 6D). Age-dependent effects on apoptosis (measured as the percentage of cleaved caspase 3 cells) were only observed in the CA3 of sham-operated animals and in the CA1 of injured animals. However, a noticeable I/R-dependent increase was observed in all of the structures for both young and old animals (Figure 6A-C).

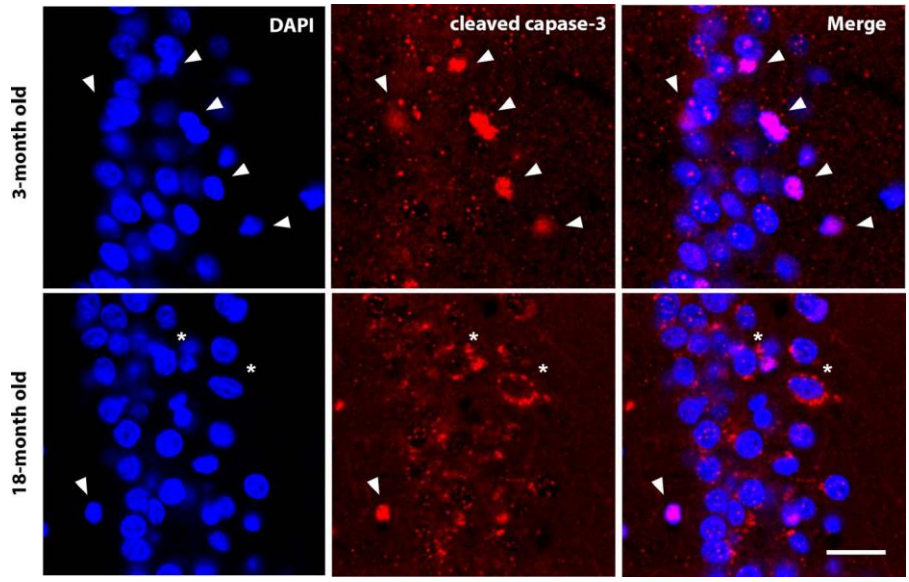

Figure 5. Different labelling patterns of apoptosis. Labelling of cleaved caspase-3 shows two different patterns: nuclear labelling (B) (arrows), which is predominant in young animals; and cytoplasmic labelling (E) (asterisks), which is predominant in old animals. Nuclear labelling with DAPI (A and D) and merged images (C and F). Bar = 20 µm.

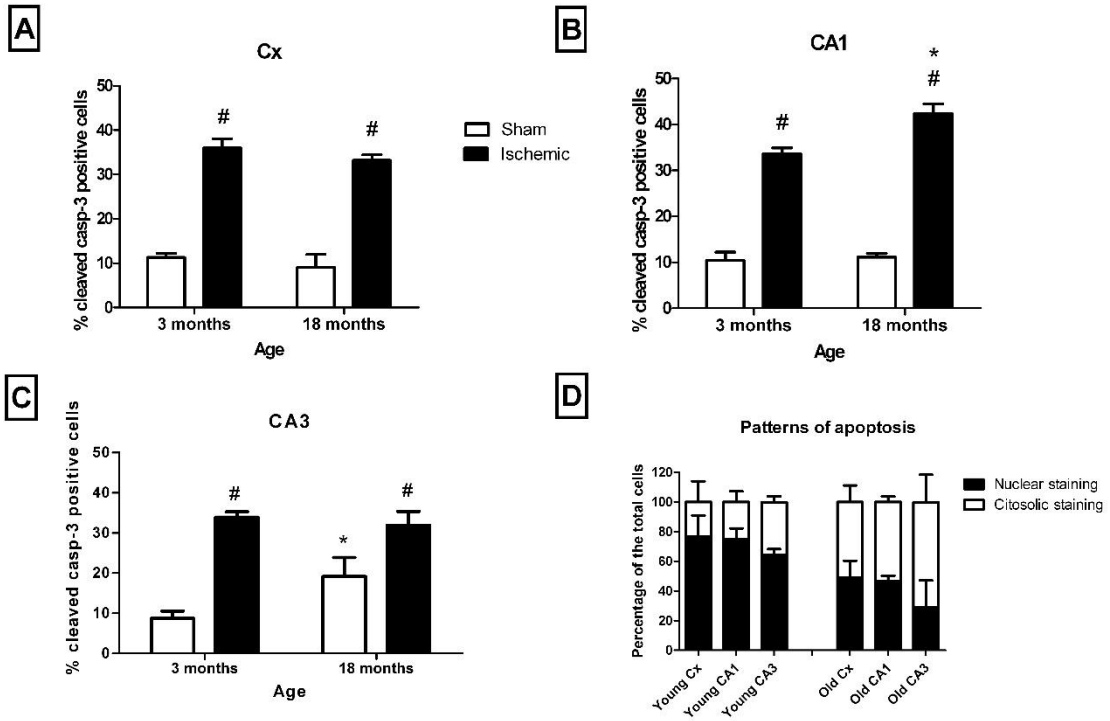

Figure 6. Age- and I/R-dependent apoptosis. Comparison of the percentage of apoptosis between young and old animals in the CX (A), CA1 (B), and CA3 (C) in sham-operated (open columns) and I/R injured (black columns) animals. The pattern of staining in both young and old I/R injured animals in the different structures are also shown (D). Age-dependent significant differences are represented by * and I/R-dependent significant differences are represented by #. No significant interactions between age and I/R were found ($p < 0.05$, two way ANOVA, $n = 5$).

Discussion

The main results of this study can be summarized as follows: a) the effects on the leukocyte transmigration markers, E-selectin, VCAM-1 and ICAM-1 transcription is modified by both ischemia and age and there is a significant interaction between these two factors; b) some of the results did not reach significance in the protein analysis of this process but significant effects of both age and ischemia and its interaction is consistent with the mRNA results; and c) in a similar way the results of GFAP as a marker of gliosis and the cleaved caspase-3 as a marker of cell mortality show the effect of age and ischemia and their significant interaction.

Selection of times and markers

The process of brain inflammation that follows I/R starts within the first hours after injury and continues for weeks (Schilling et al. 2003; Tanaka et al. 2003; Yilmaz et al. 2006). However, the maximal recruitment of circulating inflammatory cells in the brain occurs two days after ischemia (Stevens et al. 2002b; Gelderblom et al. 2009; Jin et al. 2010). Thus, comparison between young and old animals at this time is crucial to determining age-dependent differences. The onset of apoptotic morphology in the core of the lesion has been described to occur between 6–12 h, but the development of cell death in the penumbra is difficult to know (Lipton, 1999). Some studies on focal ischemia indicate that 48 h after ischemia, 30% of cells in the ischemic core appear damaged, but show no signs of death, and 15% of cells are apparently healthy (Li et al. 1998). On the other hand, 48 h after ischemia is considered the limit of the viability for cells in the penumbra area (Meisel et al. 2005; Durukan and Tatlisumak, 2007; Kadhim et al. 2008; Lakhan et al. 2009; Kriz and Lalancette-Hebert, 2009; Candelario-Jalil, 2009). Thus, we chose this time for the study because it seems to be critical in the analysis for both inflammation and mortality.

One of the hallmarks of inflammation in the brain is the activation of glia, and GFAP is probably the best marker of gliosis (Busch and Silver, 2007; Rolls et al. 2009). In this regard, gliosis drives a change in morphology that requires the expression of GFAP, which is a necessary marker to evaluate neuroinflammation. Adhesion molecules are markers that should be monitorized since the recruitment of neutrophils requires an adhesion process to allow the cell transmigration across the vascular endothelium

(Wang et al. 2007). In this regard, selectins and CAMs are the most relevant molecules involved in the adhesion process (Stanimirovic and Satoh, 2000; Wang et al. 2007; Petri et al. 2008). In an attempt to estimate the role of neuroinflammation in apoptosis we used the effector cleaved caspase-3, which is considered the main marker in apoptosis (He et al. 2006; Wang et al. 2013; Fan et al. 2014).

Cell death

Although we did not find age-dependent changes in the number of apoptotic cells at 48 hours after I/R, differences in the apoptotic activity modulated by age have been described at 8 days after global ischemia in the hippocampal CA1 (He et al. 2006). Our results show differences in the apoptotic labelling, indicating age-dependent differences in the time-course of apoptosis. In this regard, the pattern of a predominant nuclear staining has been described as a later stage in the apoptosis process than the cytoplasmic staining (Eckle et al. 2004). Our data indicate that at 48 hours after I/R, old animals exhibit earlier apoptotic stages than young animals, which could represent a higher ratio of mortality in young rats, or age-dependent differences in the time-course of the apoptosis. The similar amounts of the total number of neuronal nuclei for the different conditions and the general similar percentages of apoptotic cells, led us to assume that differences in the pattern of caspase labelling mirrors differences in the apoptotic time-course rather than the total amount of death due to apoptosis. Studies carried out using a middle cerebral artery occlusion (MCAO) model indicate that cell death in aged animals is higher after 3 days of the injury (Popa-Wagner *et al.,* 2007). However, the time course of cell death in this model and the one studied here is difficult to compare. The areas studied in the MCAO model are close to the infarct core (Popa-Wagner *et al.,* 2007) while our model simulates only the penumbra area. The distance of a cell to the infarct core is crucial in deciding whether the cell survives or dies and obviously the onset of apoptosis can be radically different. A secondary conclusion of the results of the analysis of the ischemic and sham-operated cell ratios in both young and old animals is that 48 h after I/R is too early to properly measure age-related differences in the caspase-dependent delayed cell death.

The low affinity binding

Our data show that both P and E selectins are expressed in brains of young (3 month) and old (24 month) rats, and that there are age-dependent differences between them

in the 48 h I/R response. Thus, while E-selectin transcript levels observed in old sham-operated animals are lower than their corresponding young sham-operated animals, 48 h I/R rats reveal an age-dependent increase in transcription. This indicates that E-selectin transcription is maintained at least until the age studied in this report, which is in contrast with our initial hypothesis. In this regard, we thought that age-dependent decreases in the enzymatic activity (Sinha et al. 2005; Bala et al. 2006) could be due to decreases in their expression.

E-selectin has been reported to induce the expression of CD11/CD18 integrins, which are required for the neutrophils to bind with high affinity to vascular CAMs (Petri et al. 2008). Thus, our results (both in mRNA and protein) support that the low affinity binding (rolling) is maintained in at least the old animals studied here. Protein results also indicate that CA3 and Cx, but not CA1, presented and increased I/R-dependent responses in young animals, which correlates with the lower vulnerability of the CA3 and cortex to ischemic damage. However, this difference was not maintained in the older animals, as has been recently reported (Lalonde and Mielke, 2014).

P-selectin presented a constitutive expression in peripheral tissues, but not in the cerebral endothelium (Gotsch et al. 1994; Barkalow et al. 1996). The mRNA transcript levels were too low to study accurately and, therefore, we only analysed the P-selectin protein levels. Our data suggest that in old animals, this protein presents a lessened ability of response, in contrast to what was observed for E-selectin. It is also possible that at 48 hours after I/R that P-selectin is not at its highest concentration since it is released earlier than E-selectin (Zhang et al. 1998). Therefore, we must note that, although the transcription of the E-selectin gene is maintained, we cannot be sure what happened with P-selectin since it could follow a different time-course. We also found I/R-dependent differences in P-selectin in young animals, both in the cerebral cortex and CA3, but not in CA1, as was observed for E-selectin, although in P-selectin the CA3 and CX present a diametric response. These types of differences suggest different types of regulation of the cerebrovascular unit in different areas of the brain. Differences in the endothelium along different areas of the brain have already been described (McIntosh and Warnock, 2013). Our data support that these differences could be lessened by age.

High affinity binding

Our results indicate an age-dependent diametric response in the CAMs and E-selectin transcripts in sham-operated animals, thus indicating that the transcriptional response of the molecules related with low and high affinity binding of neutrophils is modified by aging. The protein response is not as clear, but it must be taken into account that the method of protein detection is less accurate than qPCR detection. In addition, some overlap in the function of ICAM-1 and selectins (Salas et al. 2006) could explain why the differences are less evident when protein expression was compared. The results for ICAM-1 expression support the idea that transmigration or the high affinity binding is maintained or even increased in all of the structures of older animals after the ischemic damage.

Thus, the response of the selectins and CAMs observed in I/R injured animals adds further support to the idea that there are age-dependent differences for the molecules involved in low and high affinity binding of the neutrophils. Thus, this study shows that age modifies the response of these adhesion molecules either by altering their transcription or their time-course expression.

GFAP

One of the most noticeable findings in our study was the diametric response of GFAP to the ischemic insult in young and old animals. The results from the young animals confirm the ischemia-dependent decrease in GFAP expression that was previously described 48 h after reperfusion in a 4VO model of global ischemia in young Wistar rats (Zhang et al. 2007). Several studies provide evidence that aging brain reacts stronger to ischemia reperfusion with an early inflammation response (Badan *et al.,* 2003, Popa-Wagner *et al.,* 2007; Buga et al 2013) and it has been reported that aged Sprague-Dawley rats present an early glial scar in an MCAO model (Popa-Wagner *et al.,* 2006). Also, GFAP reactivity in humans has been described to depend on the age of patient (Dziewulska, 1997), which agrees with our results. However, a perfusion model of global ischemia showed increases in GFAP expression at 6 h of I/R in the cerebellum of 4–5 months old Wistar rats (Blanco et al. 2007). Also, a haemorrhagic animal model of stroke revealed increases in immunopositive GFAP cells in young animals when compared to old animals 3 days after I/R (Gong et al. 2004). Thus, results seem to be dependent on the model

used, but all of the reports show differences in GFAP protein expression between young and old animals.

The hippocampus and cerebral cortex have been reported to have different vulnerabilities to the ischemia (Kirino et al. 1985; Dijkhuizen et al. 1998; Xu et al. 2001). This difference is consistent with differences observed in the expression of different neurotransmitter system genes (Montori et al. 2010a; Montori et al. 2010b; Montori et al. 2010c) or markers of reticulum stress (Llorente et al. 2013b). Our results show that changes induced by age modify this structure-dependent vulnerability.

In summary, this study shows different responses in old and young animals at 48 h of I/R, including different patterns of apoptotic labelling, GFAP reactivity, and molecules involved in high and low affinity binding of neutrophils. We think that these age-dependent differences represent changes in the time-course response to I/R and should be taken into account in the treatments of or during the development of therapeutic targets for stroke.

CHAPTER 2

Post-ischemic salubrinal treatment results in a neuroprotective role in global cerebral ischemia

Background

Stroke is reported to be one of the major causes of death, the leading cause of permanent disability and the second-ranked cause of dementia in developed countries (Donnan *et al.* 2008; World Health Organization (WHO) 2011). Its main cause is a reduction in blood flow (ischemic stroke) that leads to an impairment in neural tissue homeostasis. The extent of brain damage after stroke depends on the ability of the brain to recover homeostasis (Doll *et al.* 2015; Posada-Duque *et al.* 2014). At the cellular level, ischemia results in accumulation of unfolded proteins in the ER stress. This elicits the so-called UPR, which attempts to restore cell homeostasis and prevent cell death (Kaufman 1999; Walter and Ron 2011). At a systemic level, ischemia elicits a protective inflammatory response whose excess results in the so-called sterile inflammation that contributes to increase the neural damage (Ceulemans *et al.* 2010; Corps *et al.* 2015). Much evidence supports the crosstalk between UPR and inflammation, suggesting new targets for stroke therapies (Aarts *et al.* 2003; Hasnain *et al.* 2012; Zhang and Kaufman 2008).

The ischemia-induced inflammatory response has been reported to modify the BBB, also called the neurovascular unit (Hawkins and Davis 2005). Inflammation contributes to BBB impairment by increasing the expression of the CAMs in the endothelium (Jin *et al.* 2010), as well as promoting the release of MMPs. These enzymes degrade the extracellular matrix and assist leukocyte migration through the endothelium, allowing blood proteins to extravasate into the cerebral parenchyma (Wang *et al.* 2007; Yilmaz and Granger 2010). In turn, this increases the BBB permeability and the inflammatory response, increasing the ischemia-induced damage.

One key marker of inflammation is TNF-α, the major pro-inflammatory cytokine (Joussen *et al.* 2009), which ignites the canonical NF-κB activation and is considered the main

pathway in the inflammatory response (Rius *et al.* 2008). TNF-α promotes the expression of CAMs and MMPs and is also a strong inducer of ER stress (Li *et al.* 2011; Xue *et al.* 2005). In turn, ER-stress is able to induce a non-canonical activation of NF-κB, inhibiting the canonical NF-κB activation induced by the inflammatory stimuli (Kitamura 2009; Nakajima and Kitamura 2013). The earlier UPR pathway is activated by PERK (Nakka *et al.* 2014). The PERK pathway is characterized by eIF2α phosphorylation (Schroder and Kaufman 2005; Schroder 2008), which leads to a general blocking of protein translation (Fernandez *et al.* 2002; Harding *et al.* 2000). The eIF2α phosphorylation has been reported to be the necessary and sufficient requirement for the non-canonical ER-stress dependent activation of NF-κB (Deng *et al.* 2004; Jiang *et al.* 2003). Salubrinal, an inhibitor of phosphatase PP1, blocks the dephosphorylation of eIF2α (Boyce *et al.* 2005), thus enhancing the PERK pathway. This enhancement could be a protective therapeutic strategy to prevent vascular inflammation (Halterman *et al.* 2008; Li *et al.* 2011). In fact, treatment with salubrinal prior to ischemic insult presents a neuroprotective effect (Nakka *et al.* 2010) and a recent study has also demonstrated a neuroprotective role of salubrinal in traumatic brain injury (Rubovitch *et al.* 2015).

We hypothesize that the enhancement of UPR would reduce both ER stress and the inflammatory response, thus reducing the ischemic damage. In this report we demonstrate for the first time the neuroprotective role of salubrinal treatment administered after an ischemic insult and show that this agent modifies the inflammatory response triggered by ischemia. We also show that ischemic insult induces structure-dependent differences in the BBB permeability.

Material and methods

Animals

Sixty three-month-old Sprague-Dawley male rats (350–450 g) were housed at standard temperature (22 ± 1 ºC) in a 12 h light/dark cycle with food (Panlab, Barcelona, Spain) and water *ad libitum*. The experimental groups were set up as indicated in Table 1.

Table 1. Experimental groups

Time of I/R	Sham animals		Ischemic animals	
5 h			Treated (5IR-Sal)	Vehicle(5IR-Vehicle)
24 h	Treated (24S-Sal)	Vehicle (24S-Vehicle)	Treated (24IR-Sal)	Vehicle(24IR-Vehicle)
48 h	Treated (24S-Sal)	Vehicle (24S-Vehicle)	Treated (48IR-Sal)	Vehicle(48IR-Vehicle)
7 days		Vehicle (7D-S)	Treated (7DIR-Sal)	Vehicle(7DIR-Vehicle)

All experimental procedures were carried out in compliance with the ARRIVE guidelines, in accordance with the Guidelines of the European Union Council (63/2010/EU) following Spanish regulations (RD 53/2013, BOE 8/2/2013) for the use of laboratory animals and were approved by the Scientific Committee of the University of Leon. All efforts were made to minimize animal suffering and to reduce the number of animals used.

Transient global cerebral ischemia

Animals injured following a two-vessel occlusion global cerebral ischemia model (IR) and their corresponding sham operated controls (without carotid clamping) were obtained following the procedure previously described (Vieira et al. 2014). Briefly, induction of anesthesia was carried out with 4% isoflurane (IsoFlo, Abbott Laboratories Ltd) in 3 L/min in 100% oxygen and then animals were maintained under anesthesia with a flux of 1.5–2.5% isoflurane at 800 mL/min in 100% oxygen, through a face mask. After exposing both carotid arteries, the femoral artery was exposed and catheterized to record blood pressure along the whole procedure. This pathway was also used to maintain a moderate hypotension (40–50 mm Hg) by partial exsanguination (about 8 ml of blood slowly extracted at 1 ml/min) to prevent the blood flow to the brain through the paravertebral arteries. To prevent clot formation, 50 UI heparin/kg were supplied to the animal through this catheter and 50 UI heparin were maintained in 3 ml saline in the syringe used for storing extracted blood. When hypotension values were stable, the transient global ischemia was induced by clamping both common carotid arteries for 15

min. Temperature of the body was maintained at 36 ± 1 °C during surgery with a feedback-regulated heating pad using a rectal probe. After ischemia, blood was returned to the animal at 1 ml/min until the arterial blood pressure recovered. After removing the catheter, the animal was sutured and once consciousness returned it was transported to an air-conditioned room at 22 ± 1 °C until sacrificed. The same procedure was carried out in sham operated rats, except the carotid arteries clamping.

Salubrinal treatment

One hour after surgery, all animals were injected intraperitoneally either with 1 mg/kg of salubrinal (TOCRIS, Bristol, UK) in saline with 1.5% DMSO, or vehicle. Animals with 48h and 7 days of IR were injected with a second dose of salubrinal or vehicle 24 h after surgery.

Tissue dissection ant total RNA and protein extraction

After decapitation, brains were quickly removed and placed on a brain rodent matrix (ASI Instruments, Warren, MI) at 4 ºC to obtain 2 mm thick sagittal slices at a distance of 1 mm to the medial line. *Cornu Ammonis 1* (CA1) and *Cornu Ammonis* 3 (CA3) hippocampal regions, as well as the cerebral cortex (Cx) above them, were dissected under a light microscope. Samples were frozen in dry ice and stored at -80ºC. Total RNA and protein were extracted from each dissected brain region using the Tripure Isolation Reagent® (Roche Diagnostics, Barcelona, Spain) following the manufacturer's instructions and then stored at -80ºC.

Reverse transcriptase reaction and qPCR

All qPCR assays in this study were performed following the Minimal Information for Publication of Quantitative Real-Time PCR Experiments (MIQE) Guidelines (Taylor *et al.* 2010). RNA integrity and retrotranscription was performed as previously described (Anuncibay-Soto *et al.* 2014). Quantitative PCR (qPCR) was performed in a Step One Plus thermocycler (Applied Biosystems, Foster City, CA) using the following primers: *mmp-9*: (f5'ttctgtccagaccaagggtaca, r5'gcgcatggccgaactc, NM_ 031055.1); *vcam-1*: (f5'tgctcctgacttgcagcaccac, r3'tgtcatcgtcacagcagcaccc, NM_ 012889.1); *icam-1*: (f5'tgcagccggaaagcagatggtg, r3'atggacgccacgatcacgaagc, NM_012967.1); *gapdh*: (f5'gggcagcccagaacatca, r3'tgaccttgcccacagcct, NM_017008).

Optimal qPCR conditions in our assays were obtained using 2 µl of 1/10 cDNA and 300 nM of, using SYBR Green Master Mix as the fluorescent DNA dye (Applied Biosystems,

Foster City, CA). The results were analysed following the $2^{-\Delta\Delta Ct}$ method (Livak and Schmittgen 2001). using *gapdh* housekeeping gene as a reference to normalize the Ct values for each gene to be analysed. Fold changes were expressed as $2^{-\Delta\Delta Ct}$, where ΔΔCt represents the transcript variation between the different conditions $(\Delta Ct_{ischemic} - \Delta Ct_{sham})$ and $(\Delta Ct_{salubrinal} - \Delta C_{tvehicle})$.

Western blot analysis

Protein samples were resuspended in 8 M urea with 4% SDS in the presence of a protease inhibitor (complete protease inhibitor cocktail EDTA free; Applied Biosystems, Foster City, CA) and quantified using a DC Protein Assay Kit (Bio-Rad, Hercules, CA). Band gels were obtained from 25 µg of each sample as previously described(Anuncibay-Soto *et al.* 2014) using the following primary antibodies: NF κB raised in rabbit (Abcam, Cambridge, UK, 1 µg/ml); MMP-9 raised in rabbit (Abcam, 1 µg/ml); ICAM-1 raised in rabbit (Abcam, 0.75 µg/ml); GFAP raised in rabbit (Dako, Glostrup, Denmark, 1 µg/ml); TNF-α raised in rabbit (Abcam, 1 µg/ml) and β-actin raised in mouse (Sigma Aldrich, Madrid, Spain, 0.2 µg/ml).

The resulting bands were digitalized in a GS-800 Calibrated Densitometer (Bio-Rad, Hercules, CA) and band optical densities were quantified with ImageJ Software (NIH, Washington, MD). The corresponding β-actin bands were used to normalize the optical density of the bands.

Immunofluorescence assays

Another 15 rats with 7 days of reperfusion were euthanized with an intraperitoneal dose of 200 mg/kg of sodium pentobarbital (Vetoquinol, Vernois, France) and immediately perfused via intra-aortic delivery of 4% paraformaldehyde as previously described (Anuncibay-Soto *et al.* 2014). Fixed brains were cut in 40 µm thick coronal sections for immunohistochemical assays.

An epitope-retrieval step was conducted transferring the sections to 0.05% Tween-20 in 10 mM sodium citrate buffer, pH 6.0, at 80 ºC for 30 minutes followed by blocking in 20% goat serum with 0.2% TritonX-100 in PBS for 1 h at RT. Sections were incubated overnight at 4 ºC with anti-NeuN antibody raised in mouse (1:500) (Millipore, Darmstadt, Germany) and then with a rabbit anti-mouse IgG conjugated with Alexa-568 (1:500)(Life Technologies, Carlsbad, CA). Nuclei were counterstained with DAPI (Sigma, Madrid, Spain) and sections mounted using Fluoromount G Mounting Medium (Life

Technologies, Carlsbad, CA). The number of cells stained with NeuN in different areas was measured following the principles of the optical dissector method (serial random sections, section sampling fraction, area sampling fraction and thickness sampling fraction) (Gundersen et al. 1988; Zarow et al. 2005). Six equidistant non-overlapping 40 µm thick sections between Bregma -1.8 to -4.3 mm (rostro-caudal axis), following Paxinos and Watson (1996), were analysed per animal using optical dissectors with 50 x 50 µm grid squares and a height of 30 µm for the fractionator volume (5 µm of both the top and the bottom of the section with putative damage from the cutting process were discarded). Five equidistant dissectors in the layer III of the frontoparietal cortex, motor area between 1 and 5 mm lateral to the midline, 5 equidistant dissectors in hippocampal CA1 and 4 in hippocampal CA3 areas were analyzed per section. Final results are expressed as the number of cells/mm3. Image acquisition was carried out with a Nikon Eclipse TE-2000 Confocal Microscope (Nikon Instruments, Amsterdam, Netherlands). Image processing and analysis were performed using ImageJ Software (NIH, Washington, MD).

C reactive protein:

Blood samples from each animal were centrifuged at 1500 x g for 15 minutes and the supernatant was frozen at -80 ºC until the ELISA test for C-reactive protein (RayBiotech, Norcross, GA) could be performed following the manufacturer's instructions.

Statistical analysis

Graph Pad Prism 6.0 Software (Graph Pad Software Inc, La Jolla, CA) was used for statistical analyses. Quantitative results are expressed as mean ± SEM. Two-way ANOVA following by Bonferroni post-hoc test, one-way ANOVA following by Tukey post-hoc test or Student t test followed by unpaired t test were conducted setting the confidence level at 95%.

Results

Salubrinal effect on UPR-PERK pathway

The treatment previous to the ischemic insult with salubrinal has been reported to increase the eIF2α phosphorilation in the first hours after the insult (Nakka *et al.* 2010)

. We observed that the post-ischemic treatment with salubrinal also increased the IF2α phosphorylation 5 h after ischemia in treated vs. non-treated insulted animals. We analysed it to prove the UPR enhancement in the model here presented (Fig. 1A). This effect disappeared at 24 hours. (Fig. 1B).

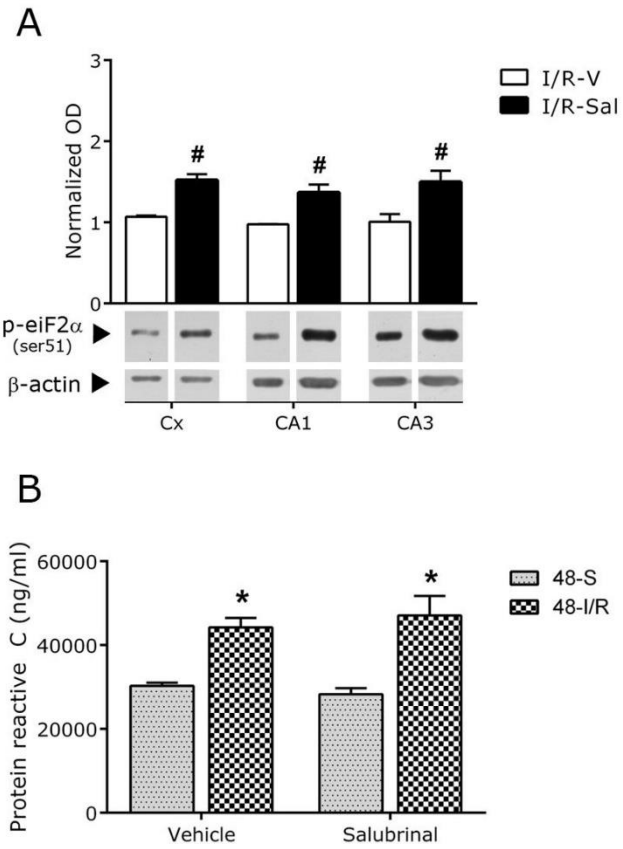

Figure 1. Effects of salubrinal on UPR and inflammation. Salubrinal treatment elicited an enhancement of UPR in the different structures studied but did not promote a significant effect on blood inflammation markers. Representative protein bands of A) phosphorylated eIF2α (38 kDa) at 5 IR hours, B) phosphorylated eIF2α (38 kDa) at 24h IR hours and C) C reactive protein at 48 IR hours. The averages of the densitometric analysis corresponding to five rats (mean ± SEM) normalized with respect to β-actin (40 kDa) are indicated above the bands. # indicates significant differences between the IR-Sal and IR-vehicle groups. * indicates significant differences between IR and sham in treated and non-treated animals. In all cases $p<0.05$ by two tails unpaired Student t test, n=5.

Inflammation markers

C-reactive protein, TNF-α, and NF-κB were used as inflammation parameters. **C-reactive protein** blood levels were measured at 48 h and appeared significantly increased as a consequence of IR. Salubrinal treatment following IR did not present significant changes (Fig. 1B). **TNF-α** levels were almost undetectable in Cx both at 24 h and 48 h after the insult; however, hippocampal levels were noticeable at both times (Fig. 2A, B). Significant ischemia-dependent TNF-α increases were observed in CA1 comparing 48IR-

vehicle with 48S-vehicle animals (Fig. 2B) and in CA3 comparing 24IR-vehicle with 24S-vehicle animals (Fig. 2A). Also, strikingly higher levels of TNF-α were observed in both structures comparing 48IR-vehicle with 24IR-vehicle animals. Interestingly, the treatment with salubrinal decreased the TNF-α levels in sham animals both at 24 and 48 h but resulted in significant increases in 24IR-Sal compared to 24IR-vehicle and non-significant when 48IR-Sal were compared to 48IR-vehicle animals. Significant interactions between salubrinal treatment and IR were observed in CA1 at 24 h.

NF-κB levels were detectable in all the structures studied (Fig. 2C, D). Significantly increased levels of this protein as a consequence of the IR were observed only in CA3 at 24 h. After salubrinal treatment we observed significant increases in NF-κB in Cx when comparing 24IR-Sal with 24IR-vehicle animals, and in CA1 when comparing 24S-Sal with 24S-vehicle animals (Fig. 2C). This contrasts with the significant decreases observed for 48IR-Sal with respect to 48IR-vehicle animals (Fig.2D). The same comparisons in CA3 revealed a diametric response to that observed in Cx and CA1 with a salubrinal-dependent decrease at 24 h and a salubrinal-dependent increase at 48 h. A significant interaction between salubrinal treatment and IR was observed in Cx at 48 h.

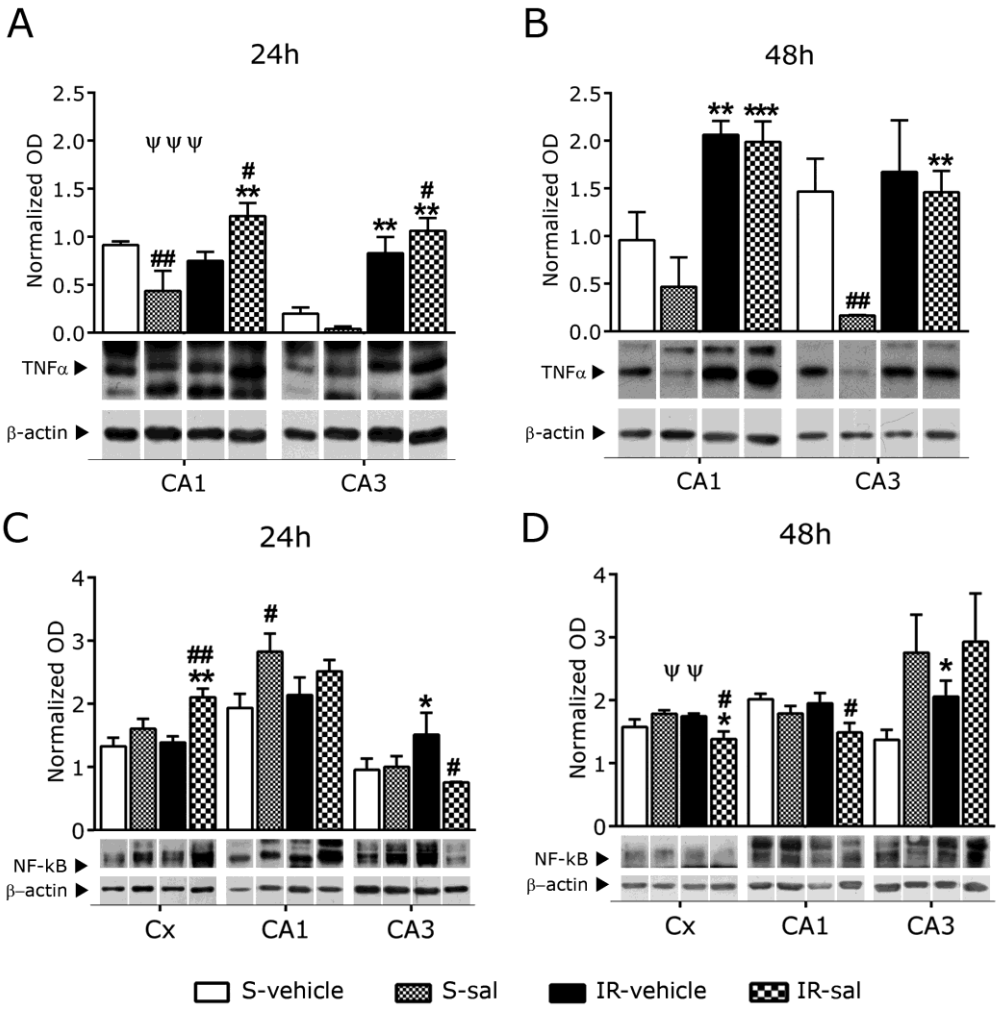

Figure 2. Effect of IR time and treatment on protein levels of inflammatory markers. Representative protein bands of TNF-α (23 kDa) at A) 24 h and B) 48 h and NF-κB (55 kDa) at C) 24 h and D) 48 h in the different structures studied. Averages of the densitometric analysis corresponding to five rats (mean ± SEM) normalized with respect to β-actin (40 kDa) are indicated above the bands. Of note, TNF-α expression is undetectable in Cx. Statistics between the different conditions, indicated at the bottom of the image, are represented by an asterisk when IR are compared, by a number sign when treatments are compared and by a yen sign for significant interactions between IR and treatment. In all cases $p<0.05$ by two way ANOVA, n=5.

Neurovascular unit

GFAP is used as an inflammatory marker of the brain (Wang *et al.* 2007). IR animals treated with salubrinal showed a significant decrease in their GFAP levels at 24 h in Cx and CA1 when compared with sham animals (Fig 3A). This effect disappeared at 48 h (Fig 3B). In turn, CA3 displayed a different response, with no changes under the different conditions at 24 h and significant increases as a result of the ischemic insult (48 IR-vehicle versus 48S-vehicle), in contrast with the significant decreases as a result of the salubrinal treatment (48IR-Sal compared to 48S-Sal). Also, salubrinal treatment

significantly increased the CA3 GFAP protein levels in sham animals at 48 h. This effect also seemed to appear at 24 h but we failed to detect any statistical significance (Fig 3B). **Matrix metalloproteinase 9** (MMP-9) protein levels appeared significantly increased as a consequence of the ischemia in all the structures at 48 h but only in the Cx at 24 h (Fig 3 C, D). The treatment with salubrinal resulted in significant decreases of MMP-9 levels in Cx and CA1 (48IR-Sal compared with 48IR-vehicle). Interestingly, this comparison in CA3 revealed a diametrically opposed effect with a significant salubrinal-induced increase in MMP-9 levels. A significant interaction between ischemia and salubrinal was observed in Cx at 48 h.

MMP-9 transcript level did not reveal significant differences in any of the structures studied when ischemic vehicle animals where compared to sham vehicle animals (Fig 4 A, B). The treatment with salubrinal resulted in significant MMP-9 transcript level decreases in all the structures when ischemic treated animals were compared with the corresponding sham treated animals at 24 h (Fig 4A). However, at 48 h, only CA1 still showed these significant transcript decreases observed in the treated animals (Fig 4B). Similar levels of MMP-9 transcripts were observed between sham animals treated and non treated with salubrinal, except in CA1 at 24 h (Fig 4C). Interestingly, this comparison in ischemic animals revealed that salubrinal induced significant decreases in CA1 and CA3 at 24 h and in CA1 at 48 h (Fig 4 C, D).

ICAM-1 protein levels significantly increased as a consequence of the IR in CA3 at 24 h as well as in CA1 and in Cx at 48 h (Fig 3E, F). The treatment with salubrinal in IR animals showed a trend to decrease the ICAM-1 levels in CA1 and Cx that was significant in CA3 at 24 h and in Cx at 48 h. Interestingly, the treatment with salubrinal was able to increase the ICAM-1 levels in CA3 of sham animals at 24 h, but decreased them in the Cx.

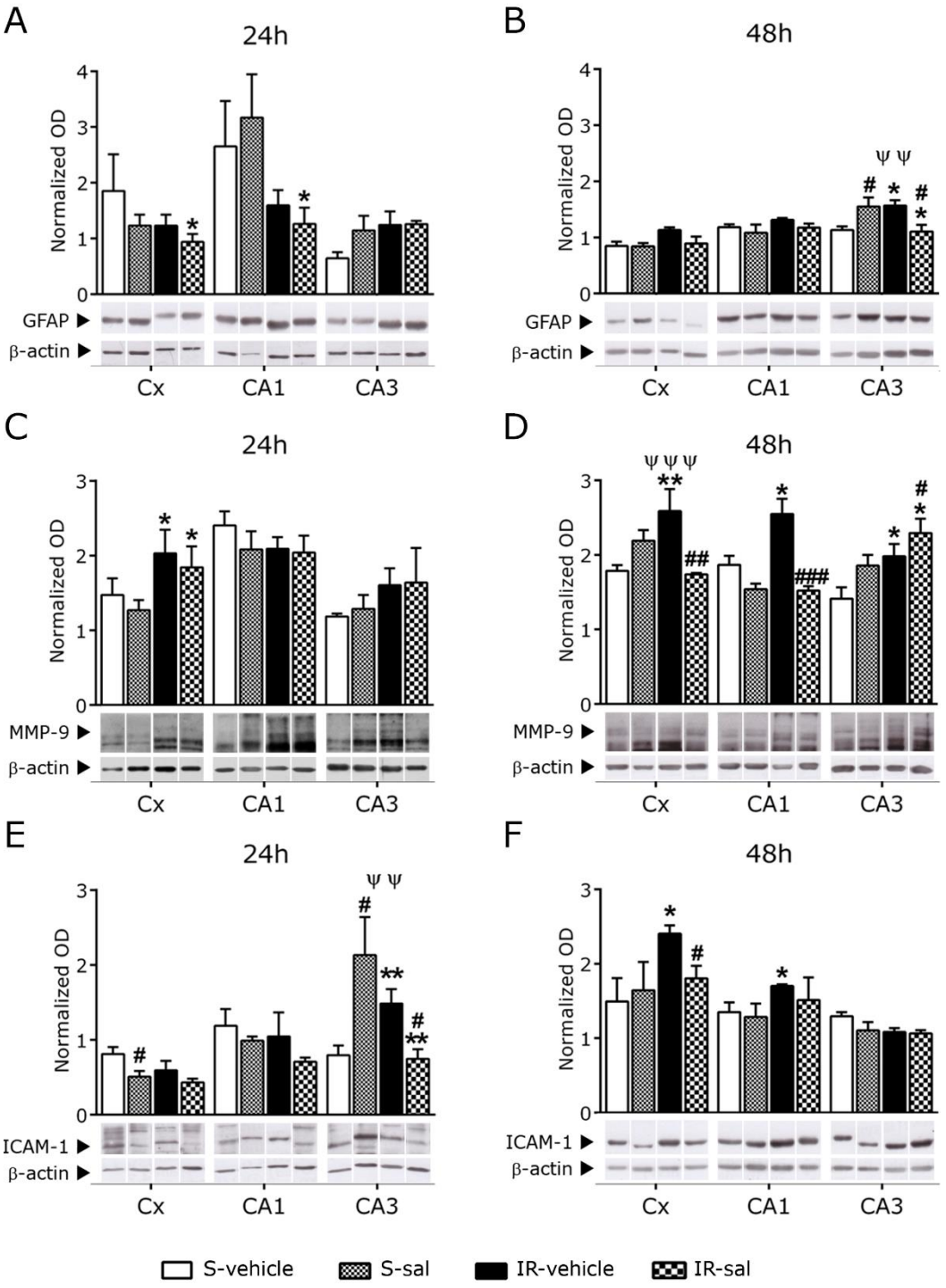

Figure 3. Effect of IR time and treatment on protein levels of different neurosvacular unit components. Representative protein bands of GFAP (50 kDa) at A) 24 h and B) 48 h, MMP-9 (87 kDa) at C) 24 h and D) 48 h and ICAM-1 (58 kDa) at E) 24 h and F) 48 h in the different structures studied. Averages of the densitometric analysis corresponding to five rats (mean ± SEM) normalized with respect to β-actin (40 kDa) are indicated above the bands. Statistics between the different conditions, indicated at the bottom of the image, are represented by an asterisk when IR are compared, by a number sign when treatments are compared and by a yen sign for significant interactions between IR and treatment. In all cases $p<0.05$ by two way ANOVA, n=5.

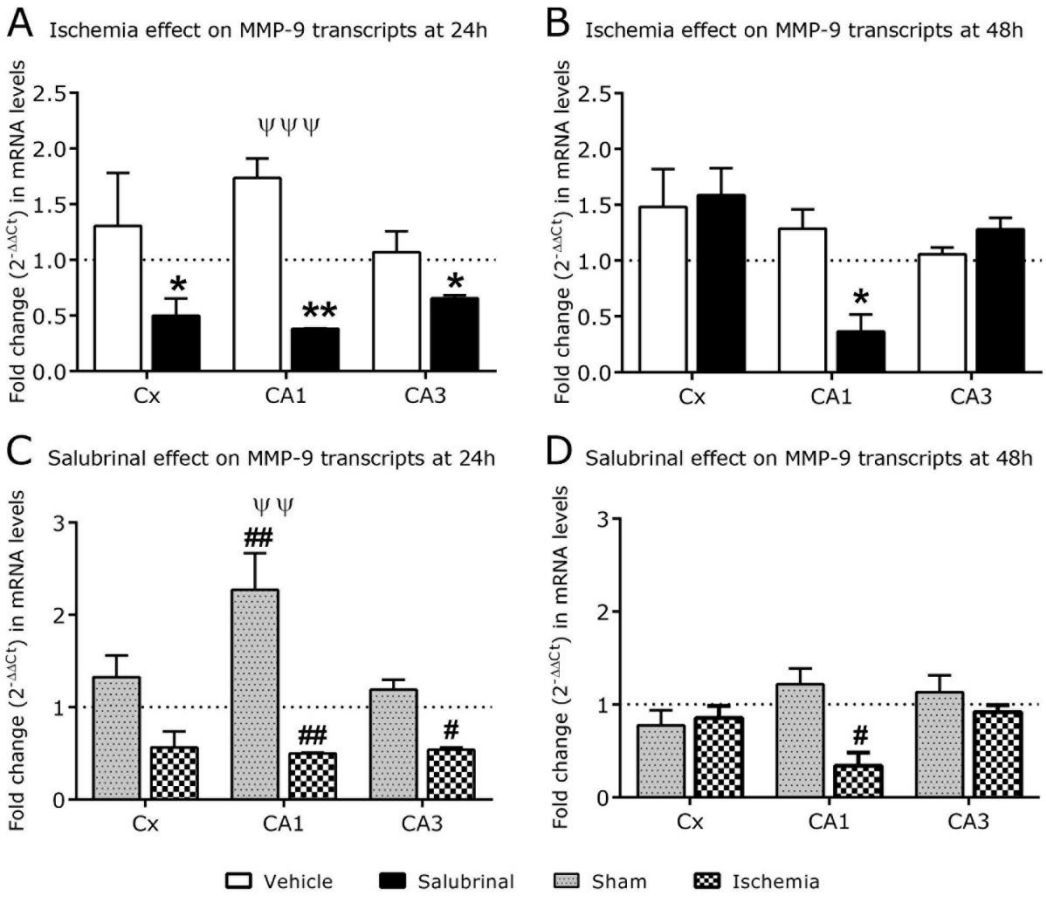

Figure 4. Effect of IR time and salubrinal treatment on neurovascular unit MMP-9 mRNA levels. Fold changes ($2^{-\Delta\Delta Ct}$) at 24 and 48 hours showing the effect of ischemia (A, B) and the effect of salubrinal (C, D) on MMP-9 transcripts. The controls (respective sham animals in A and B, and respective non-treated animals in C,D) are represented by a value of 1, dotted line. Statistics between the different conditions are represented by * when IR are compared, by # when treatments are compared and a ¥ for significant interactions between IR and treatment. In all cases $p<0.05$ by two way ANOVA, n=5.

ICAM-1 transcript levels appeared significantly increased by IR in CA3 at 24 h (Fig 5A, C) and in Cx and CA1 at 48 h (Fig 5B, D). The treatment with salubrinal resulted in blocking or decreasing the effect of the IR both at 24 h and 48 h (Fig 5A, B). In sham animals, the salubrinal treatment did not elicit an intrinsic effect on ICAM-1 transcript levels, but decreased them significantly in all the structures in 48IR animals (Fig 5C, D). Significant interactions between salubrinal treatment and IR were observed in CA3 at 24 h and in all structures at 48 h.

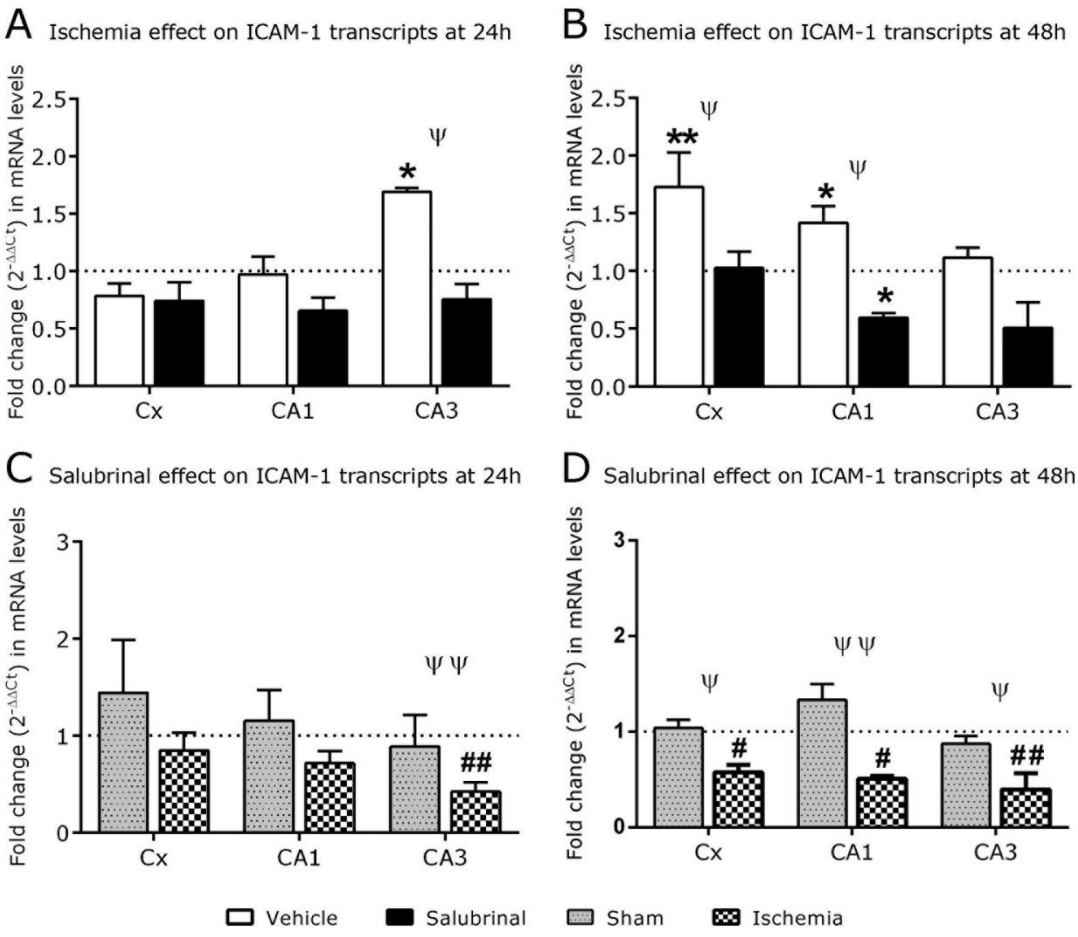

Figure 5. Effect of IR time and salubrinal treatment on neurovascular unit ICAM-1 mRNA levels. Fold changes ($2^{-\Delta\Delta Ct}$) at 24 and 48 hours showing the effect of ischemia (A, B) and the effect of salubrinal (C, D) on ICAM-1transcripts. The controls (respective sham animals in A and B, and respective non-treated animals in C,D) are represented by a value of 1, dotted line. Statistics between the different conditions are represented by * when IR are compared, by # when treatments are compared and a ¥ for significant interactions between IR and treatment. In all cases $p<0.05$ by two way ANOVA, n=5.

VCAM-1 transcript levels increased significantly as a consequence of IR in Cx and CA1 at 48 h but only in Cx at 24 h. These ischemia-induced increases in VCAM-1 mRNA levels were abolished or decreased by the treatment with salubrinal (Fig 6). Of note, the salubrinal treatment resulted in a tendency to increase these transcripts in CA3 both at 24 h and 48 h that was significant in the comparison between IR treated and non-treated animals (Fig 6A, C). No intrinsic effect of salubrinal on these transcripts was observed in sham animals (Fig 6C, 6D). Significant interactions between salubrinal treatment and IR were observed for Cx at 24h and 48 h, in CA3 at 24 h and in CA1 at 48 h.

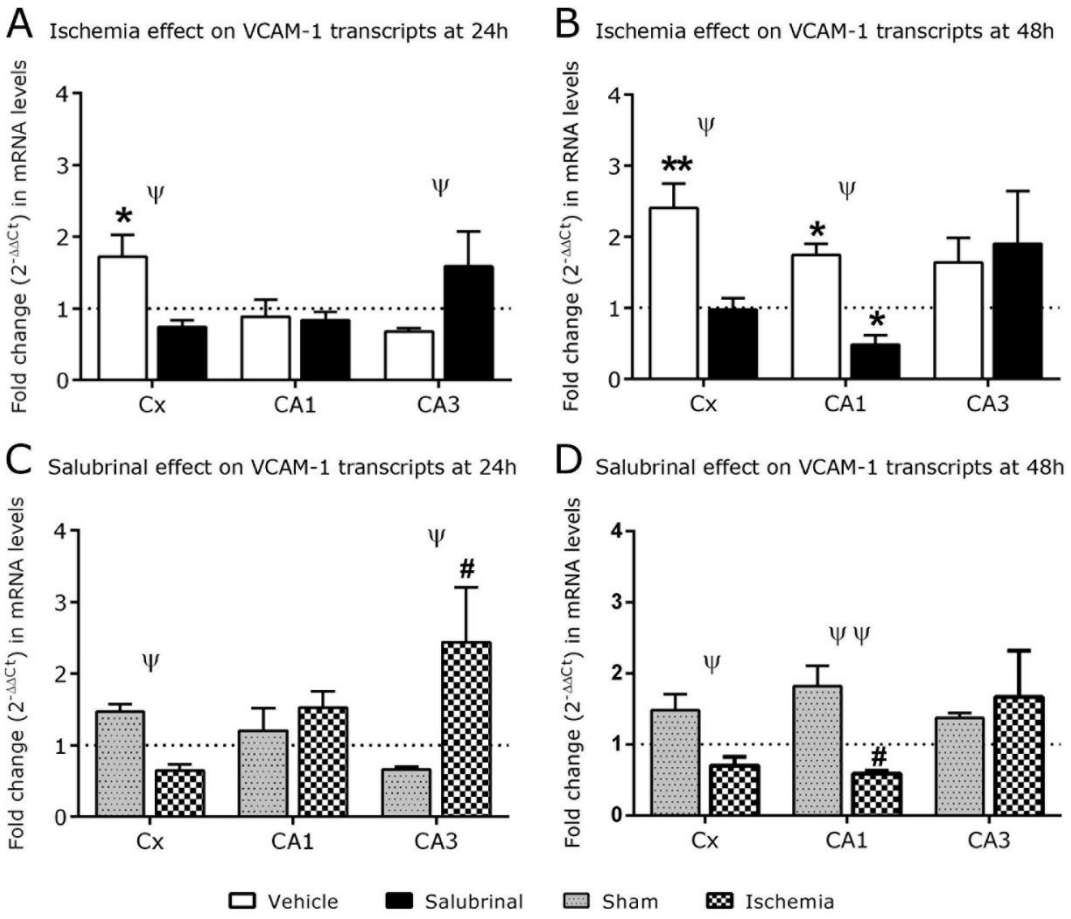

Figure 6. Effect of IR time and salubrinal treatment on neurovascular unit VCAM-1 mRNA levels. Fold changes ($2^{-\Delta\Delta Ct}$) at 24 and 48 hours showing the effect of ischemia (A, B) and the effect of salubrinal (C, D) on VCAM-1 transcripts. The controls (respective sham animals in A and B, and respective non-treated animals in C,D) are represented by a value of 1, dotted line. Statistics between the different conditions are represented by * when IR are compared, by # when treatments are compared and a ¥ for significant interactions between IR and treatment. In all cases $p<0.05$ by two way ANOVA, n=5.

Cell demise

An IR-induced significant decrease in the number of NeuN-labelled cells was observed in pyramidal layers of CA1, CA3 and Cx. The treatment with salubrinal significantly reduced the neuronal demise only in the CA1 pyramidal layer (Fig 7A, B).

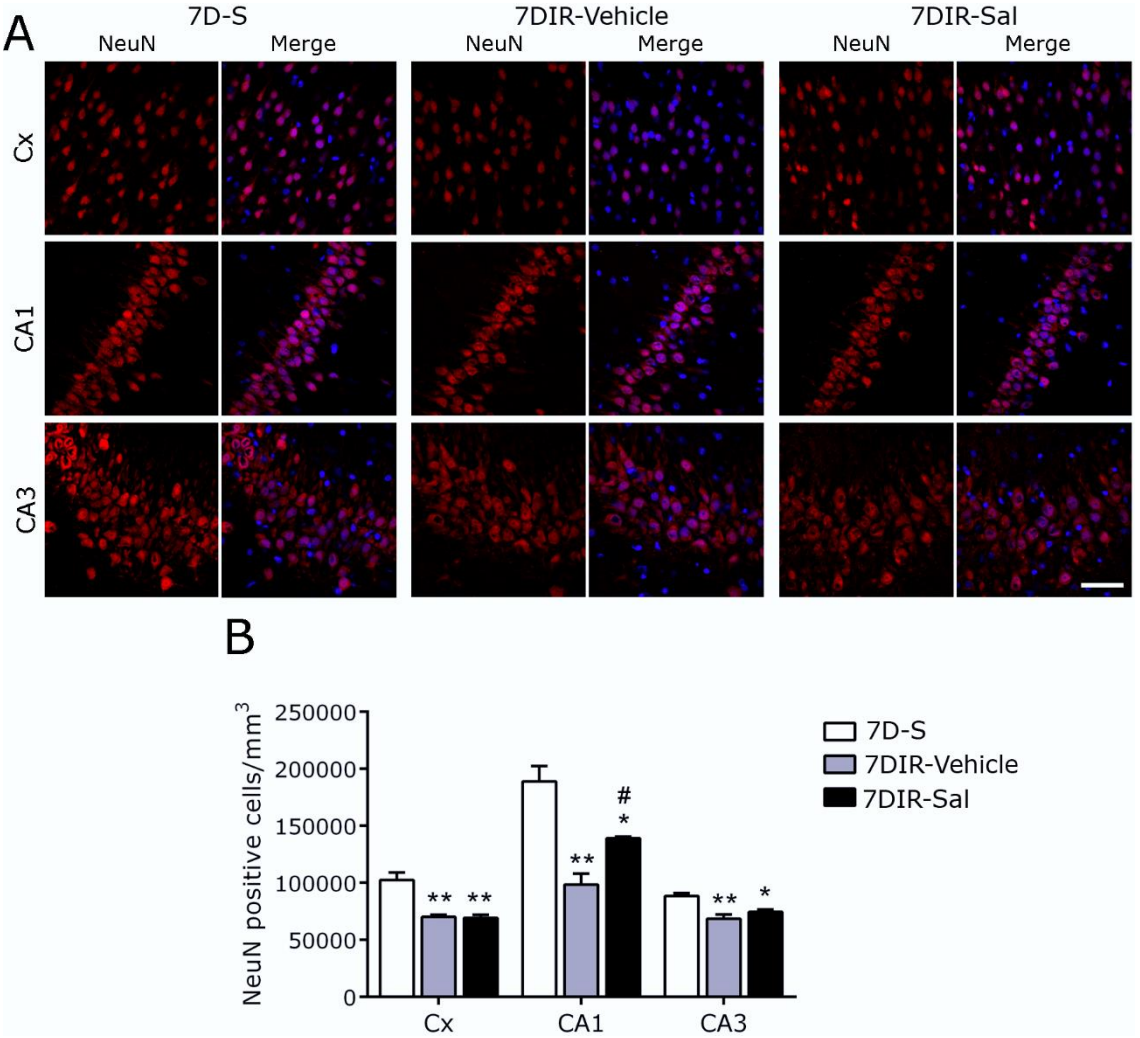

Figure 7. Neuronal demise after salubrinal treatment. A) Cortex, CA1 and CA3 labelled with NeuN and with NeuN+DAPI in the the different conditions studied. Bar= 50 µm. B) Graph shows the number of neurons stained with NeuN in IR non-treated (white columns) and treated (black columns) with salubrinal. Significant differences as a consequence of IR are represented by * and significant differences between treatments are indicated by #. ($p<0.05$, one way ANOVA, n=5).

Discussion

The inflammatory response after global ischemia is structure-dependent

TNF-α levels observed in this study reveal a lower inflammatory response in Cx compared to hippocampus, suggesting that hippocampus would be more prone to sterile inflammation. In addition, the inflammatory response is different in CA3 and CA1. Thus, CA3 presented a faster response that disappeared at 48 h, compared to the delayed and striking response at 48 h observed in CA1. This suggests that the hippocampal sterile inflammation is limited to CA1 and could account for its greater

neuronal demise at 7 days, in accordance with the greater ischemic-induced vulnerability described for CA1 (Kirino *et al.* 1985; Petito *et al.* 1987; Zhu *et al.* 2012). Moreover, the treatment with salubrinal brings forward to 24 h the CA1 TNF-α peak and increases the TNF-α levels in CA3 at 24 h, indicating that enhancing UPR-PERK pathway modifies the time course of the inflammation, which would be in agreement with the increases of NF-κB observed at 24 h. Of note, salubrinal acts at a local level and does not modify the inflammation markers in blood, as reveals the lack of reponse of C-reactive protein in the blood.

UPR inhibits NF-κB activation by inflammatory stimuli (canonical pathway) but ER stress is able to activate NF-κB through the non-canonical pathway, as described in cell culture (Deng *et al.* 2004; Jiang *et al.* 2003). Thus the similarity in the NF-κB levels in Cx and CA1, despite their striking differences in the TNF-α inflammatory stimulus, suggests an almost exclusively non-canonical expression of NF-κB in Cx, in a similar way as reported in cell culture (Nakajima *et al.* 2011). In CA1, NF-κB levels could mirror the balance between the activation of the canonical and non-canonical pathways. Thus, the similarity in NF-κB levels and differences in TNF-α levels support the idea of different inflammatory properties for Cx and CA1, although additional experimental support is required to prove it. In addition, the salubrinal-induced decrease in CA3 NF-κB levels at 24 h contrasts with the later CA1 and Cx decrease (at 48 h), suggesting a delayed response in these structures. The faster IR-dependent increases in CA3 TNF-α levels compared to those in CA1 provides additional support for the idea of different properties in BBB permeability between this structures.

How long lasting is the salubrinal effect? Our data on phosphorylated eIF2α showed a salubrinal-induced enhancement of UPR-PERK pathway at 5 h, in agreement with previous reports (Nakka *et al.* 2010). The inflammatory effect elicited by eIF2α phosphorylation does not require sustained phosphorylation in cell culture (Kitamura 2009) which would agree with our data where eIF2α show similar phosphorylation for treated and non treated ischemic animals at 24 hours. We think that the second dose of salubrinal has no effect on the inflammatory markers, since it resulted in a decrease in NF-κB levels and in TNF-α levels in treated and non-treated IR animals at 48 h.

Different response to ischemia in different cell types of the neurovascular unit

The distinct levels of TNF-α in Cx, CA1 and CA3 reveal local differences in the inflammatory response. These differences also appeared after the salubrinal treatment, adding consistency to the data. It is not clear to what extent the different cells that form the BBB contribute to their local properties and we hypothesized that local inflammatory properties in the different structures mirror not only differences in the neuronal response, but also differences in the neurovascular unit. To prove this hypothesis we studied the ischemic response of the cell types that form the neurovascular unit in different brain structures.

Astrocytes

Following salubrinal treatment, GFAP decreases at 24 h in CA1 and Cx while no changes are detected at 48 h, contrasting with the lack of response at 24 h and the decrease at 48 h in CA3.This supports the idea of a delayed response in CA3 with respect to CA1 and Cx and our hypothesis of local properties for the BBB. In addition, our data together with the lack of response to salubrinal reported at 72 h after spinal cord injury (Ohri et al. 2013) suggests that ER stress in astrocytes is limited to a few days rather than a lack of responsiveness.

Pericytes

Pericytes are the main producers of MMP-9 (Takata *et al.* 2011), a typical marker of BBB impairment (Rosenberg *et al.* 1992; Rosenberg *et al.* 1996; Ueno *et al.* 2009) that in our hands prove a general ischemic-induced BBB impairment at 48 h. The early increase in MMP-9 expression and the maintenance of this high level of expression in Cx compared with the delayed MMP-9 increase in CA1 suggest that BBB damage occurs more rapidly in Cx. Given the reduced vulnerability to ischemia of Cx compared to CA1 (Kirino *et al.* 1985; Petito *et al.* 1987; Zhu *et al.* 2012), the faster peak in Cx MMP-9 expression supports the idea that vulnerability depends on an intrinsic neuronal resistance to ischemia (Tecoma and Choi 1989) rather than a greater protective role of the neurovascular unit in this structure. The different time courses of BBB impairment in the different structures studied also provides support for local inflammatory properties in the neurovascular unit.

Salubrinal treatment was not able to prevent the early BBB impairment observed in Cx; however, its effects on MMP-9 at 48 h reveal two critical aspects: 1) the enhancement of differences between CA1, CA3 and Cx by salubrinal, supporting structure-dependent properties in the neurovascular unit following ischemia, and 2) the ability of salubrinal to prevent or at least minimize the late BBB impairment in CA1 and Cx. The MMP-9 mRNA levels at 24 h suggest that the response observed in the protein at 48 h has already been elicited 24 hours earlier in all the structures studied. The decreased levels of both MMP-9 mRNA and protein in CA1 and Cx after the treatment with salubrinal suggest that the UPR enhancement helps to decrease the BBB impairment. Interestingly, salubrinal was not able to prevent the BBB impairment in CA3 in spite of the ability of this agent to increase the eIF2α phosphorylation.

Endothelial response

Changes in the role of endothelial cells in the properties of the BBB have been related with age. Thus, embryonic neural progenitor cells have been reported as inducers of BBB properties in cerebral endothelial cells (Weidenfeller *et al.* 2007). Also, ICAM-1 and VCAM-1, the key players in the adhesion of circulating blood cells to the endothelium (Li *et al.* 2011; Norman *et al.* 2008), present aging-dependent differences in various brain areas after ischemic insult (Anuncibay-Soto *et al.* 2014). Here we show that structural differences in the endothelial cells also appear in young adult animals. Therefore, local differences in expression and time course of adhesion molecules support a role for endothelial cells in local differences of the neurovascular unit in response to the ischemic insult.

The time-course pattern of MMP-9 expression after the ischemic insult seemed to be delayed 24 h with respect to that observed for ICAM-1, suggesting an increased adhesion between endothelium and circulating blood cells at 48 h in CA1 and Cx. The treatment with salubrinal also reproduced the delayed time-course of expression for these molecules. Therefore, the consecutive steps played by these molecules in BBB impairment, described for MCAO (Wang *et al.* 2007), also appear in global ischemia.

Ischemia-induced changes in ICAM-1 expression in CA3 appeared 24 h earlier than in Cx and CA1. This is corroborated by the VCAM-1 increase in CA3 at 24 h after salubrinal

treatment, contrasting with its decreased or absent effects on Cx and CA1. This provides additional support for differences in adhesion properties between CA3 and the other structures studied. Therefore, all the markers here analysed are consistent and reinforce the idea that, following ischemia, the neurovascular unit in CA3 present different properties than in CA1 and Cx. Further studies are necessary to determine if these differences also exist in naive animals or are a consequence of ischemic insult.

Neuroprotective role of post-ischemic UPR-PERK pathway modulation

Treatment with salubrinal decreased the levels of both CAMs and MMP-9 in CA1 and Cx, giving credence to the ideas that 1) a reduction in leukocyte transmigration would help to reduce BBB impairment and 2) the neuroprotective role of salubrinal involves the inflammatory response. This molecular correlation is not clear in CA3 but contributes to the hypothesis of differences in neurovascular unit properties following ischemia between different brain structures.

Is the salubrinal treatment helpful for neuronal protection? The reduction in neuronal demise in CA1 7 days after injury in salubrinal treated animals and the decrease in BBB impairment (measured as MMP-9 levels and supported by the rest of molecules here studied) support a neuroprotective effect for this agent, involving crosstalk between the inflammatory response and UPR. The smaller UPR response in CA1 using a global ischemia model (Llorente *et al.* 2013) suggests a reduced ability of CA1 to ignite the UPR that could be compensated by the salubrinal treatment. This reduced UPR could explain its greater vulnerability to ischemia and salubrinal would neuroprotect CA1 by promoting its limited UPR which in turn, would modify the inflammatory response.

In accordance with the idea of the dual role of inflammation, both protective and deleterious (Ceulemans *et al.* 2010), the comparable and strikingly high levels of TNF-α at 48 h in both treated and non-treated animals suggests that levels of sterile inflammation have been reached at 48 h in the hippocampus. Since salubrinal was able to increase inflammation at 24 h followed by reducing the BBB impairment at 48 h, we think that the effect of salubrinal on inflammation at 24 h is still protective.

CONCLUSIONS

In conclusion, this study shows that salubrinal treatment presents a neuroprotective role in CA1. We suggest that CA1 presents a limited UPR against the ischemia and salubrinal treatment enhances this response thus reducing the cell delayed mortality. We also suggest that the neurovascular unit presents structure-dependent inflammatory properties to ischemic injury and differences in the time course of the inflammatory response for CA1/Cx and CA3, which is also supported by the salubrinal treatment. In addition, our study demonstrates the responsiveness of endothelial cells and, to a much lesser degree, of astrocytes to the salubrinal treatment. Therefore, the salubrinal treatment affects in different way the different cell populations, resulting in local rather than systemic effects. Finally, this study demonstrates that UPR modulators are able to modify the inflammatory response. The effectiveness of salubrinal when administered after the ishemic insult suggest therapeutic posibilites for UPR modulators in stroke that, up to date, have not been taken into accout.

CHAPTER 3

The detrimental effect of robenacoxib can be prevented when combined with salubrinal, which leads to a synergic decrease of glial activation in a global cerebral ischemia model

Background

The impairment of the BBB that follows a cerebrovascular accident is one of the most critical events in the progression of neuronal death, since it plays a crucial role in the inflammatory response(Berezowski *et al.,* 2012; Rom *et al.,* 2016). The BBB is crucial in the recovery of brain functionality (Abbott, 2013) and has been recently renamed as the NVU to include the different components involved in its complex functionality. Thus, the NVU includes astrocytes, endothelial cells, pericytes, and neurons (Abbott *et al.,* 2010), and some authors include the surrounding microglia (da Fonseca *et al.,* 2014). Hallmarks of the impairment of the NVU are the release of MMP-9 as well as increases in CAMs involved in the transmigration of leukocytes through the BBB endothelium (Rosenberg *et al.,* 1996). CAMs promote the so-called firm adhesion of endothelial cells to leukocytes, a critical step that allows the blood cells to cross the BBB and reach the neural parenchyma (Jin *et al.,* 2009). Another cell type, astrocytes, exerts multiple effects in the NVU, including neuronal support, modulation of endothelial cells, regulation of glutamate uptake, and different roles in the brain inflammatory response. In fact, the overexpression of GFAP, a typical astrocyte marker, is used as a neuroinflammation marker (Pekny *et al.,* 2016; Wang *et al.,* 2007). The impairment of the NVU breaks the immunoprivileged state of the brain, increases the neural damage, and results in local recruitment of microglia, enhancing its macrophagic function (Pun *et al.,* 2009; Yenari *et al.,* 2006). In normal conditions, resting microglia cells present small somata whose long processes show many branches, displaying a ramificate shape. After ischemic injury, microglia activate, which is mirrored by striking changes in cell morphology that show an ameboid shape with large somata and short processes with few ramifications (Walker *et al.,* 2014; Yenari *et al.,* 2010).

Stroke has been reported to increase the unfolded/misfolded proteins in the cell, a phenomenon described as ER stress, which exacerbates the cell damage (Kaufman, 1999; Walter and Ron, 2011). Control of ER stress by pharmacological agents that enhance cell survival has been widely described in *in vivo* and *in vitro* models (Cai *et al.,* 2014; Kitamura, 2009; Nakajima and Kitamura, 2013; Nakka *et al.,* 2010). In recent years, evidence of crosslinking between inflammation and ER stress response has suggested the possibility of modulating one another (Hasnain *et al.,* 2012; Zhang and Kaufman, 2008). Thus, the use of agents, such as salubrinal (Sal), that reduce ER stress by enhancing the UPR has been reported to reduce NVU impairment and to play a role in the inflammatory response (Anuncibay-Soto *et al.,* 2016; Barreda-Manso *et al.,* 2017).

Anti-inflammatory agents have been considered as neuroprotective agents against neurodegenerative diseases, stroke, and traumatic brain injury (Perez-Polo *et al.,* 2013; Szekely and Zandi, 2010; Yilmaz and Granger, 2010). COX-1 blocking induces gastrointestinal side effects elicited by traditional NSAIDs. The lack of selectivity of NSAIDs has driven the pharmaceutical industry to develop selective anti COX-2 treatments (Patrono, 2016a). This has led to the development of different families of NSAIDs, namely the coxib family, with the most recent developed in the 1990's (King *et al.,* 2009). Some of these coxibs (rofecoxib and valdecoxib) have been withdrawn based on their cardiovascular risks (Roumie *et al.,* 2008). These risks have been related with both the vascular damage dependent on the inhibition of COX-2 as well as the platelet activation as a consequence of the lack of COX-1 inhibition (Cairns, 2007). The debacle in the use of NSAIDs has provided essential notions on the different and non-exchangeable roles of COX-1 and COX-2, whose specific cell-type roles remain indispensable for some functions (Fiebich *et al.,* 2014). Robenacoxib (Rob), one of the most recent members of the coxib family, is used in veterinary medicine based on its preferential COX-2 inhibition. It belongs to a new generation of coxibs, without the sulphur-containing group of other coxibs (celecoxib, rofecoxib), which makes Rob chemically distinct. Moreover, its chemical composition allows quick clearance from the blood and its accumulation in inflamed tissue. These properties, together with the high specificity for COX-2 and the low and reversible inhibition of COX-1, make Rob a perfect

COX-2 inhibitor (King *et al.,* 2009). The pharmacological action of Rob has not yet been explored in global cerebral ischemia.

The quick neuroprotection assessed by the ER stress control (Anuncibay-Soto *et al.,* 2016; Barreda-Manso *et al.,* 2017; Rubovitch *et al.,* 2015), the later contribution of COX-2 to extend the damage described in global cerebral ischemia models (Candelario-Jalil *et al.,* 2003; Chu *et al.,* 2004), as well as the close relationships between inflammation and ER stress in pathological changes in neurodegenerative diseases (Hasnain *et al.,* 2012; Xin *et al.,* 2014) led us to test if the combined used of an ER stress inhibitor with an anti-inflammatory agent could enhance the neuroprotection against stroke. In this report, we describe for the first time the detrimental effect of Rob treatment after ischemia, how the combined treatment of Sal and Rob prevents the Rob effect on the neuronal damage, as well as the modifications in the glial response and the effect on some hallmarks of NVU impairment by these treatments.

Material and Methods

Animals

Eighty three-month-old Sprague–Dawley male rats (450–550 g) were housed in standard conditions: standard temperature (22 ± 1°C), 12 h light/dark cycle, and food (Panlab, Barcelona, Spain) and water *ad libitum*. The experimental groups used are indicated in Figure 1. All experimental procedures were approved by the Scientific Committee of the University of Leon and performed in compliance with the ARRIVE guidelines, in accordance with the Guidelines of the European Union Council (63/2010/EU) and Spanish regulations (RD 53/2013, BOE 8/2/2013) for the use of laboratory animals. All efforts were made to reduce the number of animals used and to minimize animal suffering.

Transient global cerebral ischemia

The ischemia/reperfusion (I/R) assays were performed in a two-vessel occlusion global cerebral ischemia model as previously described (Vieira *et al.,* 2014). In summary, anesthesia was induced with 4% isoflurane (IsoFlo, Abbott Laboratories Ltd, Madrid,

Spain) in 3 L/min in 100% oxygen. Then, a facemask was used to maintain the anesthesia using a flux of 1.5–2.5% isoflurane at 800 mL/min in 100% oxygen. Both common carotids and femoral arteries were exposed. A catheter was introduced in the femoral artery to record blood pressure along the whole procedure and control the blood volume. Blood flow to the brain through the paravertebral arteries was prevented by maintaining a moderate hypotension (40–50 mmHg) using partial exsanguination (slow draining of blood at 1 ml/min). Fifty UI heparin/kg were administered through the catheter, and 50 UI heparin were maintained in the syringe, which contained 3 mL of saline, to avoid clot formation during the blood collection.

When a stable hypotension was reached, both common carotid arteries were clamped for 15 min. Body temperature was maintained at 36 ± 1°C during surgery with a feedback-regulated heating pad monitored with a rectal probe. After ischemia, microclamps were withdrawn and returned to the animal at 1 mL/min until the recovery of arterial blood pressure. Then, the catheter was removed, and the animal was sutured and monitored during the recovery from anesthesia. The animals were then returned to the animal house and maintained in standard conditions for the different times of reperfusion to study. Sham-treated animals followed the same procedure except for the carotid clamping.

Drug treatment

The different treatments are summarized in Figure 1. Rob (10 mg/kg) was administered subcutaneously, and Sal (1mg/kg in vehicle 1.5% DMSO) was administered intraperitoneally.

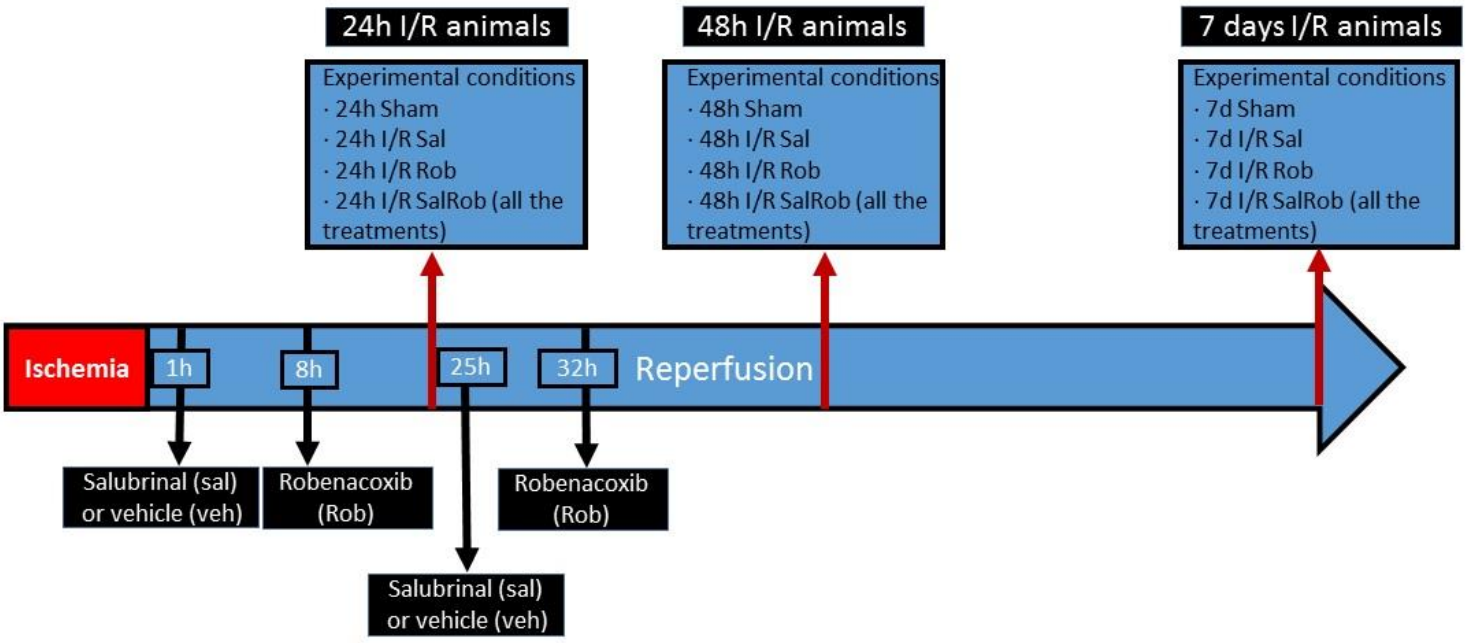

Figure 1. Experimental procedure.

Tissue dissection and total RNA extraction

Fifty animals (25 after 24 h I/R and 25 after 48 h I/R) were used for RNA assays. After decapitation, the brains were quickly removed and placed on a brain rodent matrix (ASI Instruments, Warren, MI, USA) at 4°C. Using the sagittal guides of the matrix for inserting the blades, 2-mm-thick sagittal slices were obtained at a distance of 1 mm to the medial line, In these slices, the Cornu Ammonis 1 (CA1) hippocampal region, as well as the cerebral cortex (Cx) above its was dissected under microscopy. Samples were frozen in dry ice and stored at -80°C. From each brain area dissected, total RNA was extracted using the Tripure Isolation Reagent (Roche Diagnostics, Barcelona, Spain), following the manufacturer's instructions, and then stored at -80°C.

Reverse transcriptase reaction and qPCR

Minimal Information for Publication of Quantitative Real-Time PCR Experiments (MIQE) Guidelines (Taylor *et al.,* 2010) were followed in the quantitative PCR (qPCR) assays. RNA integrity and retrotranscription were performed as previously described (Anuncibay-Soto *et al.,* 2014). The following primers were used for qPCR: *mmp-9*: (f5'ttctgtccagaccaagggtaca, r5'gcgcatggccgaactc, NM_ 031055.1); vascular adhesion molecule 1 (*vcam-1*): (f5'tgctcctgacttgcagcaccac,r5'tgtcatcgtcacagcagcaccc, NM_

012889.1); intercellular adhesion molecule 1 (*icam-1*): (f5'tgcagccggaaagcagatggtg, r5'atggacgccacgatcacgaagc, NM_012967.1); glyceraldehyde 3-phosphate dehydrogenase (*gapdh*): (f5'gggcagcccagaacatca, r5'tgaccttgcccacagcct,NM_017008). The qPCR was performed as previously described (Anuncibay-Soto *et al.,* 2016) using a Step One Plus thermocycler (Applied Biosystems, Foster City, CA, USA). The results were analyzed following the 2ΔΔCt (Livak and Schmittgen, 2001) method using the *gapdh* housekeeping gene. Fold changes were expressed as $2^{-\Delta\Delta Ct}$, where ΔΔCt represents the transcript variation between the different conditions (ΔCtischemic-ΔCtsham).

Immunofluorescence assays

Thirty rats with 48 h or seven days of reperfusion were killed with an intraperitoneal dose of 200 mg/kg of sodium pentobarbital (Vetoquinol, Vernois, France) and immediately perfused via intra-aortic delivery of 4% paraformaldehyde (PFA) as previously described (Anuncibay-Soto *et al.,* 2014). The brain was cut in 40 µm-thick coronal slices with a freezing microtome.

Sections were incubated in 0.05% Tween-20 in 10 mM sodium citrate buffer, pH 6.0, at 80°C for 30 min for epitope-retrieval. Then a successive blocking of endogenous biotin with an avidin-biotin kit and immunoglobulins (Ig) with 1% bovine serum albumin (BSA) in 0.2% Triton X-100 in phosphate buffer saline (PBS) at room temperature was performed. A summary of the antibodies (Ab) used is shown in Table I. Double staining for microglia and astroglia was carried out, incubating the sections overnight at 4°C in 1% BSA, 0.2% Triton X-100 in PBS with anti-IBA-1 (ionized calcium binding adaptor molecule 1) Ab and anti-GFAP Ab. Anti-IBA-1 Ab was recognized by a biotinylated Ab, which, in turn, was labelled with extravidin conjugated with Alexa-647 (1:500). A secondary Ab complexed with Alexa-488 was used to recognize the anti-GFAP Ab. Afterwards, sections were incubated overnight at 4°C in anti-NeuN Ab in 1% BSA and 0.2% Triton X-100 in PBS and then recognized with a secondary Ab complexed with Alexa-568. Nuclei were counter-stained with 4,6-diamidino-2-phenylindole (DAPI), and sections were mounted using Fluoromount G mounting medium.

Host species and specificity	Target	Concentration	Brand
Mouse monoclonal	Anti-NeuN	1:500	Millipore
Goat polyclonal	Anti-IBA-1	1:2000	Abcam
Rabbit polyclonal	Anti-GFAP	1:500	Dako
Horse polyclonal	Anti-goat IgG biotinilated	1:500	Vector
Goat polyclonal	Anti-rabbit IgG Alexa 488	1:500	Life Technologies
Horse polyclonal	Anti-mouse IgG Alexa 568	1:500	Life Technologies

Image acquisition

Image analysis was made on animals perfused with 4% PFA. For each brain, three coronal sections were obtained every 960 µm between Bregma -2.30 mm and Bregma -4.30 mm (Figure 2A). Sections were immunolabeled for IBA-1, GFAP, and NeuN, and nuclei were stained with DAPI and images obtained with a Zeiss LSM 800 confocal microscope. Each section was scanned to obtain a tile image of the whole hippocampus with a resolution of 1.25 µm/pixel using the Tile Scan Module (included in Zen Blue software) with a Plan-Apochromat 10x/0.45 M27 objective. An optical dissector method was used to count cells and to perform morphometric and densitometric analyses of glial populations. In brief, three equidistant dissectors of 0.255 mm2 with a lateral resolution of 0.156 µm/pixel were obtained with a Plan-Apochromat 40x/1.3Oil DIC (UV) VIS-IR M27 along the hippocampal CA1 pyramidal layer. Each dissector was formed by nine images were taken each 3 µm (21 µm in total) in z-axis. The different immunofluorescence stainings were included in each image. Bias in image quantification was prevented by keeping constant the detector gain, pinhole, laser power, and pixel

dwell.

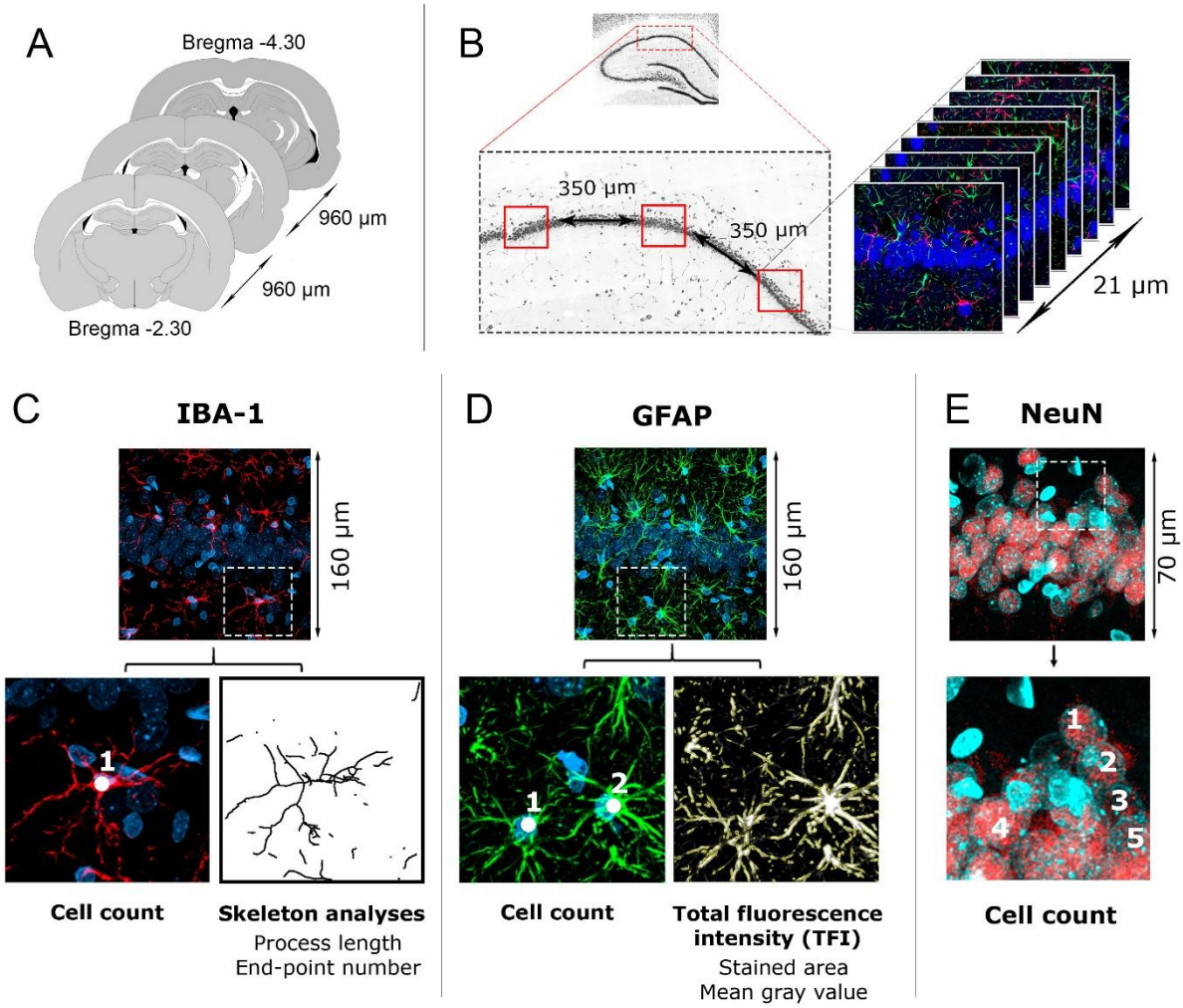

Figure 2. Microscope image analysis workflow. A) Schematic representation of the sections included in analysis of each animal. Three 960 µm equidistant coronal sections obtained between bregma -2.30 mm and bregma -4.30 mm were used. **B)** In each section, three equidistant optical dissectors (160 x 160 µm, separated 350 µm between them) along the hippocampal CA1 pyramidal layer were obtained**.** Each dissector is formed by nine images separated 3 µm in z-axis, which discards about 7 µm top and 7 µm bottom regions of the 40 µm-thick section. The triple immunolabeling allowed us to use the same images of each dissector for the study of astroglia, microglia, and neurons. **C)** Workflow used to measure microglia process branches and length. A skeletonization of IBA-1 z-stack images was used by converting microglia processes in interconnected tridimensional 1 pixel-thick lines. Skeleton analysis allowed to estimate the process length and the end-point number per cell. **D)** Workflow to estimate astrocyte area and GFAP TFI. Each GFAP z-stack image was converted to 256 gray levels. Each image was also binarized, thus creating a mask to measure both the area of GFAP labeling and its gray average value (TFI value). TFI values for each of the nine images of the z-stack were summed and divided by the number of astrocyte nuclei, expressing the final results as TFI/cell. **E)** Workflow used to neuron count. A second dissector of 70 x 70 µm was obtained from each image and NEUN+ cells were counted in the nine z-stack levels. Results were estimated as NEUN+ cells/dissector.

Microglia activation analysis

The density of microglia indicated as cells/mm^3 was obtained from the average of IBA-1-labeled cells in all dissectors in each region. The degree of microglia activation was estimated by quantifying the number of branches and the cell process length following the method developed by Morrison and Filosa, 2013, with minor modifications. In brief, each IBA-1 image of the z-stack was transformed to an 8 bits grayscale image and then binarized, skeletonized, and analyzed with Analyze Skeleton 2D/3D plugin in ImageJ. The number of microglia nuclei in each dissector was used for normalize the results and obtain the averages of the number of process endpoints/cell and the summed process length/cell (Figure 2C).

Astroglia reactivity analysis

The degree of astroglial reactivity was estimated by measuring both the volume of astrocytes and the GFAP protein levels using image analysis. Each GFAP image of each dissector (nine images per dissector) was converted to an 8 bits grayscale image and it was also binarized. Binary images were used to create a mask outlining each astrocyte soma and its processes, thus allowing to measure the whole area of the astrocyte. The mask of each level was overlapped on the corresponding gray image, allowing to measure the mean gray value. The product of the mask area and the mean gray value has been named the total fluorescence intensity (TFI) and was measured in each level. Therefore, in each dissector, the nine TFIs (one for each level) were summed and divided by the number of astroglial nuclei, which was expressed as TFI/cell (Figure 2D).

Neuronal counting

In each dissector a central smaller 70 x 70 µm subdissector was used to count the NeuN positive cells. Thus the nine z-stack levels were used to count neurons in each dissector. Results were estimated as NEUN+ cells/subdissector.

Results

Neuronal demise

After 48 h of reperfusion, similar neuronal densities were observed in the CA1 hippocampal area when sham-, vehicle-, and Sal-treated animals were compared.

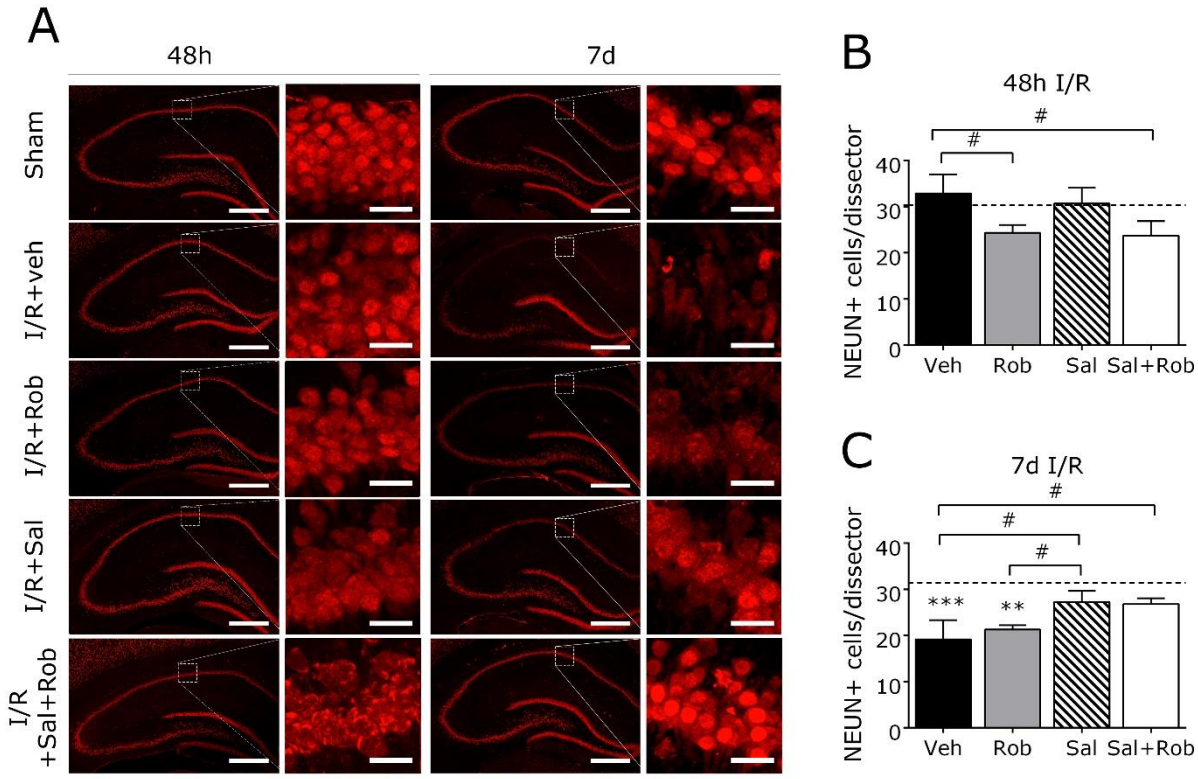

Figure 3. Neuronal demise. Neuronal densities (mean ± SEM) at 48 h (A,B) and seven days (A,C) of reperfusion in the CA1 were represented. Values of sham-operated animals are represented by a dotted line. * indicates significant differences with respect to sham-operated animals; brackets indicate the significant differences between treatments, and the # above them shows the significance: one symbol $p<0.05$, two symbols $p<0.01$, and three symbols $p<0.001$. One-way ANOVA followed by Tukey's test, n=3.

The treatment with Rob resulted in a significant neuronal demise with respect to the vehicle- or Sal-treated animals. The treatment with Sal–Rob resulted in a significant neuronal density decrease with respect to vehicle- and Sal-treated animals (Figure 3A, B).

We had previously reported that ischemia induced a significant neuronal demise seven days after the insults that was prevented by Sal in CA1 (Anuncibay-Soto *et al.,* 2016). In this structure, the neuronal demise in animals treated with Rob is similar to that observed in ischemic untreated animals at seven days. However, the treatment with

Sal–Rob presented values significantly higher than those observed in vehicle animals and similar to those observed in Sal-treated animals (Figure 3A, C).

Microglia

Microglia density

We could not detect significant changes in microglia densities in the CA1 after global cerebral ischemia at either 48 h (Figure 4A, C) or seven days (Figure 4B, F) after the insult. Interestingly, at both times, Rob treatment elicited a significant increase in the microglia density that was not observed after the treatment with Sal or the combined effect of Sal and Rob.

Microglia branch length

After 48 h of reperfusion, the branch length of microglia in vehicle animals showed a trend to increase compared to that observed in sham animals, but we could not find significant differences. Animals treated with Rob showed a significant microglia lower branch length than that observed in the CA1 in vehicle, Sal, and sham animals. The Sal–Rob combination also showed a trend to present higher branch length than the Rob treatment, but we could not find significance between them (Figure 4A, D). Seven days after the insult, the microglia branch length was significantly reduced in vehicle animals, and animals treated with Rob with respect to sham animals. Interestingly, the treatment with the combination of Sal and Rob significantly increased the branch length values (Figure 4B, G).

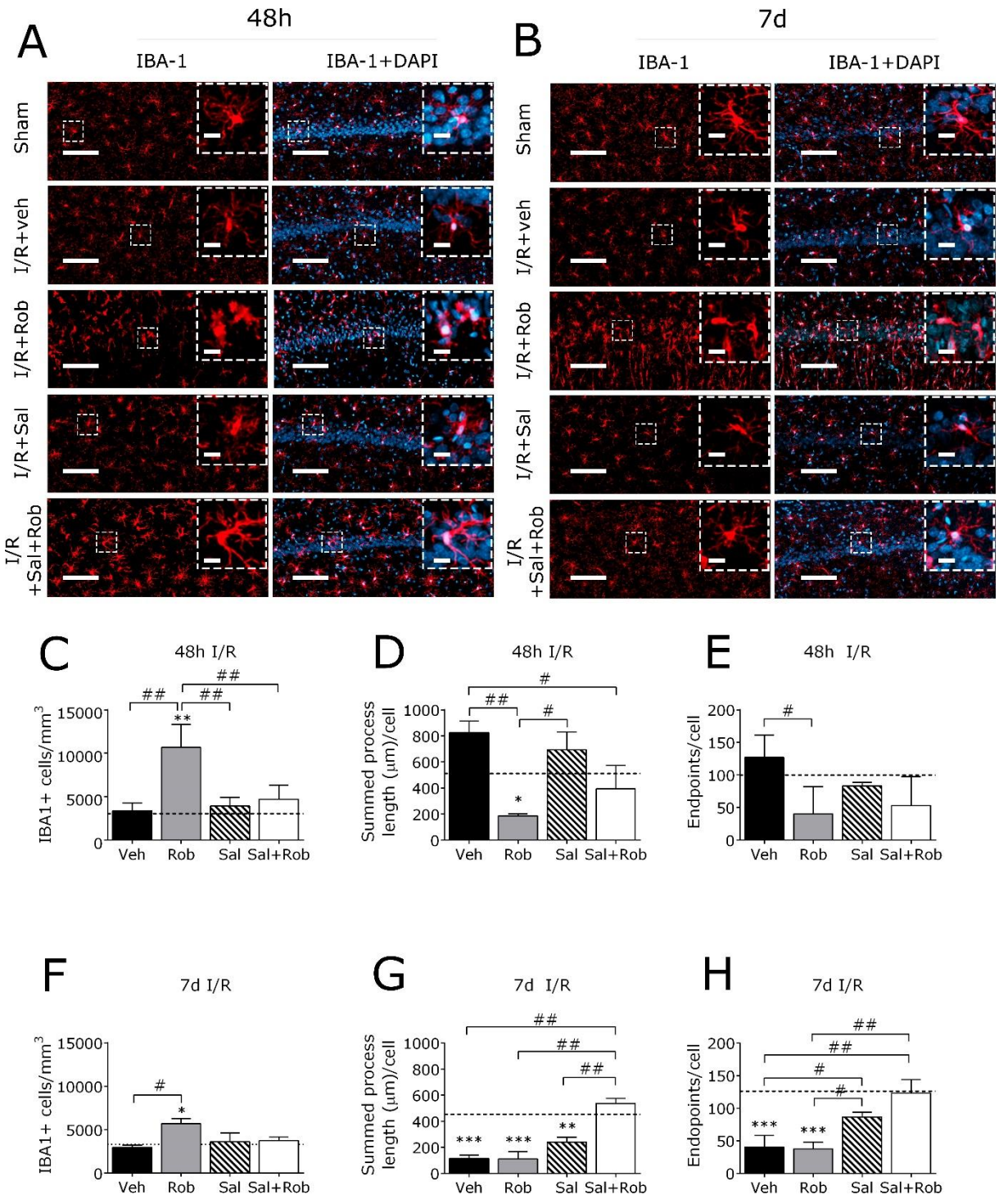

Figure 4. Ischemic-dependent effect in microglia of the CA1. Microglia density (mean ± SEM) for each experimental condition after 48 h (A, C, D, E) and seven days (B, F, G,H) after reperfusion. Figures C and F show microglia density, D and G show branch lengths (mean ± SEM) of microglial cells, and E and H show the number of endpoints (mean ± SEM) in microglial cells. Values of sham-operated animals are represented by a dotted line. * indicates significant differences with respect to sham-operated animals; brackets indicate the significant differences between treatments, and the # above them shows the significance: one symbol $p<0.05$, two symbols $p<0.01$, and three symbols $p<0.001$. One-way ANOVA followed by Tukey's test, n=3.

Microglia endpoints

After 48 h of reperfusion, the number of microglia endpoints was similar in sham, vehicle, Sal, and the combination of Sal and Rob in the CA1. The treatment with Rob resulted in a decreased number of endpoints, but we could not find significant decreases in the CA1 (Figure 4A, E).

Seven days after the insult, vehicle- and Rob-treated animals presented a significant decrease in the endpoints. The treatment with Sal resulted in a lower but non-significant number of endpoints compared with sham animals in all areas studied. The number of microglia endpoints in Sal-treated animals was significantly higher than in those of the vehicle- and Rob-treated animals. The treatment with the combination of Sal and Rob resulted in a trend to increase the microglia endpoints with respect to those observed in Sal-treated animals; therefore, this number was significantly higher with respect to those observed in vehicle- and Rob-treated animals (Figure 4B, H).

Astroglia

Density

Astroglia density was not modified by the ischemic insult after either 48 h or seven days (Figure 5A, B, C, F).

Area

The astroglial area was not significantly modified by the global ischemia after 48 h in CA1. The treatment with Rob resulted in an increased astroglial area that reached significance when compared with that observed in sham or vehicle animals 48 h after the reperfusion. In a similar way, a moderate increase was also found after the treatment with Sal (Figure 5A, D).

Seven days after the insult, we could detect only a significant decrease in the astroglia area in the CA1 as a consequence of the ischemia. The treatment with the combination of Sal and Rob displayed significant increases in astroglia area values with respect to the vehicle- and Sal-treated animals (Figure 5B, G).

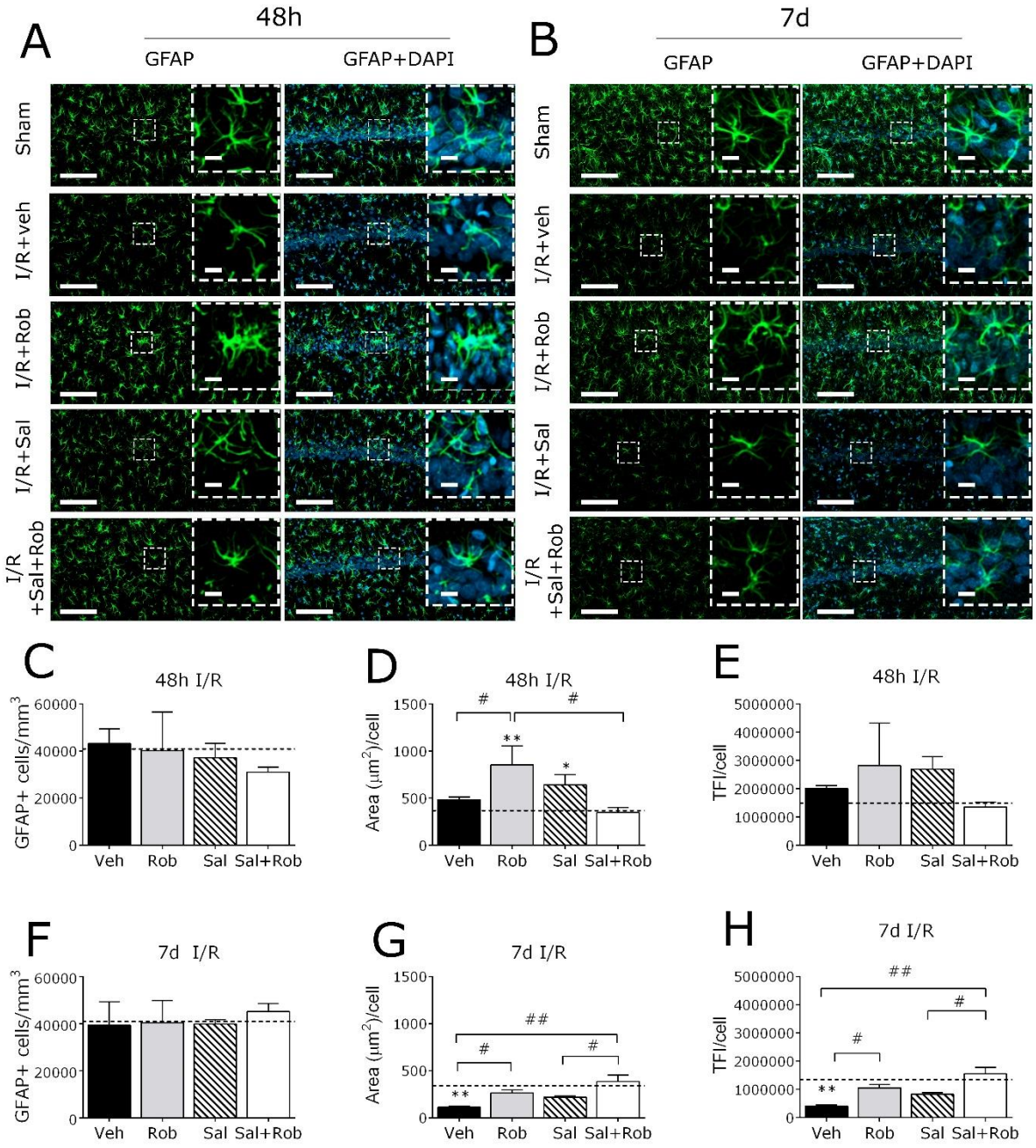

Figure 5. Ischemic-dependent effect in astroglial of cerebral CA1. Astroglia density (mean ± SEM) for each experimental condition after 48 h (A, C, D, E) and seven days (B, F, G, H) after reperfusion. Figures C and D show astroglia density, D and G show the area (mean ± SEM) of astroglia, and E and H show the TFI/cell (mean ± SEM). Values of sham-operated animals are represented by a dotted line. * indicates significant differences with respect to sham- operated animals; brackets indicate the significant differences between treatments, and the # above them shows the significance: one symbol $p<0.05$, two symbols $p<0.01$, and three symbols $p<0.001$. One-way ANOVA followed by Tukey's test, n=3.

TFI

Similar values of TFIs were observed in sham-, vehicle-, and Sal-treated animals after 48 h of reperfusion. The treatment with Rob showed a trend to increase TFI, but we failed to detect significant differences with respect to those observed in sham and vehicle animals. At this time, we could not find significant differences in the TFI values comparing the treatment with Sal, the combination of Sal and Rob, vehicle animals, or sham animals (Figure 5A, E).

After seven days of reperfusion, we detected a significant decrease in TFIs as a consequence of the ischemia in the CA1. The treatment with the combination of Sal and Rob displayed significant increases in TFI values compared with vehicle- and Sal-treated animals (Figure 5B, H).

Transcriptional levels in MMP-9 and CAMs

MMP-9

We have previously reported the effect of treatment with Sal on MMP-9 in the same model of global cerebral ischemia, indicating its ability to reduce MPP-9 transcripts in the CA1, CA3, and Cx at 24 h and in the CA1 at 48 h (Anuncibay-Soto *et al.,* 2016). Here we observed that treatment with Rob or the combined effect of Sal–Rob decreases the transcript levels of MMP-9 in the Cx at both 24 h and 48 h after ischemia with respect to sham animals. However, treatment with the combination of Sal–Rob resulted in significant decreases of MMP-9 transcript levels in the CA1, whereas treatment with Rob resulted in similar or even increased MMP-9 transcript values with respect to those observed in sham and vehicle animals (Figure 6A, B).

VCAM-1

We have previously reported an ischemic-dependent increase in the VCAM-1 transcript levels after 48 h of reperfusion in the Cx and CA1, as well as the capacity of Sal to reduce these transcript levels after 48 h of reperfusion (Anuncibay-Soto *et al.,* 2016). The treatment with Rob at 24 h resulted in significant decreases of the VCAM-1 transcript levels with respect to those of the vehicle and sham animals in the Cx and CA1. The treatment with the combination of Sal–Rob resulted in a more moderate reduction of

VCAM-1 transcript levels, only reaching significance in the hippocampal areas studied compared to those observed after the treatment with only Rob after 24 h of reperfusion. After 48 h of reperfusion, treatment with Rob and with Sal–Rob showed a similar response, with similar values with respect to sham animals in the Cx, and significantly lower VCAM-1 transcript levels in the CA1. Importantly, these treatments resulted in significantly lower values compared to those observed in the vehicle (Figure 6C, D).

ICAM-1

We have previously reported an increase in the ICAM-1 transcript levels especially after 48 h of reperfusion in the Cx and CA1, as well as the capacity of Sal to reduce these transcript levels after 48 h of reperfusion (Anuncibay-Soto *et al.,* 2016). We included the treatment with Rob and the combination of Sal and Rob at both 24 h and 48 h that resulted in significant decreases of the ICAM-1 transcript levels with respect to those of vehicle and sham animals in the Cx. The treatments with Rob and with Sal–Rob resulted in similar significant decreases of the ICAM-1 transcript levels (Figure 6F, G).

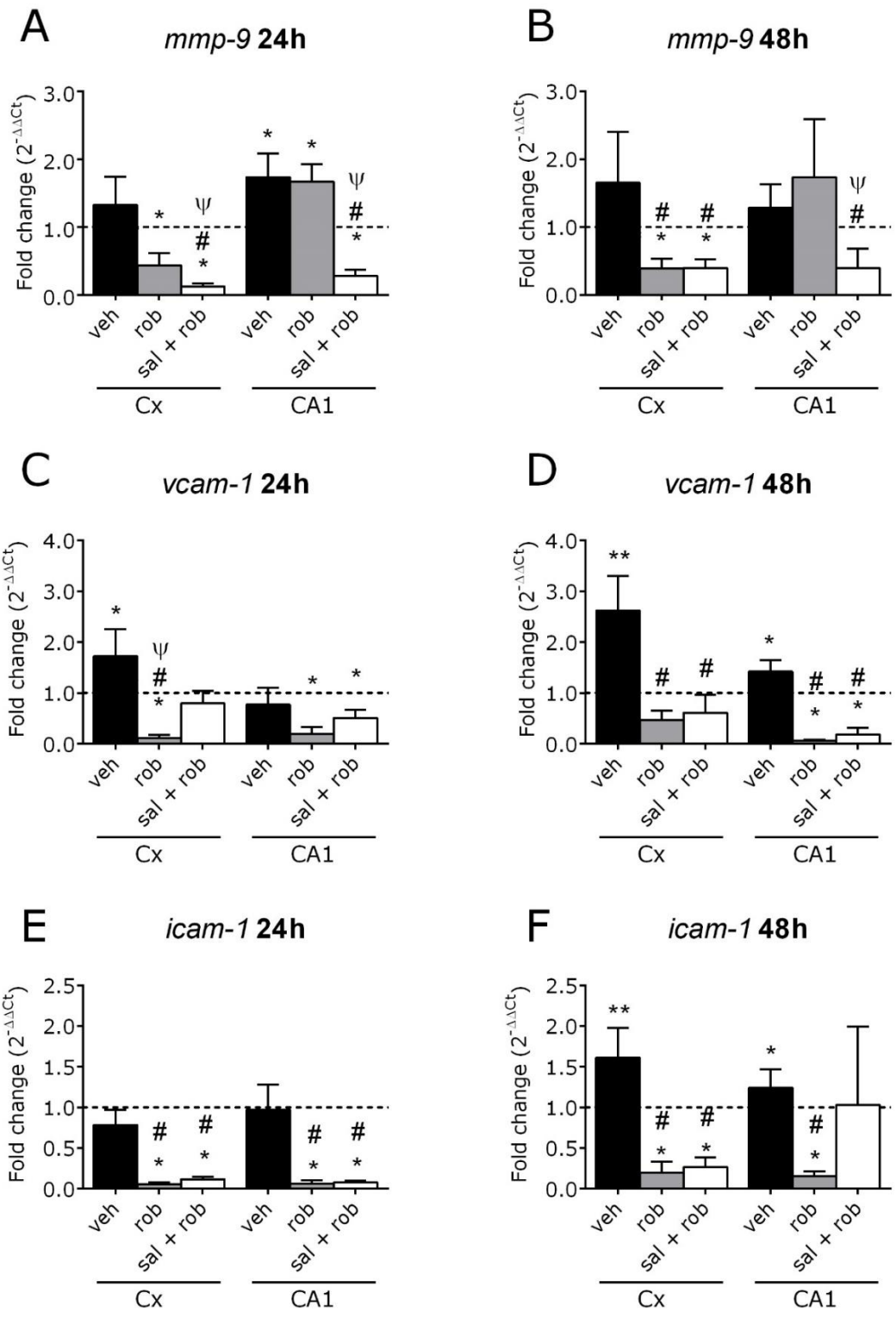

Figure 6. Effect of I/R time and treatments on the neurovascular unit in mRNA levels. Fold changes of MPP-9 ($2^{-\Delta\Delta Ct}$) after 24 h I/R (A) and 48 h I/R (B). Fold changes of VCAM-1 ($2^{-\Delta\Delta Ct}$) at 24 h I/R (C) and 48 h I/R (D). Fold changes of ICAM-1 ($2^{-\Delta\Delta Ct}$) at 24 h I/R (E) and 48 h I/R (F). Values of sham-operated animals are represented by a dotted line. * indicates significant differences with respect to sham-operated animals; # indicates significant differences between the treatment and the vehicle. Y indicates significant differences between the treatment with Rob and Sal–Rob. One symbol represents $p<0.05$, two symbols $p<0.01$, and three symbols $p<0.001$. One-way ANOVA followed by Tukey's test, n=5.

Discussion

Looking for a synergic effect against stroke

We have previously demonstrated in the same global cerebral ischemia model that Sal administered 1 h and 24 h after insult results in increased neuroprotection of the CA1 (Anuncibay-Soto *et al.,* 2016), one of the most ischemic-vulnerable brain areas (Kirino *et al.,* 1985; Petito *et al.,* 1987; Zhu *et al.,* 2012). The Sal treatment included anti-inflammatory changes that suggested that its combination with anti-inflammatory agents could result in positive synergic effects against stroke. In this regard, the neuroprotective effect of some anti-inflammatory agents such as meloxicam or 2-OAA has been proved in global and other cerebral brain ischemia models (Llorente *et al.,* 2015; De los Reyes and Céspedes 2014; Ugidos *et al.,* 2017). The development of preferential COX-2 inhibitors such as "coxibs" has resulted in surprisingly different effects, making it necessary to test for each coxib member the risks and benefits in each application (Cairns, 2007). In this regard, detrimental effects by increasing the risks of cardiovascular events and stroke have been reported for some members of the coxib family, such as rofecoxib (Jüni *et al.,* 2004) or valdecoxib (Patrono, 2016b), although other "coxibs" do not seem to increase the stroke risk (Roumie *et al.,* 2008). The effects of Rob on these pathologies have not been published, as far as we know. However, the strong preferential effect of Rob on COX-2:COX-1 in isolated cells (967:1) (King *et al.,* 2009) seemed to make this drug ideal for testing specific effects of blocking COX-2 as well as detecting possible synergies of anti-COX2 agents and Sal. In addition, Rob can be administered subcutaneously (King *et al.,* 2009), which makes easier the combined treatment and the use of the same vehicle in both Sal and Rob, thus reducing the number of experimental groups.

The problem with robenacoxib

Neuronal demise in the global cerebral ischemia model has been widely described to be detected at seven days after the ischemic insult (Castro *et al.,* 2014; Hartman *et al.,* 2005; Pulsinelli *et al.,* 1982). Then, why the treatment with the anti-inflammatory agent Rob accelerates the neuronal loss and therefore becomes detrimental in CA1? This detrimental effect (Figure 3) could be the result of the COX-2 blocking in the endothelial cells, which could lead to vasoconstriction. Clot formation by platelet activation would

not be prevented by coxibs, since they do not block COX-1 (Cairns, 2007; Patrono, 2016b). In fact, tromboembolic complications due to inflammation-induced platelet activation are among the most common problems in patients with cerebrovascular disease (Koudstaal *et al.,* 1993). However, the combined administration of a single dose of Sal 1 h after the insult followed by Rob administration was able to prevent the ischemic-induced neuronal loss detected at seven days, in contrast with the inability of Rob to prevent this demise. These data support the hypothesis that ER stress plays a crucial role in the progression of the inflammatory response (Hasnain *et al.,* 2012; Xin *et al.,* 2014). Therefore, the effect of preventing neuronal demise after Sal–Rob administration seems to be dependent only on Sal. In addition, animals treated with Sal at 1 h and 24 h present the same neuronal demise as those treated by the combination of Sal at 1 h and Rob at 8 h and 32 h, indicating that the second dose of Sal 24 h after insult has low or no efficacy, as previously hypothesized (Anuncibay-Soto *et al.,* 2016). In fact, our data showed that two doses of Rob are able to elicit a detrimental effect in the CA1, suggesting that this coxib would increase the cerebrovascular accident damage. This supports the notion that early control of ER stress is crucial in neuroprotection.

Glia, the NVU, and imbalance in the activity of COX isoforms

The glial response to Rob treatment provides some hints about the detrimental effect of Rob on the neuronal population. In this regard, Rob treatment unexpectedly promotes strong microglia activation in the CA1 at 48 h, despite its anti-inflammatory effects, which can be observed on the BBB parameters analyzed here (MMP-9 and those CAMs responsible for firm adhesion) (Figure 6). Microglia activation has been hypothesized to be responsible for neuronal death (Baron *et al.,* 2014), which would be consistent with our data of high microglia density, neuronal loss, and high MMP-9 transcript levels, indicating strong damage to the BBB in the CA1. In fact, Sal treatment and the Sal–Rob combined treatment led to the decrease or absence of microglia activation and did not reveal cell death seven days after the insult in the CA1 (Figure 4). Modifications in the balance in the activity of COX-1 or COX-2 that play different indispensable functions and cannot functionally substitute one another (Fiebich *et al.,* 2014) could explain the detrimental effect of a selective blocking of COX-2 with Rob. A two-hit model involving COX-1 and COX-2 activities has been proposed to explain the neuroinflammation process. COX-1 has been described as the predominant form of COX

in resting microglia and its activation. The first hit would result in microglial activation (Aïd and Bosetti, 2011; Choi *et al.,* 2009; Schwab and McGeer, 2008; Tecoma and Choi, 1989) and the second hit would be elicited by neuronal injury, death, or persistent glial activation, resulting in potentiation of the microglial activation. Thus, neuroinflammation activated by COX-1 induced by ischemia is not stopped by Rob. This imbalance would explain the microglia reactivity and neuronal damage. The presence of Sal counteracts the neuroinflammation induced by microglia reactivity (Huang and Feng, 2013; Logsdon *et al.,* 2016), which is confirmed in this report mainly at seven days. The highest combined effect of Sal and Rob on the microglia activation seems to depend on a decrease in both isoforms of COX. In fact, a primary contribution of COX-1 and a delayed contribution of COX-2 in the progression of the damage have been reported in a global cerebral ischemia model (Candelario-Jalil *et al.,* 2003). Thus, the use of NSAIDs with activity against COX-1 and COX-2, which have proved to have a strong neuroprotective effect in tMCAO models, has been claimed (Candelario-Jalil and Fiebich, 2008; Ugidos *et al.,* 2017). Traditional NSAIDs seem to be able to balance the inhibition of the synthesis of platelet tromboxane (anti-trombotic activity) and the synthesis of prostacyclin in endothelial cells (prothrombotic activity). This balance involves the modulation of COX-1 and COX-2 activities and could explain the absence of cardiovascular risk and stroke with these agents (FitzGerald *et al.,* n.d.; Roumie *et al.,* 2008).

Why does a selective anti-COX-2 promote BBB impairment in the CA1? The effect of Rob on both area and TFI parameters shows astroglia activation that is reduced in Sal and Sal–Rob treatment (Figure 5) and is consistent with that observed in microglia. These results provide additional support to the detrimental effect of Rob that can be remedied when administered in combination with Sal.

CAMs are expressed mainly by vascular endothelial cells (Feng *et al.,* 2017; Jin *et al.,* 2010). The specific intrinsic COX-2 activity in the endothelial vascular cells (Patrono, 2016a) would explain why Rob treatment decreases VCAM-1 and ICAM-1 transcription, thus preventing impairment of the NVU at an endothelial level. However, the treatment with Sal reveals that ER stress seems to present a striking effect on the BBB impairment in the CA1 mirrored by the MMP-9 release (Anuncibay-Soto *et al.,* 2016). This would

explain why Rob is unable to protect from the MMP-9 release, but the combination with Sal results in a decrease of MMP-9 (Figure 6). Therefore, reducing the ER stress seems to play a more crucial role than inhibiting COX-2 in preventing BBB impairment. In fact, the prevention of BBB impairment by Sal treatment has been reported in other models (Barreda-Manso *et al.,* 2017; Logsdon *et al.,* 2016).

The detrimental effects of treatment with Rob could be the consequence of an imbalance in COX-1 and COX-2 activities. In this regard, the treatment with Rob would inhibit COX-2, resulting in an intrinsic detrimental effect in vascular endothelial cells, while microglia activation would not be stopped, since COX-1 is not inhibited. The early neuroprotection provided by Sal, which reduces microglia activation and protects the BBB, could provide time for a beneficial effect based on late blocking of COX-2. However, we cannot deny that Rob presents additional detrimental effects unrelated to its anti-COX2 properties.

In summary, this study shows that the use of the highly selective anti-COX2 Rob, despite its anti-inflammatory effect, moves the neuronal demise forward instead of increasing neuroprotection. However, the combined effect of Sal and Rob prevents the early neuronal loss induced by this anti-inflammatory agent. This study also confirms that acute treatment with Sal provides a neuroprotective effect that can be observed even seven days after insult. We also prove that glial activation is strongly increased by Rob, poorly or non-activated by Sal, and reverted by the combined administration of Sal–Rob. Finally, the synergic action on the microglia by the combined effect of an anti-ER stress agent followed by an anti-inflammatory agent suggests that a proper combination of different neuroprotective agents could provide a stronger neuroprotective effect, although the agents and times have to be chosen carefully.

CONCLUSIONS

Conclusions

1) The comparative study between young and old animals reveals that the inflammatory response induced by ischaemia-reperfusion are age-dependent.
2) Age modifies the time course of apoptosis and the pattern of labelling, but does not seem to modulate the cell demise.
3) Age modifies the adhesion molecules involved in the recruitment of neutrophils, leading to differential changes in the low-affinity binding and the high-affinity binding to leukocytes.
4) Age lessens the differences in vulnerability to ischaemia between cerebral cortex and hippocampus and supports the idea of local differences in the BBB.
5) The enhancement of the UPR–PERK pathway is able to reduce the inflammatory response and suggest new therapeutic possibilities for UPR modulators in stroke.
6) Salubrinal treatment has a neuroprotective role in CA1 in the global cerebral ischaemia model. In this model of ischaemia, CA1 presents a limited UPR, and salubrinal treatment enhances the ability of CA1 to overcome ER stress, thus reducing delayed cell death.
7) Treatment with salubrinal provided additional support to our hypothesis of local differences in the neurovascular unit response to inflammation.
8) Salubrinal treatment elicit different responses in the neurovascular unit components that range from practically no response in astrocytes to a strong endothelial and neuronal response, resulting in local rather than systemic effects.
9) Post-ischaemic treatment with the selective COX-2 inhibitor robenacoxib results in a detrimental effect on the neuronal population and an exacerbation of glial activation.

10) The combined treatment of robenacoxib and salubrinal results in a neuroprotective effect that seems to be provided by the acute administration of salubrinal.

11) The combined treatment of robenacoxib and salubrinal results in a synergic decrease in glia activation, which suggests that a proper combination of ER stress inhibitors and anti-inflammatory agents could result in an enhanced neuroprotective effect.

Conclusiones

1) El estudio comparativo entre animales jóvenes y viejos muestra que la respuesta inflamatoria inducida por el proceso de isquemia-reperfusión es dependiente de la edad.
2) La edad modifica la dinámica temporal y el patrón de marcaje de la apoptosis, pero no parece modular la pérdida celular.
3) La edad modifica las moléculas de adhesión involucradas en el reclutamiento de los neutrófilos, dando lugar a cambios diferenciales en las moléculas relacionadas con la adhesión de baja afinidad y en las de alta afinidad a leucocitos.
4) La edad disminuye la vulnerabilidad diferencial frente a la isquemia entre la corteza cerebral y el hipocampo y da soporte a la idea de propiedades locales a lo largo de la barrera hematoencefálica.
5) El aumento de la activación de la vía UPR-PERK es capaz de reducir la respuesta inflamatoria, proponiendo de manifiesto las posibilidades de los moduladores de la UPR como terapia frente al accidente cerebrovascular.
6) El tratamiento con salubrinal presenta un papel neuroprotector en CA1 en el modelo de isquemia cerebral global. El CA1 parece que presenta una limitada capacidad para activar la UPR en este modelo de isquemia y que el tratamiento con salubrinal mejora la capacidad del CA1 para hacer frente al estrés de retículo endoplasmático, reduciendo así la muerte celular retrasada.
7) El tratamiento con salubrinal proporciona un soporte adicional nuestra hipótesis de la existencia de diferencias locales en la respuesta de la unidad neurovascular a la inflamación.
8) El tratamiento con salubrinal provoca una respuesta diferencial en los componentes de la unidad neurovascular, desde una respuesta prácticamente nula en astrocitos hasta una fuerte sensibilidad en

neuronas y en células endoteliales, dando lugar a efectos a nivel local más que a nivel sistémico.

9) El tratamiento post-isquémico con robenacoxib, un inhibidor selectivo de COX-2, provoca un efecto perjudicial en la población neural y aumenta la activación glial.

10) El tratamiento combinado con robenacoxib y salubrinal da lugar a un efecto neuroprotector que parece ser debido a la administración aguda de salubrinal.

11) El tratamiento combinado de robenacoxib y salubrinal provoca un descenso sinérgico en la activación glial. Esto sugiere que la combinación de agentes inhibidores del estrés de retículo endoplasmático y agentes anti-inflamatorios podría resultar en un mayor efecto neuroprotector.

REFERENCES

References

- Aarts M., Iihara K., Wei W. L., Xiong Z. G., Arundine M., Cerwinski W., MacDonald J. F. and Tymianski M. **(2003)** A key role for TRPM7 channels in anoxic neuronal death. *Cell*. 115, 863-877.
- Abbott J., Rönnbäck L. and Hansson E. **(2006)** Astrocyte–endothelial interactions at the blood–brain barrier. *Nat Rev Neurosci.* 7, 41-53.
- Abbott J., Patabendige A., Dolman D., Yusof S. and Begley D. **(2010)** Structure and function of the blood-brain barrier. *Nerurobiol Dis.* 37, 13–25.
- Abbott J. **(2013**) Blood–brain barrier structure and function and the challenges for CNS drug delivery. *J Inherit Metab Dis.* 36, 437–449.
- Abraham H. and Lazar G. **(2000)** Early microglial reaction following mild forebrain ischemia induced by common carotid artery occlusion in rats. *Brain Res.* 862, 63–73.
- Adams H. P. Jr, Effron M. B., Torner J., Dávalos A., Frayne J., Teal P., Leclerc J., Oemar B., Padgett L., Barnathan E. S., Hacke W. and AbESTT-II Investigators. **(2008)** Emergency administration of abciximab for treatment of patients with acute ischemic stroke: results of an international phase III trial: Abciximab in Emergency Treatment of Stroke Trial (AbESTT-II) *Stroke*. 39, 87–99.
- Aïd S. and Bosetti F. **(2011)** Targeting cyclooxygenases-1 and -2 in neuroinflammation: therapeutic implications. *Biochimie*. 93, 46–51.
- Alliot F., Godin I. and Pessac B. (**1999**) Microglia derive from progenitors, originating from the yolk sac, and which proliferate in the brain. *Brain Res Dev Brain Res.* 117, 145-52.
- Amantea D., Nappi G., Bernardi G., Bagetta G. and Corasaniti M. T. **(2009)** Post-ischemic brain damage: pathophysiology and role of inflammatory mediators. *FEBS J.* 276, 13-26.
- Amor S., Puentes F., Baker D. and van der Valk P. **(2010)** Inflammation in neurodegenerative diseases. *Immunology.* 129, 154-169.
- Anderson P. and Kedersha N. **(2002)** Visibly stressed: the role of eIF2, TIA-1, and stress granules in protein translation. *Cell Stress Chaperones.* 7, 213-221.
- Anthony D.C., Bolton S.J., Fearn S. and Perry V.H. **(1997)** Age-related effects of interleukin-1 beta on polymorphonuclear neutrophil-dependent increases in blood-brain barrier permeability in rats. *Brain.* 120, 435-444.

- Antithrombotic Trialists' Collaboration. **(2002)** Collaborative meta-analysis of randomised trials of antiplatelet therapy for prevention of death, myocardial infarction, and stroke in high risk patients. *BMJ.* 234, 71-86.
- Antithrombotic Trialists' (ATT) Collaboration, Baigent C., Blackwell L., Collins R., Emberson J., Godwin J., Peto R., Buring J., Hennekens C., Kearney P., Meade T., Patrono C., Roncaglioni M. C. and Zanchetti A. **(2009)** Aspirin in the primary and secondary prevention of vascular disease: collaborative meta-analysis of individual participant data from randomised trials. *Lancet.* 373, 1849-1860.
- Anuncibay-Soto, B., Perez-Rodriguez D., Santos-Galdiano M., Font E., Regueiro-Purriños M. and Fernández-López A. **(2016)** Post-ischemic salubrinal treatment results in a neuroprotective role in global cerebral ischemia. *J Neurochem.* 138, 295-306.
- Anuncibay-Soto B., Perez-Rodriguez D., Llorente I. L., Regueiro-Purrinos M., Gonzalo-Orden J. M. and Fernandez-Lopez A. **(2014)** Age-dependent modifications in vascular adhesion molecules and apoptosis after 48-h reperfusion in a rat global cerebral ischemia model. *Age*. 36, 9703.
- Anwar M., Buchweitz-Milton E. and Weiss H. R. (1988) Effect of Prazosin on microvascular perfusion during middle cerebral artery ligation in the rat. *Circ Res.* 63, 27–34.
- Anyanwu E.C. **(2007)** Neurochemical changes in the aging process: implications in medication in the elderly. *Sci World J.* 7, 1603-1610.
- Arboix A. **(2002)** Diseases simulating transitory ischemic attacks or established strokes. *Neurología.* 17, 353-354.
- Arumugam T.V., Phillips T.M., Cheng A., Morrell C.H., Mattson M.P. and Wan, R. **(2010)** Age and energy intake interact to modify cell stress pathways and stroke outcome. *Ann Neurol*. 67, 41-52.
- Asai M., Tsukamoto O., Minamino T., Asanuma H., Fujita M., Asano Y., Takahama H., Sasaki H., Higo S., Asakura M., Takashima S., Hori M. and Kitakaze M. **(2009)** PKA rapidly enhances proteasome assembly and activity in in vivo canine hearts. *J Mol Cell Cardiol.* 46, 452-462.
- Ay H., Koroshetz W. J., Vangel M., Benner T., Melinosky C., Zhu M., Menezes N., Lopez C. J. and Sorensen A. G. **(2005)** Conversion of ischemic brain tissue into infarction increases with age. *Stroke*. 36, 2632-2636.
- Ayuso M.I., Garcia-Bonilla L., Martin M.E. and Salinas, M. **(2010)** Assessment of protein expression levels after transient global cerebral ischemia using an antibody microarray analysis. *Neurochem Res*. 35, 1239-1247.
- Back T. **(1998)** Pathophysiology of the ischemic penumbra--revision of a concept. *Cell Mol Neurobiol.* 18, 621-638.

- Badawi Y., Ramamoorthy P., Shi H. **(2012)** Hypoxia-inducible factor 1 protects hypoxic astrocytes against glutamate toxicity." *ASN Neuro* 4, 231-41.
- Bai J. and Lyden P. D. **(2015)** Revisiting cerebral postischemic reperfusion injury: new insights in understanding reperfusion failure, hemorrhage, and edema. *Int J Stroke.* 10, 143-52.
- Bal K., Tripathy B.C. and Sharma D. **(2006)**. Neuroprotective and anti-ageing effects of curcumin in aged rat brain regions. *Biogerontology,* 7, 81-89.
- Baltan S., Besancon E. F., Mbow B., Ye Z., Hamner M. A. and Ransom B. R. **(2008)** White matter vulnerability to ischemic injury increases with age because of enhanced excitotoxicity. *J Neurosci.* 28, 1479-1489.
- Bargatze R. F., Kurk S., Butcher E. C. and Jutila M. A. **(1994)** Neutrophils roll on adherent neutrophils bound to cytokine-induced endothelial cells via L-selectin on the rolling cells. *J Exp Med.* 180, 1785-92.
- Barnett, H. J. **(2002)** Stroke prevention in the elderly. *Clin Exp Hypertens.* 24, 563–571.
- Baron R., Babcock A., Nemirovsky A., Finsen B. and Monsonego A. **(2014)** Accelerated microglial pathology is associated with Aβ plaques in mouse models of Alzheimer's disease. *Aging Cell.* 13, 584–595.
- Barone F. C. and Feuerstein G. Z. **(1999)** Inflammatory mediators and stroke: new opportunities for novel therapeutics. *J Cereb Blood Flow and Metabol.* 19, 819–834.
- Barkalow F. J., Goodman M. J., Gerritsen M. E. and Mayadas T. N. **(1996)** Brain endothelium lack one of two pathways of P-selectin-mediated neutrophil adhesion. *Blood*. 88, 4585-4593.
- Barreda-Manso M. A., Yanguas-Casás N., Nieto-Sampedro M. and Romero-Ramírez L. **(2017)** Neuroprotection and blood-brain barrier restoration by Salubrinal after a cortical stab injury. *J Cell Physiol.* 232, 1501–1510.
- Barreiro O., Yanez-Mo M., Serrador J. M., Montoya M. C., Vicente-Manzanares M., Tejedor R., Furthmayr H. and Sanchez-Madrid F. **(2002)** Dynamic interaction of VCAM-1 and ICAM-1 with moesin and ezrin in a novel endothelial docking structure for adherent leukocytes. *J Cell Biol.* 157, 1233-1245.
- Barreiro O., Vicente-Manzanares M., Urzainqui A., Yáñez-Mó M. and Sánchez-Madrid F. **(2004)** Interactive protrusive structures during leukocyte adhesion and transendothelial migration. *Front Biosci.* 9, 1849-1863.
- Bauer A. T., Bürgers H. F., Rabie T. and Marti H. H. **(2010)** Matrix metalloproteinase-9 mediates hypoxia-induced vascular leakage in the brain via tight junction rearrangement. *J Cereb Blood Flow Metab.* 30, 837-848.

- Bechmann I., Goldmann J., Kovac A. D., Kwidzinski E., Simbürger E., Naftolin F., Dirnagl U., Nitsch R. and Priller J. **(2005**) Circulating monocytic cells infiltrate layers of anterograde axonal degeneration where they transform into microglia. *FASEB J.* 19, 647-649.

- Belayev L., Pinard E., Nallet H., Seylaz J., Liu Y., Riyamongkol P., Zhao W., Busto R. and Ginsberg M. D. **(2002)** Albumin therapy of transient focal cerebral ischemia: in vivo analysis of dynamic microvascular responses. 33, 1077-1084.

- Bendel O., Alkass K., Bueters T., von Euler M. and von Euler G. **(2005)** Reproducible loss of CA1 neurons following carotid artery occlusion combined with halothane-induced hypotension. *Brain Res*. 1033, 135-142.

- Berezowski V., Fukuda A., Cecchelli R. and Badaut J. **(2012)** Endothelial cells and astrocytes: a *Concerto En Duo* in ischemic pathophysiology. *Int J Cell Biol.* 2012, 1–16.

- Blais J. D., Chin K. T., Zito E., Zhang Y., Heldman N., Harding H. P., Fass D., Thorpe C. and Ron D. **(2010)** A small molecule inhibitor of endoplasmic reticulum oxidation 1 (ERO1) with selectively reversible thiol reactivity. *J Biol Chem.* 285, 20993-21003.

- Blamire A. M., Anthony D. C., Rajagopalan B., Sibson N. R., Perry V. H. and Styles P. **(2000)** Interleukin-1beta -induced changes in blood-brain barrier permeability, apparent diffusion coefficient, and cerebral blood volume in the rat brain: a magnetic resonance study. *J Neurosci*. 20, 8153-8159.

- Blanco S., Castro L., Hernandez R., Del Moral M. L., Pedrosa J. A., Martinez-Lara E., Siles E. and Peinado M. A. **(2007)** Age modulates the nitric oxide system response in the ischemic cerebellum. *Brain Res.* 1157, 66-73.

- Boyce M., Bryant K. F., Jousse C., Long K., Harding H. P., Scheuner D., Kaufman R. J., Ma D., Coen D. M., Ron D. and Yuan J. **(2005)** A selective inhibitor of eIF2alpha dephosphorylation protects cells from ER stress. *Science.* 307, 935-939.

- Braughler J. M., Duncan L. A. and Chase R. L. **(1985)** Interaction of lipid peroxidation and calcium in the pathogenesis of neuronal injury. *Cent Nerv Syst Trauma*. 2, 269-283.

- Broderick J. P. **(1997)** Intracerebral hemorrhage after intravenous t-PA therapy for ischemic stroke. The NINDS T-PA stroke study group. *Stroke*. 28, 2109–2118.

- Broderick J. P. **(2004)** William M. Feinberg Lecture: stroke therapy in the year 2025: burden, breakthroughs, and barriers to progress. *Stroke*. 35, 205-211.

- Broughton B. R., Reutens D. C. and Sobey C. G. **(2009)** Apoptotic mechanisms after cerebral ischemia. *Stroke*. 40, e331-339.

- Broughton B. R., Lim R., Arumugam T. V., Drummond G. R., Wallace E. M. and Sobey C. G. **(2012)** Post-stroke inflammation and the potential efficacy of novel stem cell therapies: focus on amnion epithelial cells. *Front Cell Neurosci.* 6, 66.
- Brouns R and De Deyn P. P. **(2009)** The complexity of neurobiological processes in acute ischemic stroke. *Clin Neurol Neurosurg.* 111, 483-495.
- Brown A. W., Marlowe K. J. and Bjelke B. **(2003)** Age effect on motor recovery in a post-acute animal stroke model. *Neurobiol Aging.* 24, 607-614.
- Busch S. A. and Silver J. **(2007)** The role of extracellular matrix in CNS regeneration. *Curr Opin Neurobiol*. 17, 120-127.
- Cacheaux L. P., Ivens S., David Y., Lakhter A. J., Bar-Klein G., Shapira M., Heinemann U., Friedman A. and Kaufer D, **(2009)**. Transcriptome profiling reveals TGF-beta signaling involvement in epileptogenesis. *J Neurosci*. 29, 8927-8935.
- Cai X. H., Li X. C., Jin S. W., Liang D. S., Wen Z. W., Cao H. C., Mei H.F., Wu Y., Lin Z. D. and Wang L. X. **(2014)** Endoplasmic reticulum stress plays critical role in brain damage after chronic interittent hypoxia in growing rats. *Exp Neurol.* 257, 148-156.
- Cairns J. A. **(2007)** The Coxibs and raditional nonsteroidal anti-inflammatory drugs: a current perspective on cardiovascular risks. *Can J Cardiol.* 23, 125–131.
- Candelario-Jalil E., González-Falcón A., García-Cabrera M., Álvarez D., Al-Dalain S., Martínez G., León O. and Springer J. E. **(2003)** Assessment of the relative contribution of COX-1 and COX-2 isoforms to ischemia-induced oxidative damage and neurodegeneration following transient global cerebral ischemia. *J Neurochem.* 86, 545–555.
- Candelario-Jalil E. and Fiebich B. L. **(2008)** Cyclooxygenase inhibition in ischemic brain injury. *Curr Pharm Des.* 14, 1401–1418.
- Candelario-Jalil E. **(2009)** Injury and repair mechanisms in ischemic stroke: considerations for the development of novel neurotherapeutics. *Curr Opin Investig Drugs.* 10, 644-654.
- Carlos T. M. and Harlan J. M. **(1994)**. Leukocyte-endothelial adhesion molecules. *Blood* 84, 2068–2101.
- Castro C. C., Pagnussat A. S., Moura N., da Cunha M.J., Machado F.R., Wyse A. T. and Netto C. A. **(2014)** Coumestrol treatment prevents Na+, K+ -ATPase inhibition and affords histological neuroprotection to male rats receiving cerebral global ischemia. *Neurol Res.* 36, 198–206.
- Carman C. V. and Springer T. A. **(2004)** A transmigratory cup in leukocyte diapedesis both through individual vascular endothelial cells and between them. *J Cell Biol*. 167, 377-388.

- Ceulemans A. G., Zgavc T., Kooijman R., Hachimi-Idrissi S., Sarre S. and Michotte Y. **(2010)** The dual role of the neuroinflammatory response after ischemic stroke: modulatory effects of hypothermia. *J Neuroinflam*. 7, 74-94.
- Chamorro A. and Hallenbeck J. **(2006)** The harms and benefits of inflammatory and immune responses in vascular disease. *Stroke*. 37, 291-293.
- Chan P. H., Kerlan R. and Fishman R. A. **(1983)** Reductions of gamma-aminobutyric acid and glutamate uptake and (Na+ + K+)-ATPase activity in brain slices and synaptosomes by arachidonic acid. *J Neurochem.* 40, 309-316.
- Chan P. H. **(2001)** Reactive oxygen radicals in signaling and damage in the ischemic brain. *J Cereb Blood Flow Metab*. 21, 2–14.
- Chapman R. C. and Walter P. **(1998)** Intracellular signalling from the endoplasmic reticulum to the nucleus. *Ann Rev Cell Dev Biol.* 14, 459-85.
- Chariot A. **(2009)** The NF-κB-independent functions of IKK subunits in immunity and cancer. *Trends Cell Biol*. 19, 404-413.
- Che X., Ye W., Panga L., Wu D. C. and Yang G. Y. **(2001)** Monocyte chemoattractant protein-1 expressed in neurons and astrocytes during focal ischemia in mice. *Brain Res.* 902, 171-177.
- Cheng W. P., Wang B. W. and Shyu K. G. **(2009)**. Regulation of GADD153 induced by mechanical stress in cardiomyocytes." *Eur J Clinic Invest.* 39, 960-971.
- Choi S. H., Aid S. and Bosetti F. **(2009)** The distinct roles of cyclooxygenase-1 and -2 in neuroinflammation: implications for translational research. *Trends Pharmacol Sci.* 30, 174–181.
- Chong, Z. Z., Xu Q. P. and Sun J. N. **(2001)**. Effects and mechanisms of triacetylshikimic acid on platelet adhesion to neutrophils induced by thrombin and reperfusion after focal cerebral ischemia in rats. *Acta Pharmacol Sin.* 22, 679-684.
- Choudhri T. F., Hoh B. L., Zerwes H. G., Prestigiacomo C. J., Kim S. C., Connolly E. S. Jr, Kottirsch G. and Pinsky D. J. **(1998)** Reduced microvascular thrombosis and improved outcome in acute murine stroke by inhibiting GP IIb/IIIa receptor-mediated platelet aggregation. *J Clin Invest.* 102, 1301-1310.
- Christou I., Alexandrov A. V., Burgin W. S., Wojner A. W., Felberg R. A., Malkoff M. and Grotta J. C. **(2000)** Timing of recanalization after tissue plasminogen activator therapy determined by transcranial doppler correlates with clinical recovery from ischemic stroke. *Stroke.* 31, 1812-1816.
- Chu K., Jeong S. W., Jung K. H., Han S. Y., Lee S. T., Kim M. and Roh J. K. **(2004)** Celecoxib induces functional recovery after intracerebral hemorrhage with

reduction of brain edema and perihematomal cell death. *J Cereb Blood Flow Metab.* 24, 926-33.

- Clayton D. A., Mesches M. H., Alvarez E., Bickford P. C. and Browning M. D. **(2002)** A hippocampal NR2B deficit can mimic age-related changes in long-term potentiation and spatial learning in the Fischer 344 rat. *J Neurosci*. 22, 3628-3637.
- Colangelo A. M., Alberghina L. and Papa M. **(2014)** Astrogliosis as a therapeutic target for neurodegenerative diseases. *Neurosci Lett.* 565, 59-64.
- Collard C. D. and Gelman S. **(2001)** Pathophysiology, clinical manifestations, and prevention of ischemia-reperfusion injury. *Anesthesiology* 94, 1133-38.
- Collins T. C., Petersen N. J., Menke T. J., Souchek J., Foster W. and Ashton C. M. **(2003)** Short-term, intermediate-term, and long-term mortality in patients hospitalized for stroke. *J Clin Epidemiol*. 56, 81-87.
- Corps K. N., Roth T. L. and McGavern D. B. **(2015)** Inflammation and neuroprotection in traumatic brain injury. *JAMA Neurol*. 72, 355-362.
- Creutzfeldt C. J. and Holloway R. G. **(2012)** Treatment decisions after severe stroke: uncertainty and biases. *Stroke.* 43, 3405-3408.
- Crofford L. J., Wilder R. L., Ristimäki A. P., Sano H., Remmers E. F., Epps H. R. and Hla T. **(1994)** Cyclooxygenase-1 and -2 expression in rheumatoid synovial tissues. Effects of interleukin-1 beta, phorbol ester, and corticosteroids. *J Clin Invest.* 93, 1095-1101.
- Cybulsky A. V., Takano T., Papillon J. and Bijian K. **(2005)** Role of the endoplasmic reticulum unfolded protein response in glomerular epithelial cell injury. *J Biol Chem.* 280, 24396–24403.
- da Fonseca A. C., Matias D., Amaral R., Geraldo L. H., Freitas and Lima F. R. **(2014)** The impact of microglial activation on blood-brain barrier in brain diseases. *Fron Cell Neurosci.* 3, 362.
- Davis M., Mendelow A. D., Perry R. H., Chambers I. R. and James O. F. **(1995)** Experimental stroke and neuroprotection in the aging rat brain. *Stroke*. 26, 1072–1078.
- Davoust N., Vuaillat C., Androdias G. and Nataf S. **(2008)** From bone marrow to microglia: barriers and avenues. *Trends Immunol*. 29, 227–234.
- De los Reyes, L. M. and Céspedes A. E. **(2014)** Atorvastatin-meloxicam association inhibits neuroinflammation and attenuates the cellular damage in cerebral ischemia by arterial embolism. *Biomedica.* 34, 366-378.

- del Zoppo,G. J., Schmid-Schönbein G. W., Mori E., Copeland B. R. and Chang C. M. **(1991)** Polymorphonuclear leukocytes occlude capillaries following middle cerebral artery occlusion and reperfusion in baboons. *Stroke.* 22, 1276–1283.
- del Zoppo G. J. **(1998)** The role of platelets in ischemic stroke. *Neurol.* 51, 9-14.
- DeGracia D. J., Kumar R., Owen C. R., Krause G. S. and White B. C. **(2002)** Molecular pathways of protein synthesis inhibition during brain reperfusion: implications for neuronal survival or death. *J Cereb Blood Flow Metab.* 22, 127-141.
- Deng J., Lu P. D., Zhang Y., Scheuner D., Kaufman R. J., Sonenberg N., Harding H. P. and Ron D. **(2004)** Translational repression mediates activation of nuclear factor kappa B by phosphorylated translation initiation factor 2. *Mol Cell Biol.* 24, 10161-10168.
- Didion S. P., Ryan M. J., Baumbach G. L., Sigmund C. D. and Faraci F. M. **(2002)**. Superoxide contributes to vascular dysfunction in mice that express human renin and angiotensinogen. *Am J Physiol.* 283, 1569-1576.
- Dijkhuizen R. M., Knollema S., van der Worp H. B., Ter Horst G. J., De Wildt D. J., Berkelbach van der Sprenkel J. W., Tulleken K. A. and Nicolay K. **(1998)** Dynamics of cerebral tissue injury and perfusion after temporary hypoxia-ischemia in the rat: evidence for region-specific sensitivity and delayed damage. *Stroke*. 29, 695-704.
- Dirnagl U., Iadecola C. and Moskowitz M. A. **(1999)**. Pathobiology of ischaemic stroke: an integrated view. *Trends Neurosci.* 22, 391–397.
- Doll D. N., Hu H., Sun J., Lewis S. E., Simpkins J. W. and Ren X. **(2015)** Mitochondrial crisis in cerebrovascular endothelial cells opens the blood-brain barrier. *Stroke.* 46, 1681-1689.
- Dong Y. and Benveniste E. N. **(2001)**. Immune function of astrocytes. *Glia*. 36, 180–190.
- Donnan G. A., Fisher M., Macleod M. and Davis S. M. **(2008)** Stroke. *Lancet.* 371, 1612-1623.
- Durukan A. and Tatlisumak T. **(2007)** Acute ischemic stroke: overview of major experimental rodent models, pathophysiology, and therapy of focal cerebral ischemia. *Pharmacol Biochem Behav.* 87, 179-197.
- Duverger D. and MacKenzie E. T. **(1988)** The quantification of cerebral infarction following focal ischemia in the rat: influence of strain, arterial pressure, blood glucose concentration, and age. *J Cereb Blood Flow Metab.* 8, 449-461.
- Dziennis S., Mader S., Akiyoshi K., Ren X., Ayala P., Burrows G. G., Vandenbark A. A., Herson P. S., Hurn P. D. and Offner H. A. **(2011)** Therapy with recombinant T-

cell receptor ligand reduces infarct size and infiltrating inflammatory cells in brain after middle cerebral artery occlusion in mice. *Metab Brain Dis*. 26, 123-133.

- Dziewulska D. **(1997)** Age-dependent changes in astroglial reactivity in human ischemic stroke. Immunohistochemical study. *Folia Neuropathol.* 35, 99-106.
- Eckle V. S., Buchmann A., Bursch W., Schulte-Hermann R. and Schwarz M. **(2004)** Immunohistochemical detection of activated caspases in apoptotic hepatocytes in rat liver. *Toxicol Pathol.* 32, 9-15.
- Elvers M., Stegner D., Hagedorn I., Kleinschnitz C., Braun A., Kuijpers M. E., Boesl M., Chen Q., Heemskerk J. W., Stoll G., Frohman M. A. and Nieswandt B. **(2010)** Impaired alpha(IIb)beta(3) integrin activation and shear-dependent thrombus formation in mice lacking phospholipase D1. *Sci Signal.* 3, 1.
- Engelhardt B. and Ransohoff R. M. **(2012)** Capture, crawl, cross: the T cell code to breach the blood–brain barriers. *Trends Immunol.* 33, 579-589.
- Engin F. and Hotamisligil G. S. **(2010)** Restoring endoplasmic reticulum function by chemical chaperones: an emerging therapeutic approach for metabolic diseases. *Diabetes Obes Metab.* 12, 108-115.
- Enzmann G., Mysiorek C., Gorina R., Cheng Y. J., Ghavampour S., Hannocks M. J., Prinz V., Dirnagl U., Endres M., Prinz M., Beschorner R., Harter P. N., Mittelbronn M., Engelhardt B.and Sorokin L. **(2013)** The neurovascular unit as a selective barrier to polymorphonuclear granulocyte (PMN) infiltration into the brain after ischemic injury. *Acta Neuropathol.* 125, 395-412.
- Farfel-Becker T., Vitner E. B., Pressey S. N., Eilam R., Cooper J. D. and Futerman A. H. **(2011)** Spatial and temporal correlation between neuron loss and neuroinflammation in a mouse model of neuronopathic Gaucher disease. *Human Mol Genet.* 20, 1375-1386.
- Fan W., Dai Y., Xu H., Zhu X., Cai P., Wang L., Sun C., Hu C., Zheng P. and Zhao B. Q. **(2014)** Caspase-3 modulates regenerative response after stroke. *Stem Cells* 32, 473-486.
- Feng L., Yang X., Asweto C. O., Wu J., Zhang Y., Hu H., Shi Y., Duan J. and Sun Z. **(2017)** Genome-wide transcriptional analysis of cardiovascular-related genes and pathways induced by PM2.5 in human myocardial cells. *Environ Sci Pollut Res Int.* 24, 11683-11693.
- Fernandez J., Yaman I., Sarnow P., Snider M. D. and Hatzoglou M. **(2002)** Regulation of internal ribosomal entry site-mediated translation by phosphorylation of the translation initiation factor eIF2alpha. *J Biol Chem.* 277, 19198-19205.

- Fiebich B. L., Akter S. and Akundi R S. **(2014)** The two-hit hypothesis for neuroinflammation: role of exogenous ATP in modulating inflammation in the brain. *Front Cell Neurosci.* 8, 260.
- Fisher M. **(1993)** Increased thromboxane biosynthesis in patients with acute cerebral ischemia. *Stroke.* 24, 912.
- Fisher M. and Bastan B. **(2008)** Treating acute ischemic stroke. *Curr Opin Drug Discov Devel.* 11, 626-632.
- FitzGerald G. A., Cheng Y. and Austin S. **(2001**) COX-2 inhibitors and the cardiovascular system. *Clin Exp Rheumatol.* 19, S31-36.
- Frenette P. S., Denis C. V., Weiss L., Jurk K., Subbarao S., Kehrel B., Hartwig J. H, Vestweber D. and Wagner D. D. **(2000)** P-Selectin Glycoprotein Ligand 1 (Psgl-1) is expressed on platelets and can mediate platelet–endothelial interactions in vivo. *J Exp Med.* 191, 1413-1422.
- Fricker M., Vilalta A., Tolkovsky A. M. and Brown G. C. **(2013)** Caspase inhibitors protect neurons by enabling selective necroptosis of inflamed microglia. *J Biol Chem.* 288, 9145-9152.
- Fu H. Y., Okada K., Liao Y., Tsukamoto O., Isomura T., Asai M., Sawada T., Okuda K., Asano Y., Sanada S., Asanuma H., Asakura M., Takashima S, Komuro I., Kitakaze M and Minamino T. **(2010)** Ablation of C/EBP Homologous Protein attenuates endoplasmic reticulum–mediated apoptosis and cardiac dysfunction induced by pressure overload. *Circulation.* 122, 361-369.
- Galluzzi L. *et al.,* **(2015)** Essential versus accessory aspects of cell death: recommendations of the NCCD 2015. *Cell Death Differ* 22, 58–73.
- Garcia J. H., Liu K. F., Yoshida Y., Chen S. and Lian J. **(1994)** Brain microvessels: factors altering their patency after the occlusion of a middle cerebral artery (Wistar rat). *Am J Pathol.* 145, 728-740.
- Gardner B. M. and Walter P. **(2011)** Unfolded proteins are IRE1-activating ligands that directly induce the unfolded protein response. *Science*. 333, 1891–1894.
- Gelderblom M., Leypoldt F., Steinbach K., Behrens D., Choe C. U., Siler D. A., Arumugam T. V., Orthey E., Gerloff C. Tolosa E. and Magnus T. **(2009)** Temporal and spatial dynamics of cerebral immune cell accumulation in stroke. *Stroke*.40, 1849-185.
- Ginsberg M. D. and Pulsinelli W. A. **(1994)** The ischemic penumbra, injury thresholds, and the therapeutic window for acute stroke. *Ann Neurol*. 36, 553-554.
- Glezer I., Simard A. R. and Rivest S. **(2007)** Neuroprotective role of the innate immune system by microglia. *Neuroscience*. 147, 867–883.

- Gong Y., Hua Y., Keep R. F. Hoff J. T. and Xi G. **(2004)** Intracerebral hemorrhage: effects of aging on brain edema and neurological deficits. *Stroke*. 35, 2571-2575.
- Goodall J. C., Wu C., Zhang Y., McNeill L., Ellis L., Saudek V. and Hill Gaston J. S. **(2010)** Endoplasmic reticulum stress-induced transcription factor, CHOP, is crucial for dendritic cell IL-23 expression. *PNAS.* 107, 17698–17703.
- Gorelick P. B. **(2002)** Stroke prevention therapy beyond antithrombotics: unifying mechanisms in ischemic stroke pathogenesis and implications for therapy: an invited review. *Stroke.* 33, 862-875.
- Gotsch U., Jager U., Dominis M. and Vestweber D. **(1994)**. Expression of P-selectin on endothelial cells is upregulated by LPS and TNF-alpha in vivo. *Cell Adhes Commun.* 2, 7-14.
- Grady C. L. and Craik F. I. **(2000)** Changes in memory processing with age. *Curr Opin Neurobiol.* 10, 224-231.
- Green C. E., Pearson D. N., Camphausen R. T., Staunton D. E. and Simon S. I. **(2004)** Shear-dependent capping of L-selectin and P-selectin glycoprotein ligand 1 by E-selectin signals activation of high-avidity beta2-integrin on neutrophils. *J Immunol.* 172, 7780-7790.
- Grosser T., Yusuff S., Cheskis E., Pack M. A. and FitzGerald G. A. **(2002)** Developmental expression of functional cyclooxygenases in zebrafish. *PNAS*. 99, 8418–8423.
- Grosser T., Yu Y. and FitzGerald G. A. **(2010)** Emotion recollected in tranquillity: lessons learned from the COX-2 saga. *Annu Rev Med*. 61, 17-33.
- Gu Y., Zheng G., Xu M., Li Y., Chen X., Zhu W., Tong Y., Chung S. K., Liu K. J. and Shen J. **(2012)** Caveolin-1 regulates nitric oxide-mediated matrix metalloproteinases activity and blood-brain barrier permeability in focal cerebral ischemia and reperfusion injury. *J Neurochem.* 120, 147-156.
- Gudino-Cabrera G. and Nieto-Sampedro M. **(2000)** Schwann-like macroglia in adult rat brain. *Glia.* 30, 49-63.
- Gundersen H. J., Bagger P., Bendtsen T. F., Evans S. M., Korbo L., Marcussen N., Moller A., Nielsen K., Nyengaard J. R. and Pakkenberg B. **(1988)** The new stereological tools: disector, fractionator, nucleator and point sampled intercepts and their use in pathological research and diagnosis. *APMIS*. 96, 857-881. Hallenbeck J. M. **(1996)** Inflammatory reactions at the blood-endothelial interface in acute stroke. *Adv Neurol.* 71, 281–300.
- Hallenbeck J. M**. (2002)** The many faces of tumor necrosis factor in stroke. *Nat Med.* 8, 1363–1368.

- Halterman M. W., De Jesus C., Rempe D. A., Schor N. F. and Federoff H. J. **(2008)** Loss of c/EBP-beta activity promotes the adaptive to apoptotic switch in hypoxic cortical neurons. *Mol Cell Neurosci.* 38, 125-137.
- Hao F., Pysz M. A., Curry K. J., Haas K. N., Seedhouse S. J., Black A. R. and Black J. D. **(2011)** Protein kinase Cα signaling regulates inhibitor of DNA binding 1 in the intestinal epithelium. *J Biol Chem.* 286, 18104-18117.
- Harding H. P., Zhang Y., Bertolotti A., Zeng H. and Ron D. **(2000)** Perk is essential for translational regulation and cell survival during the unfolded protein response. *Mol Cell*. 5, 897-904.
- Harari O. A. and Liao J. K. **(2010)** NF-κB and innate immunity in ischemic stroke. *Ann N Y Acad Sci.* 1207, 32–40.
- Hartman R. E., Lee J. M., Zipfel G. J. and and Wozniak D. F. **(2005)** Characterizing learning deficits and hippocampal neuron loss following transient global cerebral ischemia in rats. *Brain Res*. 1043, 48-56.
- Hasnain S. Z., Lourie R., Das I., Chen A. C. and McGuckin M. A. **(2012)** The interplay between endoplasmic reticulum stress and inflammation. *Immunol Cell Biol.* 90, 260-270.
- Hatazawa R., Tanaka A., Tanigami M., Amagase K., Kato S., Ashida Y. and Takeuchi K. **(2007)** Cyclooxygenase-2/prostaglandin E2 accelerates the healing of gastric ulcers via EP4 receptors. *Am J Physiol Gastrointest Liver Physiol.* 293, 788-797.
- Hawkins B. T. and Davis T. P. **(2005)** The blood-brain barrier/neurovascular unit in health and disease. *Pharmacol Rev*. 57, 173-185.
- Hayakawa K., Nakajima S., Hiramatsu N., Okamura M., Huang T., Saito Y., Tagawa Y., Tamai M., Takahashi S., Yao J. and Kitamura M. **(2010)** ER stress depresses NF-kappaB activation in mesangial cells through preferential induction of C/EBP beta. *J Am Soc Nephrol.* 21, 73-81.
- Hayden M. S. and Ghosh S. **(2004)** Signaling to NF-kappaB. *Genes Dev*. 18, 2195-2224.
- He Z., Meschia J .F., Brott T. G., Dickson D. W. and McKinney M. **(2006)** Aging is neuroprotective during global ischemia but leads to increased caspase-3 and apoptotic activity in hippocampal neurons. *Curr Neurovasc Res*. 3, 181-186.
- Hirt L., Ternon B., Price M., Mastour N., Brunet J. F. and Badaut J. **(2009)** Protective role of early aquaporin 4 induction against postischemic edema formation. *J Cereb Blood Flow Metab.* 29, 423-33.
- Hoffmann A. and Baltimore D. **(2006)** Circuitry of nuclear factor kappaB signaling. *Immunol Rev.* 210, 171-186.

- Hossmann A. **(1993)** Ischemia-mediated neuronal injury. *Resuscitation*. 26, 225-235.
- Hossmann K. A. **(1994)** Viability thresholds and the penumbra of focal ischemia. *Ann Neurol*. 36, 557-565.
- Hossmann A. **(2008)** Cerebral ischemia: models, methods and outcomes. *Neuropharmacology* 55, 257-270.
- Huang Y. C. and Feng Z. P. **(2013)** The good and bad of microglia/macorphages: new hope in stroke therapeutics. *Acta Pharmacol Sin*. 34, 6-7.
- Huber J. D., Campos C. R., Mark K. S. and Davis T. P. **(2006)** Alterations in blood-brain barrier ICAM-1 expression and brain microglial activation after lambda-Carrageenan-induced inflammatory pain. *Am J Physiol*. 290, 732-740.
- Hwang, J. M., Yamanouchi J., Santamaria P., and Kubes P. (2004) A critical temporal window for selectin-dependent CD4+ lymphocyte homing and initiation of late-phase inflammation in contact sensitivity. *J Exp Med*. 199, 1223–1234.
- Iadecola C., Zhang F., Niwa K., Eckman C., Turner S.K., Fischer E., Younkin S., Borchelt D.R., Hsiao K.K. and Carlson G.A. **(1999)** SOD1 rescues cerebral endothelial dysfunction in mice overexpressing amyloid precursor protein. *Nat Neurosci*. 2, 157–61.
- Iadecola C. and Alexander M. **(2001)** Cerebral ischemia and inflammation. *Curr Opin Neurol.* 14, 89–94.
- Inagi R., Kumagai T., Nishi H., Kawakami T., Miyata T., Fujita T and Nangaku M. **(2008)** Preconditioning with endoplasmic reticulum stress ameliorates mesangioproliferative glomerulonephritis. *J American Soc Nephrol.* 19, 915-922.
- Isabel C., Calvet D. and Mas J. L. **(2016)** Stroke prevention. *Press Méd.* 45, e457–471.
- Israël A. **(2010)** The IKK complex, a central regulator of NF-kappaB activation. *Cold Spring Harb Perspect Biol* 2, a000158.
- Ivanova E. A. and Orekhov A. N. **(2016)** The role of endoplasmic reticulum stress and unfolded protein response in atherosclerosis. *Int J Mol Sci.* 17, 193.
- Ivens S., Kaufer D., Flores L. P., Bechmann I., Zumsteg D., Tomkins O., Seiffert E., Heinemann U. and Friedman A. **(2007)** TGF-beta receptor-mediated albumin uptake into astrocytes is involved in neocortical epileptogenesis. *Brain.* 130, 535-547.
- Iwakoshi N. N., Lee A. H. and Glimcher L. H. **(2003)** The X-Box Binding Protein-1 transcription factor is required for plasma cell differentiation and the Unfolded Protein Response. *Immunol Rev.* 194, 29-38.

- Jia F., Wu C., Chen Z. and Lu G. **(2012)** Atorvastatin inhibits homocysteine-induced endoplasmic reticulum stress through activation of AMP-activated protein kinase. *Cardiovasc Ther.* 30, 317-325.
- Jiang H. Y., Wek S. A., McGrath B. C., Scheuner D., Kaufman R. J., Cavener D. R. and Wek R. C. **(2003)** Phosphorylation of the alpha subunit of eukaryotic initiation factor 2 is required for activation of NF-kappaB in response to diverse cellular stresses. *Mol Cell Biol.* 23, 5651-5663.
- Jiao H., Wang Z., Liu Y., Wang P. and Xue Y. **(2011)** Specific role of tight junction proteins Claudin-5, Occludin, and ZO-1 of the blood–brain barrier in a focal cerebral ischemic insult. *J Mol Neurosci.* 4, 130-139.
- Jin R., Yang G. and Li G. **(2010)** Inflammatory mechanisms in ischemic stroke: role of inflammatory cells. *J Leukoc Biol*. 87, 779-789.
- Jornayvaz F. R. and Shulman G. I. **(2010)** Regulation of mitochondrial biogenesis. *Essays Biochem.* 47, 69-84.
- Joussen A. M., Doehmen S., Le M. L., Koizumi K., Radetzky S., Krohne T. U., Poulaki V., Semkova I. and Kociok N. **(2009)** TNF-alpha mediated apoptosis plays an important role in the development of early diabetic retinopathy and long-term histopathological alterations. *Mol Vis.* 15, 1418-1428.
- Jüni P., Nartey L., Reichenbach S., Sterchi R., Dieppe P. A. and Egger M. **(2004**) Risk of cardiovascular events and rofecoxib: cumulative meta-analysis. *Lancet*. 364, 2021-2029.
- Kadhim H. J., Duchateau J. and Sebire G. **(2008)** Cytokines and brain injury: invited review. *J Intensive Care Med*. 23, 236-249.
- Kahle K. T., Simard J. M., Staley K. J., Nahed B. V., Jones P. S. and Sun D. **(2009)** Molecular mechanisms of ischemic cerebral edema: role of electroneutral ion transport. *Physiology.*24, 257-265.
- Kaneko M. and Nomura Y. **(2003)** ER signaling in Unfolded Protein Response." Life Sci, 74, 199–205.
- Kansas G. S. **(1996)** Selectins and their ligands: current concepts and controversies. *Blood.* 88:3259–3287.
- Kaufman R. J. **(1999)** Stress signaling from the lumen of the endoplasmic reticulum: coordination of gene transcriptional and translational controls. *Genes Dev.* 13, 1211-1233.
- Kettenmann H., Hanisch U. K., Noda M. and Verkhratsky A. **(2011)** Physiology of microglia. *Physiol Rev* 91, 461-553.
- Kidwell C. S., Saver J. L., Mattiello J., Starkman S., Vinuela F., Duckwiler G., Gobin Y. P., Jahan R., Vespa P., Villablanca J. P., Liebeskind D. S., Woods R. P. and Alger

J.R. **(2001)** Diffusion-perfusion MRI characterization of post-recanalization hyperperfusion in humans. *Neurology.* 57, 2015-2021.

- Kim I., Shu C. W., Xu W., Shiau C. W., Grant D., Vasile S., Cosford N. D. and Reed J. C. **(2009)** Chemical biology investigation of cell death pathways activated by endoplasmic reticulum stress reveals cytoprotective modulators of ASK1. *J Biol Chem.* 284, 1593-1603.
- Kim J. S. **(1996)** Cytokines and adhesion molecules in stroke and related diseases. *J Neurol Sci.* 137, 69-78.
- Kimata Y. and Kohno K. **(2011)** Endoplasmic reticulum stress-sensing mechanisms in yeast and mammalian cells. *Curr Opin Cell Biol*. 23, 135-142.
- King J. N., Dawson J., Esser R. E., Fujimoto R., Kimble E. F., Maniara W., Marshall P. J., O'Byrne L., Quadros E., Toutain P. L. and Lees P. **(2009)** Preclinical pharmacology of robenacoxib: a novel selective inhibitor of cyclooxygenase-2. *J Vet Pharmacol Ther.* 32, 1-17.
- Kirino T., Tamura A. and Sano K. **(1985)** Selective vulnerability of the hippocampus to ischemia--reversible and irreversible types of ischemic cell damage. *Prog Brain Res.* 63, 39-58.
- Kitamura Y., Takata K., Inden M., Tsuchiya D., Yanagisawa D., Nakata J. and Taniguchi T. **(2004)** intracerebroventricular injection of microglia protects against focal brain ischemia. *J Pharmacol Sci.* 94, 203-206.
- Kitamura M. **(2009)** Biphasic, bidirectional regulation of NF-kappaB by endoplasmic reticulum stress. *Antioxid Redox Signal*. 11, 2353-2364.
- Kleihues P. and Hossmann K. A. **(1971)** Protein synthesis in the cat brain after prolonged cerebral ischemia. *Brain Res*. 35, 409-418.
- Kleinschnitz C. Pozgajova M., Pham M., Bendszus M., Nieswandt B. and Stoll G. **(2007)** Targeting platelets in acute experimental stroke: impact of glycoprotein Ib, VI, and IIb/IIIa blockade on infarct size, functional outcome, and intracranial bleeding. *Circulation.* 115, 2323-2330.
- Konsman J. P., Drukarch B. and Van Dam A. M. **(2007)** (Peri)vascular production and action of pro-inflammatory cytokines in brain pathology. *Clin Sci.* 112, 1–25.
- Korennykh A. and Walter P. **(2012)** Structural basis of the Unfolded Protein Response. *Annu Rev Cell Dev Biol.* 28, 251-277.
- Korennykh A. V., Egea P. F., Korostelev A. A., Finer-Moore J., Zhang C., Shokat K. M. Stroud R. M. and Walter P. **(2009)** The Unfolded Protein Response signals through high-order assembly of Ire1. *Nature*. 457-687-693.

- Krause G. S., White B. C., Aust S. D., Nayini N. R. and Kumar K. **(1988)** Brain cell death following ischemia and reperfusion: a proposed biochemical sequence. *Crit Care Med.* 16, 714-726.
- Kriz J. **(2006)** Inflammation in ischemic brain injury: timing is important. *Crit Rev Neurobiol.* 18, 145-157.
- Kriz J. and Lalancette-Hebert M. **(2009)** Inflammation, plasticity and real-time imaging after cerebral ischemia. *Acta Neuropathol*. 117, 497-509.
- Kunkel E. J., Dunne J. L. and Ley K. **(2000)** Leukocyte arrest during cytokine-dependent inflammation in vivo. *J Immunol.* 164, 3301-3308.
- Kunkel E. J. and Ley K. **(1996)** Distinct phenotype of E-selectin-deficient mice. E-selectin is required for slow leukocyte rolling in vivo. *Circ Res.* 79, 1196–1204.
- Kuroda S. and Siesjo B. K. **(1997)** Reperfusion damage following focal ischemia: pathophysiology and therapeutic windows. *Clin Neurosci.* 4, 199-212.
- Lakhan S. E., Kirchgessner A. and Hofer M. **(2009)** Inflammatory mechanisms in ischemic stroke: therapeutic approaches. *J Transl Med* 7, 97.
- Lalancette-Hebert M., Gowing G., Simard A., Weng Y. C. and Kriz J. **(2007)**. Selective ablation of proliferating microglial cells exacerbates ischemic injury in the brain. *J Neurosci.* 27, 2596–2605.
- Lalonde C. C., Mielke J. G. **(2014)** Selective vulnerability of hippocampal sub-fields to oxygen-glucose deprivation is a function of animal age. *Brain Res*. 1543, 271-279.
- Lauer R., Bauer R., Linz B., Pittner F., Peschel G.A., Ecker G., Friedl P. and Noe C. R. **(2004)** Development of an in vitro blood–brain barrier model based on immortalized porcine brain microvascular endothelial cells. *Farmaco.* 59, 133-137.
- Lee S. R., Tsuji K., Lee S. R. and Lo E. H. **(2004)** Role of matrix metalloproteinases in delayed neuronal damage after transient global cerebral ischemia. *J Neurosci.* 24, 671–678.
- Lelekov-Boissard T., Chapuisat G., Boissel J. P., Grenier E. and Dronne M. A. **(2009)** Exploration of beneficial and deleterious effects of inflammation in stroke: dynamics of inflammation cells. *Philos Trans A Math Phys Eng Sci.* 367, 4699–4716.
- Li Y., Powers C., Jiang N. and Chopp M. **(1998)** Intact, injured, necrotic and apoptotic cells after focal cerebral ischemia in the rat. *J Neurol Sci*. 156, 119-132.
- Li J., Wang J. J. and Zhang S. X. **(2011)** Preconditioning with endoplasmic reticulum stress mitigates retinal endothelial inflammation via activation of X-box binding protein 1. *J Biol Chem.* 286, 4912-4921.

- Li C., Zhao R., Gao K., Wei Z., Yin M. Y., Lau L. T., Chui D. and Hoi Yu A. C. **(2011)** Astrocytes: implications for neuroinflammatory pathogenesis of Alzheimer's disease. *Curr Alzheimer Res*. 8, 67-80.
- Li G. and Herlyn M. **(2005)** Information sharing and collateral damage. *Trends Mol Med.* 11, 350-352.
- Li J., Ma X., Yu W., Lou Z., Mu D., Wang Y., Shen B. and Qi S**. (2012)** Reperfusion promotes mitochondrial dysfunction following focal cerebral ischemia in rats. *PLoS One* 7, e46498.
- Liang D., Bhatta S., Gerzanich V. and Simard J. M. **(2007)** Cytotoxic edema: mechanisms of pathological cell swelling. *Neurosurg Focus* 22, E2.
- Lipton P. **(1999)** Ischemic cell death in brain neurons. *Physiol Rev.* 79, 1431-1568.
- Liu F. and McCullough L .D. **(2011)** Middle cerebral artery occlusion model in rodents: methods and potential pitfalls. *J Biomed Biotechnol*. 2011, 464701.
- Liu F., Benashski S. E., Persky R., Xu Y. Li J. and McCullough L. D. **(2012)** Age-related changes in AMP-activated protein kinase after stroke. *Age.* 34, 157-168.
- Liu F. and McCullough L. D. **(2012**) Interactions between age, sex, and hormones in experimental ischemic stroke. *Neurochem Int*. 61, 1255-1265.
- Liu S., Connor J., Peterson S., Shuttleworth C. W. and Liu K. J. **(2002)**. Direct visualization of trapped erythrocytes in rat brain after focal ischemia and reperfusion. *J Cereb Blood Flow Metab*. 22, 1222–1230.
- Livak K. J. and Schmittgen T. D. **(2001)** Analysis of relative gene expression data using real-time quantitative PCR and the 2(-Delta Delta CT)) Method. *Methods.* 25, 402-408.
- Logsdon A. F., Lucke-Wold B. P., Nguyen L., Matsumoto R. R., Turner R. C., Rosen C. L. and Huber J. D. **(2016)** Salubrinal reduces oxidative stress, neuroinflammation and impulsive-like behavior in a rodent model of traumatic brain injury. *Brain Res.* 1643, 140-151.
- Lively S. and Schlichter L. C. **(2012)**. Age-related comparisons of evolution of the inflammatory response after intracerebral hemorrhage in rats. *Transl Stroke Res.* 3, 132-146.
- Lo E. H. **(2008)** Experimental models, neurovascular mechanisms and translational issues in stroke research. *Br J Pharmacol.* 153, S396-S405.
- Lochhead J. J., McCaffrey G., Sanchez-Covarrubias L., Finch J. D., DeMarco K. M., Quigley C. E., Davis T. P. and Ronaldson P. T. **(2012)** Tempol modulates changes in xenobiotic permeability and occludin oligomeric assemblies at the blood-brain barrier during inflammatory pain. *Am J Physiol Heart Circ Physiol.* 302, H582–H593.

- Llorente I.L., Perez-Rodriguez D., Burgin T. C., Gonzalo-Orden J. M., Martinez-Villayandre B. and Fernandez-Lopez, A. **(2013a)**. Age and meloxicam modify the response of the glutamate vesicular transporters (VGLUTs) after transient global cerebral ischemia in the rat brain. *Brain Res Bull*. 94, 90-97.

- Llorente I. L., Burgin T. C., Perez-Rodriguez D., Martinez-Villayandre B., Perez-Garcia C. C. and Fernandez-Lopez A. **(2013b)** Unfolded protein response to global ischemia following 48 h of reperfusion in the rat brain: the effect of age and meloxicam. *J. Neurochem.* 127, 701-710.

- Llorente I. L., Landucci E., Pellegrini-Giampietro D. and Fernández-López A. **(2015)** Glutamate receptor and transporter modifications in rat organotypic hippocampal slice cultures exposed to oxygen–glucose deprivation: the contribution of cyclooxygenase-2. *Neuroscience*, 292, 118–128.

- Lucas M., Sutart L. M., Zhang A., Hodivala-Dilke K., Febbraio M., Silverstein R., Savill J. and Lacy-Hulbert A. **(2006)** Requirements for apoptotic cell contact in regulation of macrophage responses. *J Immunol.* 177, 4047-4054.

- Luheshi N., Krisztina M., Kovács J., Lopez-Castejon G., Brough D. and Denes A. **(2011)** Interleukin-1α expression precedes IL-1β after ischemic brain injury and is localised to areas of focal neuronal loss and penumbral tissues. *J Neuroinflammation.* 8, 186.

- MacManus J. P. and Buchan A. M. **(2000)** Apoptosis after experimental stroke: fact or fashion? *J Neurotrauma.* 17, 899-914.

- Maheshwari A., Badgujar L., Phukan B., Bodhankar S. L. and Thakurdesai P. **(2011)** Protective effect of etoricoxib against middle cerebral artery occlusion induced transient focal cerebral ischemia in rats. *Eur J Pharmacol* 667, 230–237.

- Malhotra J. D. and Kaufman R. J. **(2011)** ER stress and its functional link to mitochondria: role in cell survival and death. *Cold Spring Harb Perspect Biol.* 3, a004424.

- Markus T. M., Tsai S. Y., Bollnow M. R., Farrer R. G., O'Brien T. E., Kindler-Baumann D. R., Rausch M., Rudin M., Wiessner C., Mir A. K., Schwab M. E. and Kargje G. L. **(2005)** Recovery and brain reorganization after stroke in adult and aged rats. *Ann Neurol.* 58, 950-953.

- Marler J. R., Tilley B. C., Lu M., Brott T. G., Lyden P. C., Grotta J. C., Broderick J. P., Levine S. R., Frankel M. P., Horowitz S. H., Haley E. C. Jr, Lewandowski C. A. and Kwiatkowski T. P. **(2000)** Early stroke treatment associated with better outcome: the NINDS rt-PA stroke study. 55, 1649-1655.

- Marnett L. J. and DuBois M. R. **(2002)** COX-2: a target for colon cancer prevention. *Annu Rev Pharmacol Toxicol.* 42, 55-80.

- McAdam B. F., Mardini I. A., Habib A., Burke A., Lawson J. A., Kapoor S., FitzGerald G. A. **(2000)** Effect of regulated expression of human cyclooxygenase isoforms on eicosanoid and isoeicosanoid production in inflammation. *J Clin Invest.* 105, 1473-1482.

- McIntosh C. T., Warnock J. N. **(2013)** Side-specific characterization of aortic valve endothelial cell adhesion molecules under cyclic strain. *J Heart Valve Dis*. 22, 631-639.

- Mehta S. L., Manhas N. and Raghubir R. **(2007)** Molecular targets in cerebral ischemia for developing novel therapeutics. *Brain Res Rev*. 54, 34-66.

- Meisel C., Schwab J. M., Prass K., Meisel A. and Dirnagl U. **(2005)** Central nervous system injury-induced immune deficiency syndrome. *Nat Rev Neurosci*. 6, 775-786.

- Mesches M. H., Gemma C., Veng L. M., Allgeier C., Young D. A., Browning M. D. and Bickford P. C. **(2004)** Sulindac improves memory and increases NMDA receptor subunits in aged Fischer 344 rats. *Neurobiol Aging.* 25, 315-324.

- Meusser B., Hirsch C., Jarosch E. and Sommer T. **(2005)** ERAD: the long road to destruction. *Nat Cell Biol*. 7, 766-772.

- Monsel A., Zhu Y. G., Gennai S., Hao Q., Liu J. and Lee J. W. **(2014)** Cell-based therapy for acute organ injury: preclinical evidence and ongoing clinical trials using mesenchymal stem cells. *Anesthesiology.* 121, 1099-1121.

- Montori S., Dos Anjos S., Rios-Granja M. A., Perez-Garcia C. C., Fernandez-Lopez A. and Martinez-Villayandre B. **(2010a)** AMPA receptor downregulation induced by ischaemia/reperfusion is attenuated by age and blocked by meloxicam. *Neuropathol Appl Neurobiol*. 36, 436-447.

- Montori S., Martinez-Villayandre B., Dos-Anjos S., Llorente I. L., Burgin T. C. and Fernandez-Lopez A. **(2010b)**. Age-dependent modifications in the mRNA levels of the rat excitatory amino acid transporters (EAATs) at 48hour reperfusion following global ischemia. *Brain Res*. 1358, 11-19.

- Montori S., Dos-Anjos S., Martinez-Villayandre B., Regueiro-Purrinos M. M., Gonzalo-Orden J. M., Ruano D. and Fernandez-Lopez A. **(2010c)**. Age and meloxicam attenuate the ischemia/reperfusion-induced down-regulation in the NMDA receptor genes. *Neurochem Int*. 56, 878-885.

- Morales Ortiz A., Martín González M. R., Frank García A., Hernández Pérez M. A., Rodríguez-Antigüedad A., Jiménez Hernández M. D., Delgado Bona G., Peinazo Arias M., Gallardo Corral E., Martínez Vila E. and Matias Guiu J. **(2010)** Specific neurology emergency training of medical residents in Spain. *Neurologia.* 25, 557-562.

- Morrison H. W. and Filosa J. A.**(2013)** A quantitative spatiotemporal analysis of microglia morphology during ischemic stroke and reperfusion. *J Neuroinflammation* 10, 4.
-
- Mu T. W., Fowler D. M. and Kelly J. W. **(2008)** Partial restoration of mutant enzyme homeostasis in three distinct lysosomal storage disease cell lines by altering calcium homeostasis. *PLoS Biol.* 6, e26.
- Muchowski, P. J. **(2002)** Protein misfolding, amyloid formation, and neurodegeneration: a critical role for molecular chaperones? *Neuron.* 35, 9-12.
- Muntner P., Garrett E., Klag M. J. and Coresh J. **(2002)** Trends in stroke prevalence between 1973 and 1991 in the US population 25 to 74 years of age. *Stroke.* 33, 1209-1213.
- Nakagawa S., Deli M. A., Kawaguchi H., Shimizudani T., Shimono T., Kittel A., Tanaka K. and Niwa M. **(2009**) A new blood-brain barrier model using primary rat brain endothelial cells, pericytes and astrocytes. *Neurochem Int.* 54, 253-263.
- Nakajima M., Koga T., Sakai H., Yamanaka H., Fujiwara R. and Yokoi T. **(2010)** N-Glycosylation plays a role in protein folding of human UGT1A9. *Biochem Pharmacol.* 79, 1165-1172.
- Nakajima S., Hiramatsu N., Hayakawa K., Saito Y., Kato H., Huang T., Yao J., Paton A. W., Paton J. C. and Kitamura M. **(2011)** Selective abrogation of BiP/GRP78 blunts activation of NF-kappaB through the ATF6 branch of the UPR: involvement of C/EBPbeta and mTOR-dependent dephosphorylation of Akt. *Mol Cell Biol.* 31, 1710-1718.
- Nakajima S. and Kitamura M. **(2013)** Bidirectional regulation of NF-kappaB by reactive oxygen species: a role of unfolded protein response. *Free Radic Biol Med*. 65, 162-174.
- Nakka V. P., Gusain A. and Raghubir R. **(2010)** Endoplasmic reticulum stress plays critical role in brain damage after cerebral ischemia/reperfusion in rats. *Neurotox Res*. 17, 189-202.
- Nakka V. P., Prakash-Babu P. and Vemuganti R. **(2014)** Crosstalk Between Endoplasmic Reticulum Stress, Oxidative Stress, and Autophagy: Potential Therapeutic Targets for Acute CNS Injuries. *Mol Neurobiol*. 53, 532-544.
- Navarro A., Gómez C., Sánchez-Pino M. J., González H., Bández M. J., Boveris A. D. and Boveris A. **(2005)** Vitamin E at high doses improves survival, neurological performance, and brain mitochondrial function in aging male mice. *Am J Physiol Regul Integr Comp Physiol.* 289, 13292-13299.

- Nedergaard M., Gjedde A. and Diemer N. H. **(1986)** Focal ischemia of the rat brain: autoradiographic determination of cerebral glucose utilization, glucose content, and blood flow. *J Cereb Blood Flow Metab*. 6, 414-424.
- Norman M. U., James W. G. and Hickey M. J. **(2008)** Differential roles of ICAM-1 and VCAM-1 in leukocyte-endothelial cell interactions in skin and brain of MRL/faslpr mice. *J Leukoc Biol*. 84, 68-76.
- Novoa I., Zhang Y., Zeng H., Jungreis R., Harding H. P. and Ron D. **(2003)** Stress-induced gene expression requires programmed recovery from translational repression. *EMBO J.* 22, 1180-1187.
- O'Banion M. K., Winn V. D. and Young D. A. **(1992)** cDNA cloning and functional activity of a glucocorticoid-regulated inflammatory cyclooxygenase. *PNAS.* 89, 4888-4892.
- Obermeier B., Daneman R. and Ransohoff R. M. **(2013)** Development, maintenance and disruption of the blood-brain barrier. *Nat Med.* 19, 1584-1596.
- Oeckinghaus A. and Ghosh S. **(2009)** The NF-kappaB family of transcription factors and its regulation. *Cold Spring Harb Perspect Biol.* 1, a000034
- Ohri S. S., Hetman M. and Whittemore S. R. **(2013)** Restoring endoplasmic reticulum homeostasis improves functional recovery after spinal cord injury. *Neurobiol Dis*. 58, 29-37.
- Olesen J. N., Lip G. Y., Lane D. A., Køber L., Hansen M. L., Karasoy D., Hansen C. M., Gislason G. H. and Torp-Pedersen C. **(2012)** Vascular disease and stroke risk in atrial fibrillation: a nationwide cohort study. *Am J Med.* 125, 13-23.
- Ong D. S. T. and Kelly J. W. **(2011)** Chemical and/or biological therapeutic strategies to ameliorate protein misfolding diseases. *Curr Opin Cell Biol.* 23, 231-38.
- Østergaard L., Jespersen S. N., Mouridsen K., Mikkelsen I. K., Jonsdottír K. Ý., Tietze A., Blicher J. U., Aamand R., Hjort N., Iversen N. K., Cai C., Hougaard K. D., Simonsen C. Z., Von Weitzel-Mudersbach P., Modrau B., Nagenthiraja K., Riisgaard Ribe L., Hansen M. B., Bekke S. L., Dahlman M. G., Puig J., Pedraza S., Serena J., Cho T. H., Siemonsen S., Thomalla G., Fiehler J., Nighoghossian N. and Andersen G. **(2013)** The Role of the Cerebral Capillaries in Acute Ischemic Stroke: The Extended Penumbra Model. *J Cereb Blood Flow Metabol.* 33, 635-648.
- Pahl H. L. and Baeuerle P. A. **(1996)** Activation of NF-Kappa B by ER stress requires both Ca^{2+} and reactive oxygen intermediates as messengers. *FEBS Let* 39, 129-36.
- Pan, J., Konstas A. A., Bateman B., Ortolano G. A. and Pile-Spellman J.**(2007)** Reperfusion injury following cerebral ischemia: pathophysiology, MR imaging, and potential therapies. *Neuroradiology.* 49, 93-102.

- Patrono, C. **(2016a)** Cardiovascular effects of cyclooxygenase-2 inhibitors: a mechanistic and clinical perspective. *Br J Clin Pharmacol*. 82, 957–964.
- Patrono, C. **(2016b)** Cardiovascular effects of nonsteroidal anti-inflammatory drugs. *Curr Cardiol Rep*. 18, 25.
- Paxinos G. and Watson C. **(1996)** The Rat Brain in Stereotaxic Coordinates. Academic Press, San Diego.
- Pekny M. and Nilsson M. **(2005)** Astrocyte activation and reactive gliosis. *Glia.* 50, 427-34.
- Pekny M, Pekna M., Messing A., Steinhäuser C., Lee J. M., Parpura V., Hol E. M., Sofroniew M. V. and Verkhratsky A. **(2016)** Astrocytes: a central element in neurological diseases. *Acta Neuropathol*. 131, 323-345.
- Pereira D. M., Valentão P., Correia-da-Silva G., Teixeira N. and Andrade P. B. **(2015)** Translating endoplasmic reticulum biology into the clinic: a role for ER-targeted natural products? *Nat Prod Rep.* 32, 705-722.
- Perez-Polo J. R., Rea H. C., Johnson K. M., Parsley M. A., Unabia G. C., Xu G., Infante S. K., Dewitt D. S. and Hulsebosch C. E. **(2013)** Inflammatory consequences in a rodent model of mild traumatic brain injury. *J Neurotrauma.* 30, 727-740.
- Perry V. H., Anthony D. C., Bolton, S. J. and Brown, H. C. **(1997)**. The blood-brain barrier and the inflammatory response. *Mol Med Today.* 3, 335-341.
- Petcu E. B., Sfredel V., Platt D., Herndon J. G., Kessler C. and Popa-Wagner A. **(2008)** Cellular and molecular events underlying the dysregulated response of the aged brain to stroke: a mini-review. *Gerontology.* 54, 6-17.
- Peters L. R. and Raghavan M. **(2011)** Endoplasmic reticulum calcium depletion impacts chaperone secretion, innate immunity, and phagocytic uptake of cells. *J Immunol.* 187, 919-31.
- Petito C. K. and Pulsinelli W. A. **(1984)**. Delayed neuronal recovery and neuronal death in rat hippocampus following severe cerebral ischemia: possible relationship to abnormalities in neuronal processes. *J Cereb Blood Flow Metab.* 4, 194-205.
- Petito C. K., Feldmann E., Pulsinelli W. A. and Plum F. **(1987)** Delayed hippocampal damage in humans following cardiorespiratory arrest. *Neurology*. 37, 1281-1286.
- Petri B., Phillipson M. and Kubes P. **(2008)** The physiology of leukocyte recruitment: an in vivo perspective. *J Immunol* 180, 6439-6446.

- Popa-Wagner A., Schroder E., Walker L. C. and Kessler C. **(1998)**. Beta-amyloid precursor protein and ss-amyloid peptide immunoreactivity in the rat brain after middle cerebral artery occlusion: effect of age. *Stroke*. 29, 2196-2202.
- Posada-Duque R. A., Barreto G. E. and Cardona-Gomez G. P. **(2014)** Protection after stroke: cellular effectors of neurovascular unit integrity. *Front Cell Neurosci*. 8, 231.
- Pulsinelli W., Brierley J. and Plum F. **(1982)** Temporal profile of neuronal damage in a model of transient forebrain ischemia. *Ann Neurol.* 11, 491-498.
- Pun P. B., Lu J. and Moochhala S. **(2009)** Involvement of ROS in BBB dysfunction. *Free Radical Res.* 43, 348–364.
- Rami A., Bechmann I. and Stehle J.H. **(2008)** Exploiting endogenous anti-apoptotic proteins for novel therapeutic strategies in cerebral ischemia. *Prog Neurobiol*. 85, 273-296.
- Rius J., Guma M., Schachtrup C., Akassoglou K., Zinkernagel A. S., Nizet V., Johnson R. S., Haddad G. G. and Karin M. **(2008)** NF-kappaB links innate immunity to the hypoxic response through transcriptional regulation of HIF-1alpha. *Nature*. 453, 807-811.
- Roda J., Bencosme J., Pérez-Higueras A. and Fraile M. **(1992)** Simultaneous multiple intracranial and spinal meningiomas. *Minim Invasive Neurosurg.* 35, 92–94.
- Roda J.M., Carceller F., Pascual J.M., Herguido M.J., González-Llanos F., Alonso de Leciñana M., Avendaño C and Díez-Tejedor E. **(1998)** Experimental animal models in cerebral ischemia. *Neurologia* 13, 427–430.
- Rodriguez-Yanez M. and Castillo J. **(2008)** Role of inflammatory markers in brain ischemia. *Curr Opin Neurol* 21,353–357.
- Rojas J. I., Zurru M. C., Romano M., Patrucco L. and Cristiano E. **(2007)** Acute ischemic stroke and transient ischemic attack in the very old--risk factor profile and stroke subtype between patients older than 80 years and patients aged less than 80 years. *Eur J Neurol*. 14, 895-899.
- Rojo A.I., McBean G., Cindric M., Egea J., López M.G., Rada P., Zarkovic N. and Cuadrado A. **(2014)** Redox control of microglial function: molecular mechanisms and functional significance. Antioxid Redox Signal. 21, 1766–1801.
- Rolls A., Shechter R. and Schwartz M. **(2009)** The bright side of the glial scar in CNS repair. *Nat Rev Neurosci*. 10, 235-241.
- Rom S., Zuluaga-Ramirez V., Reichenbach N. L., Dykstra H., Gajghate S., Pacher P. and Persidsky Y. **(2016)** . PARP inhibition in leukocytes diminishes inflammation

via effects on integrins/cytoskeleton and protects the blood-brain barrier. *J Neuroinflammation.* 13, 254.

- Rosamond W., Flegal K., Furie K., Go A., Greenlund K., Haase N., Hailpern S. M., Ho M., Howard V., Kissela B., Kittner S., Lloyd-Jones D., McDermott M., Meigs J., Moy C., Nichol G., O'Donnell C., Roger V., Sorlie P., Steinberger J., Thom T., Wilson M., Hong Y., and American Heart Association Statistics Committee and Stroke Statistics Subcommittee **(2008)** Heart disease and stroke statistics--2008 update: a report from the American Heart Association Statistics Committee and Stroke Statistics Subcommittee. *Circulation*. 117, e25-146.

- Rosell A., Ortega-Aznar A., Alvarez-Sabín J., Fernández-Cadenas I., Ribó M., Molina C.A., Lo E.H. and Montaner J. **(2006)** Increased brain expression of matrix metalloproteinase-9 after ischemic and hemorrhagic human stroke. *Stroke*. 37, 1399–1406.

- Rosenberg G. A., Kornfeld M., Estrada E., Kelley R. O., Liotta L. A. and Stetler-Stevenson W. G. **(1992)** TIMP-2 reduces proteolytic opening of blood-brain barrier by type IV collagenase. *Brain Res*. 576, 203-207.

- Rosenberg G. A., Navratil M., Barone F. and Feuerstein G. **(1996)** Proteolytic cascade enzymes increase in focal cerebral ischemia in rat. *J Cereb Blood Flow Metab*. 16, 360-366.

- Rosenberg G.A., Cunningham L.A., Wallace J., Alexander S., Estrada E.Y., Grossetete M., Razhagi A., Miller K. and Gearing A. **(2001)** Immunohistochemistry of matrix metalloproteinases in reperfusion Injury to rat brain: activation of MMP-9 linked to stromelysin-1 and microglia in cell cultures. *Brain Res*. 893, 104–12.

- Roumie C. L., Mitchel E. F. Jr, Kaltenbach L., Arbogast P. G., Gideon P. and Griffin M. R. **(2008)** Nonaspirin NSAIDs, cyclooxygenase 2 inhibitors, and the risk for stroke. *Stroke* 39, 2037-45.

- Rubovitch V., Barak S., Rachmany L., Goldstein R. B., Zilberstein Y. and Pick C. G. **(2015)** The neuroprotective effect of salubrinal in a mouse model of traumatic brain injury. *Neuromolecular Med*. 17, 58-70.

- Ruey-Horng S., Wang C. Y., and Yang C.M. **(2015)**. NF-kappaB Signaling Pathways in Neurological Inflammation: A Mini Review. *Front Mol Neurosci*. 8, 77.

- Saito A., Maier C.M., Narasimhan P., Nishi T., Song Y.S., Yu F., Liu J., Lee Y.S., Nito C., Kamada H., Dodd R.L., Hsieh L.B., Hassid B., Kim E.E., González M. and Chan PH**. (2005)** Oxidative stress and neuronal death/survival signaling in cerebral ischemia. *Mol. Neurobiol*. 31, 105–116.

- Salas A., Shimaoka M., Phan U., Kim M. and Springer T.A. **(2006)**. Transition from rolling to firm adhesion can be mimicked by extension of integrin alphaLbeta2 in an intermediate affinity state. *J Biol Chem.* 281, 10876-10882.
- Sandoval K. E. and Witt K.A. **(2008)** Blood-brain barrier tight junction permeability and ischemic stroke. *Neurobiol Dis.* 32, 200–219.
- Sato M., Hashimoto H. and Kosaka F. **(1990)** Histological Changes of Neuronal Damage in Vegetative Dogs Induced by 18 Minutes of Complete Global Brain Ischemia: Two-Phase Damage of Purkinje Cells and Hippocampal CA1 Pyramidal Cells. *Acta Neuropathol* 80,527–534.
- Saver J.L., Gornbein J., Grotta J., Liebeskind D., Lutsep H., Schwamm L., Scott P. and Starkman S. **(2009)** Number needed to treat to benefit and to harm for intravenous tissue plasminogen activator therapy in the 3- to 4.5-hour window: joint outcome table analysis of the ECASS 3 Trial. *Stroke* 40, 2433–2437.
- Schaller, B. J. **(2007)** Influence of age on stroke and preconditioning-induced ischemic tolerance in the brain. *Exp Neurol* 205,9–19.
- Schenkel A. R., Mamdouh Z., and W. A. Muller. **(2004)**. Locomotion of monocytes on endothelium is a critical step during extravasation. *Nat Immunol* 5,393–400.
- Schild, L. and Georg R. **(2005)**. Oxidative stress is involved in the permeabilization of the inner membrane of brain mitochondria exposed to hypoxia/reoxygenation and low micromolar Ca2+. *FEBS J* 272, 3593–3601.
- Schilling M., Besselmann M., Leonhard C., Mueller M., Ringelstein E. B. and Kiefer R. **(2003)** Microglial activation precedes and predominates over macrophage infiltration in transient focal cerebral ischemia: a study in green fluorescent protein transgenic bone marrow chimeric mice. *Exp Neurol*. 183, 25-33.
- Schmassmann A., Zoidl G., Peskar B.M., Waser B., Schmassmann-Suhijar D., Gebbers J.O. and Reubi J.C. **(2006)** Role of the different isoforms of cyclooxygenase and nitric oxide synthase during gastric ulcer healing in cyclooxygenase-1 and -2 knockout mice. *Am J Physiol Gastrointest Liver Physiol.* 290, 747-756.
- Scholz M., Jindrich C., Schädel-Höpfner M., and Windolf J. **(2007)** Neutrophils and the Blood-Brain Barrier Dysfunction after Trauma. *Med Res Rev* 27,401–416.
- Schönbeck U., Sukhova G. K., Graber P., Coulter S., and Libby P. **(1999)** Augmented expression of cyclooxygenase-2 in human atherosclerotic lesions. *Am J Pathol.* 155, 1281–1291.
- Schonthal A. H. **(2007)**. Induction of apoptosis by celecoxib in cell culture: an uncertain role for Cyclooxygenase-2. *Cancer Res.* 67, 5575–76.

- Schroder M. and Kaufman R. J. **(2005)** The mammalian unfolded protein response. *Annu Rev Biochem.* 74, 739-789.
- Schroder M. **(2008)** Endoplasmic reticulum stress responses. *Cell Mol Life Sci.* 65, 862-894.
- Schwab C. and McGeer P. L. **(2008)** Inflammatory aspects of Alzheimer Disease and other neurodegenerative disorders. *J Alzheimers Dis.* 13, 359-369.
- Seibert K., Masferrer J., Zhang Y., Gregory S., Olson G., Hauser S., Leahy K., Perkins W. and Isakson P. **(1995)** Mediation of inflammation by cyclooxygenase-2. *Agents Actions Suppl.* 46, 41–50.
- Sengillo J.D., Winkler E.A., Walker C.T., Sullivan J.S., Johnson M. and Zlokovic B.V. **(2013)** Deficiency in mural vascular cells coincides with blood-brain barrier disruption in Alzheimer's Disease. *Brain Pathol.* 23, 303–310.
- Seshadri S., Beiser A., Kelly-Hayes M., Kase C.S., Au R., Kannel W.B. and Wolf P.A. **(2006)** The lifetime risk of stroke: estimates from the framingham study. *Stroke*. 37, 345–350.
- Shaw S.K., Ma S., Kim M.B., Rao R.M., Hartman C.U., Froio R.M., Yang L., Jones T., Liu Y., Nusrat A., Parkos C.A. and Luscinskas F.W. **(2004)** Coordinated redistribution of leukocyte LFA-1 and endothelial cell ICAM-1 accompany neutrophil transmigration. *J. Exp. Med.* 200, 1571–1580.
- Shechter R. and Schwartz M. **(2013)** Harnessing monocyte-derived macrophages to control central nervous system pathologies: no longer 'if' but 'how.' *J. Pathol.* 229, 332–46.
- Shkoda A., Ruiz P.A., Daniel H., Kim S.C., Rogler G., Sartor R.B. and Haller D. **(2007)** Interleukin-10 blocked endoplasmic reticulum stress in intestinal epithelial cells: impact on chronic inflammation. *Gastroenterology* 132, 190–207.
- Simard J. M., Kent T. A., Chen M., Tarasov K.V. and Gerzanich V. **(2007)** Brain oedema in focal ischaemia: molecular pathophysiology and theoretical implications. *Lancet Neurol*. 6, 258–268.
- Simi A., Tsakiri N., Wang P. and Rothwell N.J. **(2007)** Interleukin-1 and Inflammatory Neurodegeneration. *Biochem. Soc. Trans*. 35, 1122–1126.
- Simmons L.J., Surles-Zeigler M.C., Li Y., Ford G.D., Newman G.D., Ford B.D. **(2016)** Regulation of inflammatory responses by neuregulin-1 in brain ischemia and microglial cells in vitro involves the NF-Kappa B pathway. *J Neuroinflammation*. 13, 237.
- Sinha N., Baquer N. Z. and Sharma D. **(2005)** Anti-lipidperoxidative role of exogenous dehydroepiendrosterone (DHEA) administration in normal ageing rat brain. *Indian. J Exp Biol*. 43, 420-424.

- Smith W. L. and Langenbach R. **(2001)**. Why there are two cyclooxygenase isozymes. *J. Clin. Invest.* 107, 1491–95.
- Sofroniew M. V. and Vinters H.V. **(2010)** Astrocytes: biology and pathology. *Acta Neuropathol*. 119, 7-35.
- Solenski N.J., diPierro C.G., Trimmer P.A., Kwan A.L. and Helm G.A. **(2002)** Ultrastructural changes of neuronal mitochondria after transient and permanent cerebral ischemia. *Stroke* 33, 816–824.
- Spindler K. R. and Hsu T.H. **(2012)** Viral disruption of the blood–brain barrier. *Trends Microbiol*. 20, 282–90.
- Stanimirovic D., Satoh K. **(2000)** Inflammatory mediators of cerebral endothelium: a role in ischemic brain inflammation. *Brain Pathol*. 10, 113-126.
- Stevens S. L., Bao J., Hollis J., Lessov N. S., Clark W. M. and Stenzel-Poore M. P. **(2002)** The use of flow cytometry to evaluate temporal changes in inflammatory cells following focal cerebral ischemia in mice. *Brain Res*. 932, 110-119.
- Sughrue M. E., Mehra A., Connolly E. S. Jr and D'Ambrosio A. L. **(2004)** Anti-adhesion molecule strategies as potential neuroprotective agents in cerebral ischemia: a critical review of the literature. *Inflamm Res*. 53, 497-508.
- Sullivan S.M., Sullivan R.K., Miller S.M., Ireland Z., Björkman S.T., Pow D.V. and Colditz P.B. **(2012)** Phosphorylation of GFAP is associated with injury in the neonatal pig hypoxic-ischemic brain. *Neurochem. Res*. 37, 2364–2378.
- Sumi N., Nishioku T., Takata F., Matsumoto J., Watanabe T., Shuto H., Yamauchi A., Dohgu S., Kataoka Y. **(2010)** Lipopolysaccharide-activated microglia induce dysfunction of the blood–brain barrier in rat microvascular endothelial cells co-cultured with microglia. *Cell. Mol. Neurobiol.* 30, 247–253.
- Sutherland G. R., Dix G. A., and Auer R.N. **(1996)** Effect of Age in Rodent Models of Focal and Forebrain Ischemia. *Stroke*. 27, 1663–1668.
- Suzuki Y., Takagi Y., Nakamura R., Hashimoto K., and Umemura K. **(2003)** Ability of nmda and non-nmda receptor antagonists to inhibit cerebral ischemic damage in aged rats. *Brain Res*. 964, 116–120.
- Szekely C. A. and Zandi P. P. **(2010)** Non-steroidal anti-inflammatory drugs and Alzheimer's disease: the epidemiological evidence. *CNS Neurol Disord Drug Targets* 9, 132-139.
- Tamura A., Graham D. I., McCulloch J. and Teasdale G.M. **(1981)** Focal cerebral ischaemia in the rat: Regional cerebral blood flow determined by [14C]iodoantipyrine autoradiography following middle cerebral artery occlusion. *J Cereb Blood Flow Metab*. 1, 61-69.

- Tanaka R., Komine-Kobayashi M., Mochizuki H., Yamada M., Furuya T., Migita M., Shimada T., Mizuno Y. and Urabe T. **(2003)** Migration of enhanced green fluorescent protein expressing bone marrow-derived microglia/macrophage into the mouse brain following permanent focal ischemia. *Neuroscience*. 117, 531-539.

- Takahashi T., Kalka C., Masuda H., Chen D., Silver M., Kearney M., Magner M., Isner J.M. and Asahara T. **(1999)** Ischemia- and cytokine-induced mobilization of bone marrow-derived endothelial progenitor cells for neovascularization. *Nat. Med*. 5,434–438.

- Takata F., Dohgu S., Matsumoto J., Takahashi H., Machida T., Wakigawa T., Harada E., Miyaji H., Koga M., Nishioku T., Yamauchi A. and Kataoka Y. **(2011)** Brain pericytes among cells constituting the blood-brain barrier are highly sensitive to tumor necrosis factor-alpha, releasing matrix metalloproteinase-9 and migrating in vitro. *J Neuroinflam*. 8, 106-2094-8-106.

- Tammela T., Zarkada G., Nurmi H., Jakobsson L., Heinolainen K., Tvorogov D., Zheng W., Franco C.A., Murtomäki A., Aranda E., Miura N., Ylä-Herttuala S., Fruttiger M., Mäkinen T., Eichmann A., Pollard J.W., Gerhardt H. and Alitalo K. **(2011)** VEGFR-3 controls tip to stalk conversion at vessel fusion sites by reinforcing notch signalling. *Nat. Cell Biol.* 13, 1202–1213.

- Taoufik, E. and Probert L. **(2008)** Ischemic Neuronal Damage. *Curr. Pharm. Des.* 14, 3565–3573.

- Taylor S., Wakem M., Dijkman G., Alsarraj M. and Nguyen M. **(2010)** A practical approach to RT-qPCR-Publishing data that conform to the MIQE guidelines. *Methods.* 50, S1-5.

- Tecoma E. S. and Choi D. W. **(1989)** GABAergic neocortical neurons are resistant to NMDA receptor-mediated injury. *Neurology*. 39, 676-682.

- Thornton P, McColl B.V., Cooper L., Rothwell N.J. and Allan S.M. **(2010)** Interleukin-1 drives cerebrovascular inflammation via map kinase-independent pathways. *Curr Neurovasc Res.* 7, 330–40.

- Traystman R. J. **(2003)** Animal models of focal and global cerebral ischemia. *ILAR J.* 44, 85–95.

- Tsujimoto Y., Nakagawa T., and Shimizu S. **(2006)** mitochondrial membrane permeability transition and cell death. *Bioch Biophys Acta*. 1757, 1297–1300.

- Uehara T., Nakamura T., Yao D., Shi Z.Q., Gu Z., Ma Y., Masliah E., Nomura Y., Lipton S.A. **(2006)** S-nitrosylated protein-disulphide isomerase links protein misfolding to neurodegeneration. *Nature*. 441, 513–517.

- Ueno M., Wu B., Nishiyama A., Huang C. L., Hosomi N., Kusaka T., Nakagawa T., Onodera M., Kido M. and Sakamoto H. **(2009)** The expression of matrix

metalloproteinase-13 is increased in vessels with blood-brain barrier impairment in a stroke-prone hypertensive model. *Hypertens Res*. 32, 332-338.

- Ugidos I. F., Santos-Galdiano M., Pérez-Rodríguez D., Anuncibay-Soto B., Font-Belmonte E., López D. J., Ibarguren M., Busquets X. and Fernández-López A. **(2017)** Neuroprotective effect of 2-hydroxy arachidonic acid in a rat model of transient middle cerebral artery occlusion. *Biochim Biophys Acta.* doi: 10.1016/j.bbamem.2017.03.009.

- Unterberg, A. W., Stover J., Kress B. and Kiening K.L. **(2004)** Edema and brain trauma. *Neuroscience*. 129, 1021–1029.

- Vandenberg R. J. and Ryan R. M. **(2013)** Mechanisms of glutamate transport. *Physiol Rev.* 93, 1621-1657.

- Vardeh D., Wang D., Costigan M., Lazarus M., Saper C.B., Woolf C.J., Fitzgerald G.A. and Samad T.A. **(2009)** COX2 in cns neural cells mediates mechanical inflammatory pain hypersensitivity in mice. *J Clin Invest*. 119, 287–294.

- Vellai T. **(2009)** Autophagy genes and ageing. *Cell Death Diff*. 16, 94–102.

- Viatour P., Merville M.P, Bours V. and Chariot A. **(2005)** Phosphorylation of NF-kappaB and IkappaB proteins: implications in cancer and inflammation. Trends Biochem Sci. 30, 43–52.

- Vieira M., Fernandes J., Carreto L., Anuncibay-Soto B., Santos M., Han J., Fernandez-Lopez A., Duarte C. B., Carvalho A. L. and Santos A. E. **(2014)** Ischemic insults induce necroptotic cell death in hippocampal neurons through the up-regulation of endogenous RIP3. *Neurobiol Dis*. 68, 26-36.

- Vitner E. B., Farfel-Becker T., Eilam R., Biton I., and Futerman A.H. **(2012)** Contribution of brain inflammation to neuronal cell death in neuronopathic forms of Gaucher's Disease. *Brain*. 135, 1724–1735.

- Walker F. R., Beynon S. B., Jones K. A., Zhao Z., Kongsui R., Cairns M. and Nilsson M. **(2014)** Dynamic structural remodelling of microglia in health and disease: a review of the models, the signals and the mechanisms. *Brain Behav Immun.* 37, 1-14.

- Walter P. and Ron D. **(2011)** The unfolded protein response: from stress pathway to homeostatic regulation. *Science*. 334, 1081-1086.

- Wang LC., Futrell N., Wang D.Z., Chen F.J., Zhai Q.H. and Schultz L.R. **(1995)** A reproducible model of middle cerebral infarcts, compatible with long-term survival, in aged rats. *Stroke*. 26, 2087–2090.

- Wang, X. Z. and Ron D. **(1996)** Stress-induced phosphorylation and activation of the transcription factor CHOP (GADD153) by p38 MAP Kinase." Science. 272, 1347–1349.

- Wang, Z., Xu X., and Wu X. **(2003)** Therapeutic effect of dexamethasone and mannitol on global brain ischemia-reperfusion injury in rats. *Beijing Da Xue Xue Bao.* 35, 303–306.
- Wang Q., Tang X. N. and Yenari M. A. **(2007)** The inflammatory response in stroke. *J Neuroimmunol.* 184, 53-68.
- Wang N., Zhang Y., Wu L., Wang Y., Cao Y., He L., Li X. and Zhao J. **(2013)** Puerarin protected the brain from cerebral ischemia injury via astrocyte apoptosis inhibition. *Neuropharmacol.* 79 , 282-289.
- Wasserman J. K., Yang H. and Schlichter L. C. **(2008)** Glial responses, neuron death and lesion resolution after intracerebral hemorrhage in young vs. aged rats. *Eur J Neurosci.* 28, 1316-1328.
- Weidenfeller C., Svendsen C. N. and Shusta E. V. **(2007)** Differentiating embryonic neural progenitor cells induce blood-brain barrier properties. *J Neurochem.* 101, 555-565.
- Winkler E.A., Sengillo J.D., Sullivan J.S., Henkel J.S., Appel S.H. and Zlokovic BV. **(2013)** Blood–spinal cord barrier breakdown and pericyte reductions in amyotrophic lateral sclerosis. *Acta Neuropathol*. 125, 111–120.
- Wiseman R.L. and Balch W.E. **(2005)** A new pharmacology – drugging stressed folding pathways. *Trends Mol Med*. 11, 347–350.
- Wolburg, H., Noell S., Mack A., Wolburg-Buchholz K. and Fallier-Becker P. **(2009)** Brain endothelial cells and the glio-vascular complex. *Cell Tissue Res* 335, 75–96.
- Wong A.D., Ye M., Levy A.F., Rothstein J.D., Bergles D.E. and Searson P.C. **(2013)** The blood-brain barrier: an engineering perspective. *Front Neuroeng.* 6, 7.
- Wong C. H. Y. and Crack P.J. **(2008)** Modulation of neuro-inflammation and vascular response by oxidative stress following cerebral ischemia-reperfusion injury. *Curr. Med. Chem*. 15, 1–14.
- World Health Organization (WHO) **(2011)** The top ten causes of death. Fact sheet number, WHO, Geneva.
- Wu, J. and Kaufman R.J. **(2006)** From acute ER stress to physiological roles of the unfolded protein response. *Cell Death Diff.* 13, 374–384.
- Xin Q., Ji B., Cheng B., Wang C., Liu H., Chen X., Chen J. and Bai B. **(2014)** Endoplasmic reticulum stress in cerebral ischemia. *Neurochem Int*. 68, 18-27.
- Xue X., Piao J. H., Nakajima A., Sakon-Komazawa S., Kojima Y., Mori K., Yagita H., Okumura K., Harding H. and Nakano H. **(2005)** Tumor necrosis factor alpha (TNFalpha) induces the unfolded protein response (UPR) in a reactive oxygen species (ROS)-dependent fashion, and the UPR counteracts ROS accumulation by TNFalpha. *J Biol Chem.* 280, 33917-33925.

- Xu X. J., Plesan A., Yu W., Hao J. X. and Wiesenfeld-Hallin Z. **(2001)** Possible impact of genetic differences on the development of neuropathic pain-like behaviors after unilateral sciatic nerve ischemic injury in rats. *Pain*. 89, 135-145.
- Yemisci M., Gursoy-Ozdemir Y., Vural A., Can A., Topalkara K. and Dalkara T. **(2009)** Pericyte contraction induced by oxidative-nitrative stress impairs capillary reflow despite successful opening of an occluded cerebral artery. *Nat. Med.* 15, 1031–1037.
- Yenari M. A., Xu L., Tang X. N., Qiao Y. and Giffard R. G. **(2006)** Microglia potentiate damage to blood-brain barrier constituents: improvement by minocycline in vivo and in vitro. *Stroke* 37, 1087-1093.
- Yenari M. A., Kauppinen T. M. and Swanson R. A. **(2010)** Microglial activation in stroke: therapeutic targets. *Neurotherapeutics.* 7, 378-391.
- Yepes, M. **(2013)** TWEAK and Fn14 in the neurovascular unit. *Front. Immunol.* 4, 367.
- Yilmaz G., Arumugam T. V., Stokes K. Y. and Granger D.N. **(2006)** Role of T lymphocytes and interferon-gamma in ischemic stroke. *Circulation*. 113, 2105-2112.
- Yilmaz G., Granger D. N. **(2008)** Cell adhesion molecules and ischemic stroke. *Neurol Res.* 30, 783-793.
- Yilmaz G. and Granger D. N. **(2010)** Leukocyte recruitment and ischemic brain injury. *Neuromolecular Med*. 12, 193-204.
- Yu Y., Cheng Y., Fan J., Chen X.S., Klein-Szanto A., Fitzgerald G.A. and Funk C.D. **(2005)**. Differential impact of prostaglandin H synthase 1 knockdown on platelets and parturition. *J Clin Invest.* 115, 986–995.
- Zeller, J. A., Lenz A., Eschenfelder C.C., Zunker P. and Deuschl G. **(2005)** Platelet-leukocyte interaction and platelet activation in acute stroke with and without preceding infection. *Arterioscler Thromb Vasc Biol*. 25, 1519–1523.
- Zarow C., Vinters H. V., Ellis W. G., Weiner M. W., Mungas D., White L. and Chui H. C. **(2005)** Correlates of hippocampal neuron number in Alzheimer's disease and ischemic vascular dementia. *Ann Neurol.* 57, 896-903.
- Zhang R., Chopp M., Zhang Z., Jiang N. and Powers C. **(1998)** The expression of P- and E-selectins in three models of middle cerebral artery occlusion. *Brain Res*. 785 , 207-214.
- Zhang M., Li W. B., Geng J. X., Li Q. J., Sun X. C., Xian X. H., Qi J. and Li S.Q. **(2007)** The upregulation of glial glutamate transporter-1 participates in the induction of brain ischemic tolerance in rats. *J. Cereb Blood Flow Metab*. 27, 1352-1368.

- Zhang K. and Kaufman R. J. **(2008)** From endoplasmic-reticulum stress to the inflammatory response. *Nature*. 454, 455-462.
- Zhang Z., Tong N., Gong Y., Qiu Q., Yin L., Lv X. and Wu X. **(2011)** Valproate protects the retina from endoplasmic reticulum stress-induced apoptosis after ischemia-reperfusion injury. *Neurosci. Lett*. 504, 88–92.
- Zhu H., Yoshimoto T., Imajo-Ohmi S., Dazortsava M., Mathivanan A. and Yamashima T. **(2012)** Why are hippocampal CA1 neurons vulnerable but motor cortex neurons resistant to transient ischemia? *J Neurochem*. 120, 574-585.